AFIT/GE/ENG/99M-23

A CLIMATOLOGY-BASED MODEL FOR LONG-TERM PREDICTION OF RADAR BEAM REFRACTION

THESIS

Todd S. Pittman, Captain, USAF

AFIT/GE/ENG/99M-23

REPORT DOCUMENTATION PAGE

Form Approved
OMB No. 0704-0188

1. AGENCY USE ONLY *(Leave blank)*	2. REPORT DATE	3. REPORT TYPE AND DATES COVERED
	March 1999	Master's Thesis

4. TITLE AND SUBTITLE
A CLIMATOLOGY-BASED MODEL FOR LONG-TERM PREDICTION OF RADAR BEAM REFRACTION

5. FUNDING NUMBERS

6. AUTHOR(S)

Todd S. Pittman, Captain, USAF

7. PERFORMING ORGANIZATION NAME(S) AND ADDRESS(ES)

Air Force Institute of Technology
2950 P. Street
WPAFB OH 45433-7765

8. PERFORMING ORGANIZATION REPORT NUMBER

AFIT/GE/ENG/99M-23

9. SPONSORING/MONITORING AGENCY NAME(S) AND ADDRESS(ES)

NAIC/TAER
4180 Watson Way
Wright-Patterson AFB OH 45433-5608

10. SPONSORING/MONITORING AGENCY REPORT NUMBER

11. SUPPLEMENTARY NOTES

Dr Vittal P. Pyati, ENG

12a. DISTRIBUTION AVAILABILITY STATEMENT

Approved for public release; distribution unlimited.

12b. DISTRIBUTION CODE

13. ABSTRACT *(Maximum 200 words)*

The National Air Intelligence Center, WPAFB, OH, needs more accurate predictions of radar beam refraction. A new model was developed for this thesis replacing the standard atmosphere approach with raytracing and climatology.

Usually a microwave radio beam bends towards the earth with a radius of curvature greater than the earth's surface. However, seasonal and climatic variations influence the bending, and at times create temperature or moisture inversions that redirect the energy along the earth's surface leaving radio holes where there is no coverage. This model uses iterative raytracing to determine the most direct path from radar to target through the climatologically predicted refractive atmosphere. The height error is calculated by comparing the geographic path to the refracted path. Only vertical refractivity variation (including the effects of ducting) is taken into account.

The model computed height errors at 17 locations worldwide for a target at 10,000 feet and 60 nautical miles that varied from 100 feet to 2260 feet compared to 804 feet predicted by standard atmosphere. The model traces to all targets when no ducting is modeled, to all targets outside the duct with surface ducting, and to some targets outside the duct with elevated ducting due to ducting ambiguities.

14. SUBJECT TERMS
Radar, Radio Beams, Atmospheric Refraction, Climatology, Radar Performance Prediction, Radar Height Error, Raytracing

15. NUMBER OF PAGES
184

16. PRICE CODE

17. SECURITY CLASSIFICATION OF REPORT	18. SECURITY CLASSIFICATION OF THIS PAGE	19. SECURITY CLASSIFICATION OF ABSTRACT	20. LIMITATION OF ABSTRACT
UNCLASSIFIED	UNCLASSIFIED	UNCLASSIFIED	UL

The views expressed in this thesis are those of the author and do not reflect the official policy or position of the Department of Defense or the U.S. Government

AFIT/GE/ENG/99M-23

A CLIMATOLOGY-BASED MODEL FOR LONG-TERM PREDICTION OF RADAR BEAM REFRACTION

THESIS

Presented to the Faculty of the Graduate School of Engineering

of the Air Force Institute of Technology

Air University

Air Education and Training Command

In Partial Fulfillment of the Requirements for the

Degree of Master of Science in Electrical Engineering

Todd S. Pittman, B.S.E.

Captain, USAF

March 1999

AFIT/GE/ENG/99M-23

A CLIMATOLOGY-BASED MODEL FOR LONG-TERM PREDICTION OF RADAR BEAM REFRACTION

Todd S. Pittman, B.S.E.
Captain, USAF

Approved:

Vittal P. Pyati — 4 Mar 99
Dr Vittal Pyati — date
Committee Chairman

Michael A. Temple — 4 Mar 99
Major Michael Temple, Ph.D. — date
Committee Member

Derrill J. Goldizen — 4 Mar 99
Major Derrill Goldizen, Ph.D. — date
Committee Member

Acknowledgments

I have learned that carrying out a thesis project is like bending a radio wave, neither one is done in a vacuum. I would, first of all, like to thank my advisor, Dr Vittal Pyati, for his guidance and encouragement. I would also like to convey my appreciation to Mr Fred Beaman, my sponsor at NAIC who was willing to make use of a poor Master's student come looking for handouts. Next, I'd like to thank the members of my committee, Maj (Dr) Mike Temple and Maj (Dr) Derrill Goldizen for the leads and the coaching that inspired several breakthroughs.

Additionally, I want to express my appreciation to Mr Wayne Patterson of the Space and Naval Warfare Systems Center. Mr Patterson's prompt helpfulness and his interest in the project were as valuable as the gold nugget of a database he provided. In the same vein, I owe a debt of gratitude to Mr Mike Squires at the AF Combat Climatology Center for his Height-Error Analysis paper and for telling me about the marvelous refractive raytracing framework laid out by Abel, *et. al.*

There's no earthly way I can thank my wife Renie for her months of work and sacrifice, so she'll have to be content to have me back. My children, Nathan and Elisabeth, had very little say in the matter, but I want them to know Daddy will have a lot more free time to wrestle from now on. Finally, I reserve my deepest gratitude for the Lord Jesus Christ, who not only gave me strength, daily guidance, and the well-timed "coincidences" that made the thesis work, but who taught me through the AFIT experience how to trust Him more surely than I ever thought I could.

Table of Contents

Page

List of Figures

Page

Page

Page

Page

Page

List of Tables

Page

Abstract

The National Air Intelligence Center, WPAFB, OH, needs to predict radar beam refraction with greater accuracy. Hitherto, beam bending has been predicted using four-thirds earth or standard atmosphere. A new and more accurate model was developed for this thesis that replaces the old rules-of-thumb with a mix of raytracing and climatology.

Usually a microwave radio beam traveling through the atmosphere bends towards the earth with a radius of curvature greater than the earth's surface. However, seasonal and climatic variations influence the amount and direction of bending, and at times create temperature or moisture inversions that act to redirect the energy along the earth's surface leaving gaping radio holes where there is no coverage.

This model uses iterative raytracing to determine the most direct path from the radar to the target through the climatologically predicted refractive atmosphere. The amount of height measurement error is calculated by comparing the geographic path to the refracted path. Only vertical refractivity variation is taken into account, and the effects of ducting and exponential refractivity are both modeled.

As a test, the model computed height error at 17 locations worldwide for a target at 10,000 feet and 60 nautical miles. The predicted errors varied from approximately 100 feet to 2260 feet – widely varying from the standard atmosphere predicted height error of 804 ft. The model traces to all targets when no ducting is modeled, to all targets outside the duct with surface ducting, and to some targets outside the duct with elevated ducting, since in this case adjacent rays sometimes cross, causing ambiguity in the estimation.

A CLIMATOLOGY-BASED MODEL FOR STRATEGIC PREDICTION OF RADAR BEAM REFRACTION

I. Introduction

As early as 1919 radio scientists were investigating the effects of tropospheric refraction or bending, of radio waves (Kerr, 1951:2). With the invention of radar, accurate prediction of radio beam refraction became especially important. Since one assumes a line-of-sight path to determine the range of a given target and any deviation from a straight line path causes erroneous measurements. Height measurement errors are of particular concern since the atmosphere primarily acts to bend the beam in a vertical direction. Beam curvature can also produce range measurement errors, but they are less significant.

With the proliferation of inexpensive yet powerful computers, radar engineers turned the algorithms compiled by people like Donald Kerr, Lamont Blake, Bean and Dutton, and others into convenient software models to be used by radar engineers, evaluators, and mission planners. Recently, the National Air Intelligence Center (NAIC), at Wright-Patterson Air Force Base, began developing AMBER, a general-purpose radar range prediction model they intend to be the most accurate yet.

Tropospheric Refraction

Everyone has observed the apparent bending of spoon sitting in a glass of water, or the shimmering effect of the air over tarmac on a blisteringly hot day. What is seen in both cases results from the bending of light waves as they pass from one medium to a another medium with different indices of refraction. This phenomenon not only applies to light, but all electromagnetic wave energy including the ultra high and higher radio frequencies used in modern radar.

The index of refraction of air depends upon temperature, pressure, and moisture content (humidity). Thus, when a radio wave propagates through the troposphere, a layer of atmosphere which extends to a height of approximately 15 km, it experiences a continually changing medium. As might be expected, the index of refraction of air varies somewhat predictably with altitude. Furthermore, it is also governed by weather, geography, time of day, and local climate. Tropospheric refractivity is a complex and largely unpredictable quantity.

For better or for worse, it is exactly that quantity which the radar engineer must predict to accurately estimate how his radar beam will perform at a given time and location. Fortunately, scientists have been studying the troposphere for decades and have not only been able to document the average refractive characteristics of the atmosphere, but have done extensive analysis on the climatological variations as well. For example, Bean and Dutton's climatological research was based on a five-year study (Bean and Dutton, 1966:109), and the NCEP/NCAR Reanalysis Project is based on 40 years of measured data (Kalnay *et. al.*, 1996).

As these and other studies have shown over and over again, the index of refraction on an average decreases exponentially with altitude. The gradient of this decrease again depends upon the temperature, pressure, and moisture content of the air. Fortunately, the air at the surface is a good index of what is happening in the upper air and we can construct a reasonable approximation to the actual profile using the surface index of refraction and the initial refractivity gradient. A radar beam propagating through such an atmosphere will gradually bend towards the earth with a radius of curvature much greater than that of the earth itself. At higher initial elevation angles, the beam bending may be insignificant, but at angles near one or two degrees the bending can be extreme causing height measurement errors of thousands of feet at ranges of a two or three hundred nautical miles. Fortunately, these errors can be predicted with some accuracy.

More generally, various meteorological and climatic effects such as extreme or rapid heating and cooling, sea breezes, thunderstorms and subsidence will cause moisture and/or temperature inversions creating regions of superrefraction in which the radio waves are bent so much they are funneled along the earth's surface for large distances. This funneling is called ducting, and can occur near the surface as well as at higher altitudes when it is referred to as elevated ducting. These ducts create radio holes, regions above (or below) the duct where the radio wave should have reached, but could not because it was redirected away from its expected path. All these effects are known as anomalous propagation, though in many places a troposphere riddled with ducts is more common than the smooth monotonic atmosphere we commonly call standard.

Modeling even the standard (non-anomalous) atmosphere relies on either current atmospheric data at the radar site, or, if that's not available, at least a knowledge of the

local climate and the average conditions that prevail. The anomalous effects can also be approximated, but with less certainty since they change continually.

Problem Statement

The current model used by NAIC implements the basic equations found in Blake (1986:179-188) and gives the option to use either an exponential refractivity profile based on the average measurements for the continental United States or a low-altitude linear approximation to that known as the effective earth approximation or 4/3 earth. Although these approximations are better than no refraction model, they rarely predict the true nature of the atmosphere with any accuracy.

There are several inherent requirements for the improved model desired by NAIC. First, it must be able to predict the radar's height and range measurement error performance with respect to a given target. Second, it must be able to be incorporated into the main AMBER model, which in turn requires well-organized, modular code with thorough documentation, and specifically requested, prototyping done in MATLAB®. Finally, the model is to be geared towards long term prediction. That is, it will be used for hypothetical scenarios, or scenarios that might occur some time in the future without the benefit of real-time weather data from the radar site. However, it is perfectly reasonable to expect to know the location of the site, the time of year, and the time of day the radar will be operating. All these requirements were either explicitly or implicitly specified by NAIC.

This third requirement suggests a model based on climatology. That is, the refractivity profile used must reflect the average conditions for the geographic location of

the radar, the time of year, and the time of day. No long-term prediction model could make use of day-to-day (synoptic) weather phenomena since those are in no way predictable. The model should, if possible, be able to take into account both the smooth, monotonic characteristics of the standard atmosphere and the anomalous propagation conditions associated with ducting, assuming enough climatological knowledge is available. At first, one might dismiss the possibility of being able to predict ducting using climatological information, but we can at least draw statistics from historical data with respect to the chances of a duct occurring and its average characteristics. So ducting also should be taken into account.

Of course, this is not the first time atmospheric refraction has been modeled using data other than the standard atmosphere. The Naval Command Control and Ocean Surveillance Center (NCCOSC) in San Diego in 1976 (Hitney and Richter, 1976) described the first of their models, Integrated Refractive Effects Prediction System (IREPS). The upgrades, Engineering Refractive Effects Prediction System (EREPS) (Patterson, 1994) and, most recently, Advanced Refractive Effects Prediction System (AREPS) (Patterson, 1998) have followed. AREPS uses a combination of geometrical optics (ray-tracing) and a model known as the electromagnetic parabolic equation to calculate power loss across a range-height field (Hitney & Richter, 1976, Patterson, 1998). AREPS accepts a variety of data input methods including direct user data entry, and an extensive (370 stations worldwide) climatological database put together by the Navy in 1987 (Patterson, 1987). In 1982, Abel, *et. al.*, described their model RAYTRA (short for Raytrace), a comprehensive raytracing model which is particularly useful for point-to-point calculation, unlike the others which provide loss predictions over a whole

range of ranges and heights. Another parabolic equation model, the Tropospheric Electromagnetic Parabolic Equation Routine (TEMPER), developed by Johns Hopkins University Applied Physics, and based on the work of Ko, Sari and Skura (1983), some advanced techniques to more accurately model anomalous conditions in the atmosphere. Another model developed at the NCCOSC (then the Naval Ocean Systems Center) is VTRPE, a third parabolic wave equation-based model developed by Frank Ryan (1991). All of these models have been tried and tested and each, to a more or less extent, is available for use. Of course, none is designed to be integrated into AMBER and only RAYTRA is wholly concerned with point-to-point height and range calculations.

The problem, then, is to develop a customized model of atmospheric refraction which will calculate the height and range measurement errors for a given radar location, time of year, time of day, elevation, and a given target height, range, and azimuthal bearing from the radar. The model should rely on climatologically-based refractivity data, and use either an existing model/algorithm or, if necessary, develop a new one.

II. Literature Review

The nature of microwave refractivity and its governing atmospherics is a complex subject. As with any real system, the factors affecting the turbulent troposphere must be prioritized and studied according to the amount of influence each has, using idealizations where necessary. Hence, this chapter can not be exhaustive. Instead, it highlights information appropriate to the modeling presented in the next chapter. First, simple refractivity and anomalous refractive behavior is described. Next, the effect of refractivity on propagation of microwave radiation is presented, including some of the raytracing mathematics used to predict beam bending. Following that is a discussion of the major meteorological and climatic factors that influence refractivity. Finally, to illustrate the effect of these factors, a brief survey of world climates is included.

N-Refractivity

A canoe paddle is dipped into the water and it seems to bend. The thirsty desert traveler peers vainly at the pools of water on the horizon, only to find he has been looking at a mirage. The distortion of light that is observed in both cases is caused by a gradient, either discrete (as in the former case above) or continuous (as in the latter), in the electromagnetic properties of the media through which the light travels. These electromagnetic properties, specifically, the dielectric constant, ε, and permeability, μ, affect the speed at which electromagnetic (E-M) waves propagate. To wit, the ratio of

the speed of the electromagnetic wave in a vacuum to the speed of electromagnetic energy in the medium is given by

$$n = \frac{c}{v} = \sqrt{\mu\varepsilon} \quad , \tag{2-1}$$

where n is commonly known as the *index of refraction*. Since n in air is approximately 1.0003, a more convenient representation has been adopted, that is

$$N = (n-1)*10^6 \quad , \tag{2-2}$$

where N is called the *refractivity* of the medium.

The simplest way to understand how a refractivity gradient causes an E-M wave to bend is by considering an interface between two media of differing refractivity. As the wavefront approaches the interface at some oblique angle, the portion of the wavefront that reaches the second medium first will either speed up or slow down depending on which medium has greater refractivity. This speed differential in the wavefront will cause it to pivot at the interface, much like a tractor does when the brake is applied on one side or the other. The result is an apparent bending of the wave as it enters the new medium. This bending is governed by Snell's Law of Refraction which is put to direct use in the later section on raytracing.

The earth's atmosphere, of course, does not consist of two homogeneous media, but of a mixture of various gases with combined pressure, temperature, and water vapor content that change with time, altitude and horizontal distance. To study radio beam bending in some local area, however, it is reasonable to ignore the horizontal variation of these atmospheric properties and consider only how they vary with height at a given time. This assumption is convenient and, in truth, necessary to limit the complexity of the

problem to within practical bounds (Kerr, 1951:46). As it turns out, the refractivity of air is defined by (Kerr,1951: 13; Bean and Dutton, 1966: 7)

$$N = \frac{77.6}{T}\left(p + \frac{4810e}{T}\right) \tag{2-3}$$

where T is temperature in Kelvins, p is pressure in millibars, and e is the partial pressure of water vapor in millibars. Although sources differ somewhat with regard to the value of the constants, these, given by Smith and Weintraub, are in widespread use (Bean and Dutton, 1966: 7, Smith and Weintraub, 1953). Further, this formulation of N is accurate for frequencies up to at least 24 gigahertz (Bean, 6). Since most, if not all, ground-based radars operate between the HF (3-30 megahertz) and C (4-8 gigahertz) bands, and most airborne radars in the X (8-12.5 gigahertz) and Ku (12.5-18 gigahertz) bands (84th Radar Evaluation Squadron, 1998: 83-87), this limitation is acceptable. Caution may be necessary when working with some of the newest ground search and terrain avoidance applications for which Ka (26.5-40 gigahertz) and millimeter-wave bands are being exploited.

Using a small weather set called a *radiosonde* that is carried aloft by balloon, scientists measure pressure, temperature, and water vapor at any desired levels up through the atmosphere to precisely determine the actual profile. Radiosonde measurements have shown refractivity generally decreases exponentially with altitude. Such a gradient causes a radio wave to bend downwards, but with a radius of curvature much greater than that of the earth's surface, eliminating the possibility of the wave returning to the earth. Typical behavior of the refractivity profile can be observed readily in the sample data for Buffalo, NY shown in Figure 2.1.

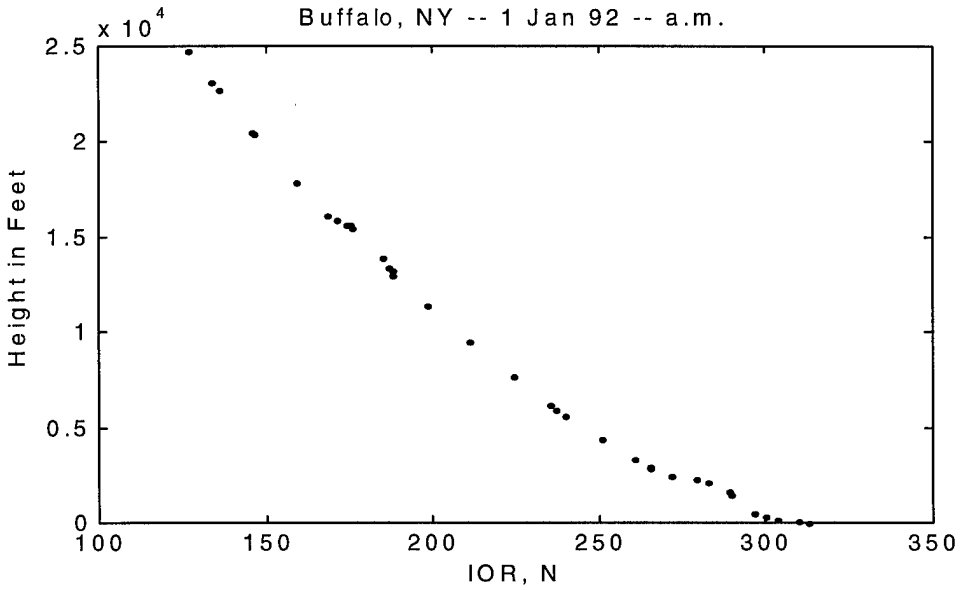

Figure 2.1 Sample *N* Profile Calculated from Radiosonde Data in the National Climatic Data Center (NOAA) Database.

Several techniques have been developed to mathematically approximate this standard refractivity profile. The traditional method used by radar engineers for quick calculations is the effective earth radius, or 4/3-earth approximation. This model, originally proposed by Schelleng, Burrows, and Ferrell (1933) is obtained by straightening the curved path of the radio waves without changing the height of the wavefront at any point along the path. The effect of this distortion is to also partially flatten the earth's surface until it has a larger radius than actual (see Figure 2.2). The *effective earth radius* is defined by

$$a_e = ka \tag{2-4}$$

where a is the actual earth radius and

$$k = \frac{1}{1 + \frac{a}{n}\frac{dn}{dh}\cos\theta} \quad , \tag{2-5}$$

where θ is the *takeoff angle* of the radar beam. Setting

$$\frac{dn}{dh} \equiv -\frac{1}{4a} \tag{2-6}$$

we get $k = 4/3$, which is the nominal value used for standard refraction. Further we can calculate the refractivity at any height using the refractivity at the surface, N_0, and the height above the earth, h:

$$N = N_0 - \frac{h}{4a} 10^6 \tag{2-7}$$

This linear approximation (Bean and Dutton, 1966: 56-58) to what really happens in the troposphere is accurate to about 10,000 feet. Above that it departs significantly from reality as shown in Figure 2.3.

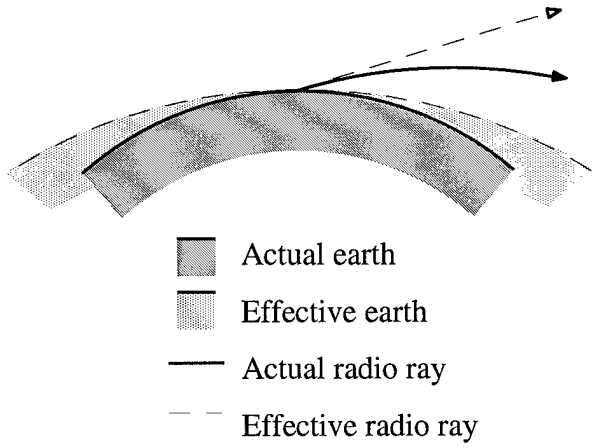

Figure 2.2 Effective Earth Approximation

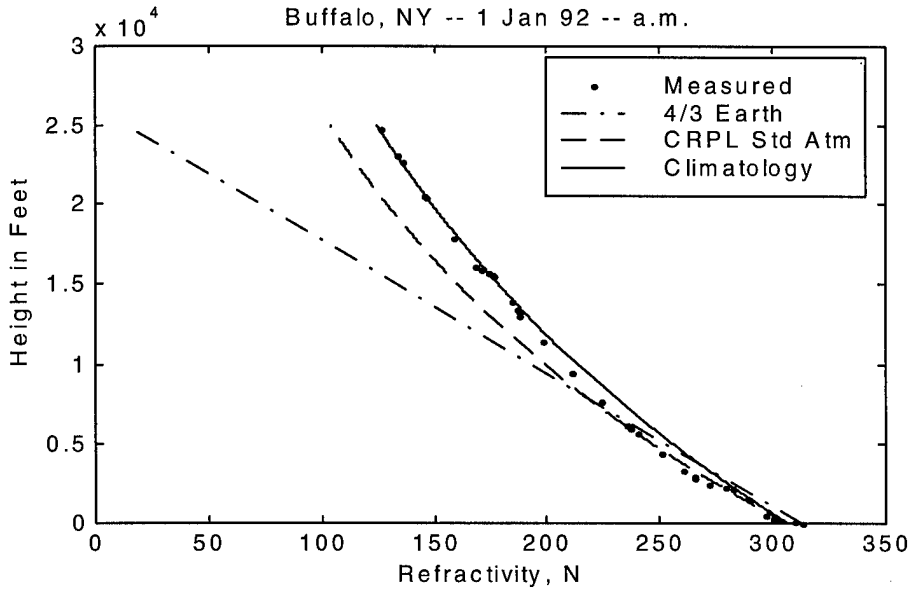

Figure 2.3 Three standard models overlaying measured data: 4/3 Effective Earth Radius model, Single Exponential Model with gradient determined using CRPL Standard Atmosphere, and Single Exponential Model with gradient drawn from climatological studies

The next model more closely approaches the exponential nature of the N-profile. In this one, the surface refractivity, N_S, and the initial gradient up to 1000 meters above the surface, ΔN, are used to calculate a single exponential distribution of N:

$$N = N_S \exp\{-c_e(h - h_S)\}, \tag{2-8}$$

where

$$c_e = \ln\frac{N_S}{N_{1km}} = \ln\frac{N_S}{N_S + \Delta N}. \tag{2-9}$$

Values for N_S may be readily obtained from surface measurements or from climatology studies, that is studies that investigate the average values for a particular location during a particular time of year. Lacking this sort of information, one can simply use the value generally considered to represent average conditions in the U.S., N_S=313 (This would

correspond to k=4/3 in the linear model). Similarly, ΔN may be derived from radiosonde measurements, or in some cases, climatology; however, this value may also be calculated from N_S using,

$$-\Delta N = 7.32 \exp\{0.005577 N_S\} \ . \tag{2-10}$$

Equations (2-8), (2-9), and (2-10) are collectively known as the Central Radio Propagation Laboratory Exponential Reference Atmosphere (Bean and Thayer, 1959). Bean and Thayer obtained this last equation after analyzing 6-year means for 45 U.S. weather stations representing all kinds of climatic conditions. Though not as accurate as a local, seasonal mean, this relationship is a good approximation and is handy when no data is available for the upper air. Figure 2.3 illustrates the exponential profiles, one using CRPL Reference Atmosphere and the other using climatology averages for the local area and time of year.

Further accuracy in modeling standard refractivity may be accomplished using the *bi-exponential*, or as it is commonly known today, the *tri-exponential* model, described thoroughly in Bean and Dutton (1966: 311-322). Refractivity, N, can be considered to be composed of a *dry term*,

$$D = \frac{77.6P}{T} \tag{2-11}$$

and a *wet term*,

$$W = \frac{3.73 \times 10^5 e}{T^2} \tag{2-12}$$

which combine to give,

$$N(h) = D_0 \exp\left\{-\frac{h}{H_d}\right\} + W_0 \exp\left\{-\frac{h}{H_w}\right\} \qquad (2\text{-}13)$$

where D_0 and W_0 are the dry and wet terms, respectively, at the surface; h is the height above the surface; and H_d and H_w are the scale heights of D and W, respectively. The scale height is, in each case, the height at which the value of the atmospheric property has decreased to 1/e of its surface value. The primary advantage of the tri-exponential model is that the contributions of the partial pressure of water vapor content and the dry pressure can be examined separately to obtain a clearer understanding of the makeup of the atmosphere. To illustrate, Bean and Dutton (1966: 312) included the following table, which includes typical values for three distinct climate types:

Table 2. 1 Typical average values of the dry and wet components of N

Station and Climate	D_0	W_0	N_0
Isachsen (78° 50' N), arctic.....	332.0	0.8	332.8
Washington, D.C. (38° 50' N),	266.1	58.5	324.6
Canton Island (2° 46' S), tropic.....	259.4	111.9	371.3

In the cold, dry arctic, the dry component makes up the vast majority of N_0, but in the tropics, where humidity is high, the wet term makes up a much greater portion of the total refractivity. Hence, this model is particularly useful for climatological studies of N.

The preceding models are predicated upon the atmosphere having a smooth, well-behaved, monotonically decreasing index of refraction. Though it may be tempting to regard this sort of atmospheric behavior as "normal," use of this particular term has been avoided so far for the simple reason that standard refraction is, in many cases, not the norm. There are many places and seasons during which refractive anomalies have a much

greater influence upon the bending of radio waves than does the pure exponential distribution.

To more easily observe anomalous behavior, it is necessary to introduce a new term, the *modified index of refraction*,

$$M = N(h) + (h / a_e)10^6 \tag{2-14}$$

with a gradient,

$$\frac{dM}{dh} = \frac{dN}{dh} + \frac{10^6}{a_e} \tag{2-15}$$

where h is height and a_e is the radius of the earth. To understand the physical significance and usefulness of this parameter, consider that the M-gradient, dM/dh, goes to zero at any altitude at which a wave launched horizontally travels a curved path that is concentric with the surface of the earth. In a standard atmosphere, M will increase monotonically and smoothly as shown in the modified version (Figure 2.4) of the now familiar Buffalo profile. More generally, however, meteorological and climatic conditions will combine to alter this simple, pleasing contour.

Though the conditions that cause refractive anomalies are discussed in a later section, it is appropriate here to understand the fundamental types of irregularity. Kerr (1951: 14,15) classifies non-standard refractivity characteristics into two categories: A layer in which the M-gradient is greater than standard throughout is termed substandard because radio frequency propagation in a sufficiently thick substandard layer is usually poorer than expected. Similarly, a layer with gradient less than standard is called

superstandard, because propagation performance in a deep enough region of this type is generally better than expected. Note that whether a layer has an *M*-gradient between zero and standard, or an *M*-gradient less than 0, it is always labeled superstandard; however, the condition leading to a negative *M*-gradient is more strictly termed an inversion. Figure 2.5 illustrates idealized *M*-profiles combining the standard profile with the chief anomalies.

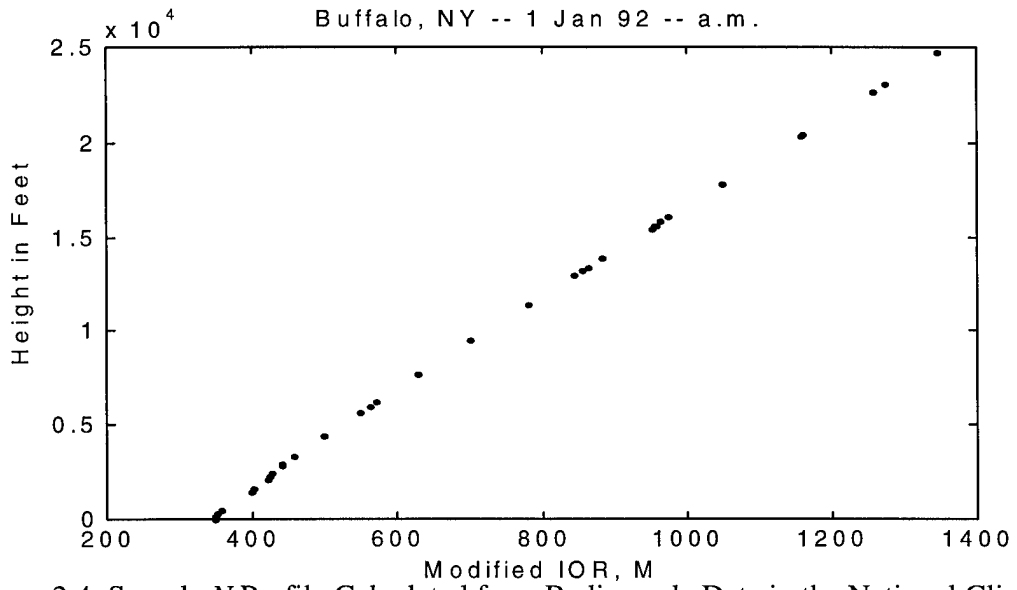

Figure 2.4 Sample *N* Profile Calculated from Radiosonde Data in the National Climatic Data Center (NOAA) Database.

Of course, this description of *N*- and *M*-profiles is only half the story. Of central importance to this thesis is exactly how microwave radiation is refracted by these various conditions in the troposphere.

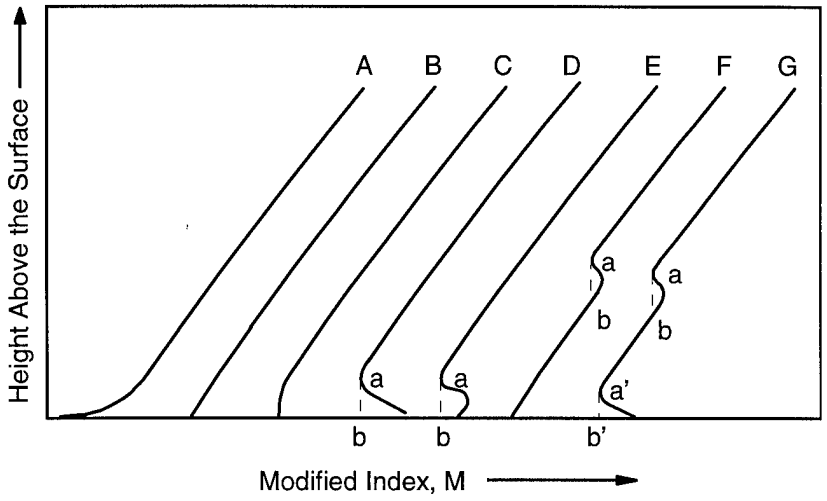

Figure 2.5 Idealized modified index profiles: (A) Substandard surface layer; (B) profile for standard refraction; (C) superstandard surface layer; (D) superstandard surface layer with surface duct; (E) elevated superstandard surface layer with surface duct; (F) elevated superstandard layer with elevated ducts; (G) surface and elevated superstandard layers with both surface and elevated ducts. In all cases the duct extends from *a* to *b* and from *a'* to *b'*. (Kerr, 1951: 14)

Tropospheric Refraction of Microwave Radio Waves

In free space electromagnetic energy travels in a straight line. In fact, the same is true for any perfectly homogeneous medium. However, when the electrical and magnetic properties along the path begin to change, segments of the wavefront begin to travel at different speeds causing the wavefront to change direction.

Consider, as the simplest case, a wavefront approaching at an oblique angle the boundary between two homogeneous media as in Figure 2.6. Snell's law,

$$\frac{n_1}{\cos\alpha_2} = \frac{n_2}{\cos\alpha_1}, \tag{2-16}$$

predicts that the wavefront will turn towards the normal when passing into a medium with higher index of refraction. This is what happens in the case of a single, discrete

change in n. If the index of refraction continues to change stepwise at equally spaced intervals, the wavefront will undergo a series of direction changes. Further, if the spacing between steps is reduced to a differential distance and the index of refraction step turned into a gradient, the path the wave follows will become a smooth curve. This is what happens in the troposphere.

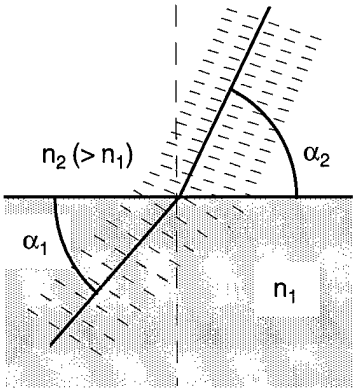

Figure 2.6 Simplest Case of Refraction

The different classifications of refractivity gradient discussed in the previous section lead to different wave propagation behaviors as shown in Figure 2.7. A substandard refractivity gradient causes the electromagnetic wave path to bend upwards. Standard refraction causes results in a path that bends down, but with a radius of curvature considerably greater than that of the earth. Hence the beam will not return to earth. Similarly, superstandard refraction will cause the beam to bend down, but with a smaller radius of curvature. These three types of bending are shown again in Figure 2.8, except that here the earth has been flattened, changing the apparent curve of the rays. When the radius of curvature is small enough to cause the elevation angle of the

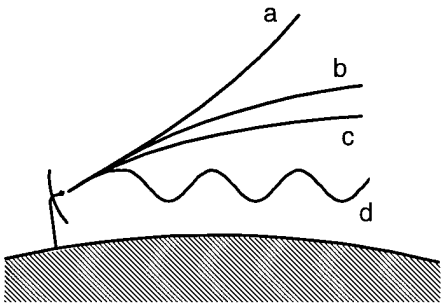

Figure 2.7 Four categories of refractive behavior: (a) subrefraction, (b) standard refraction, (c) superrefraction, (d) superrefraction with ducting

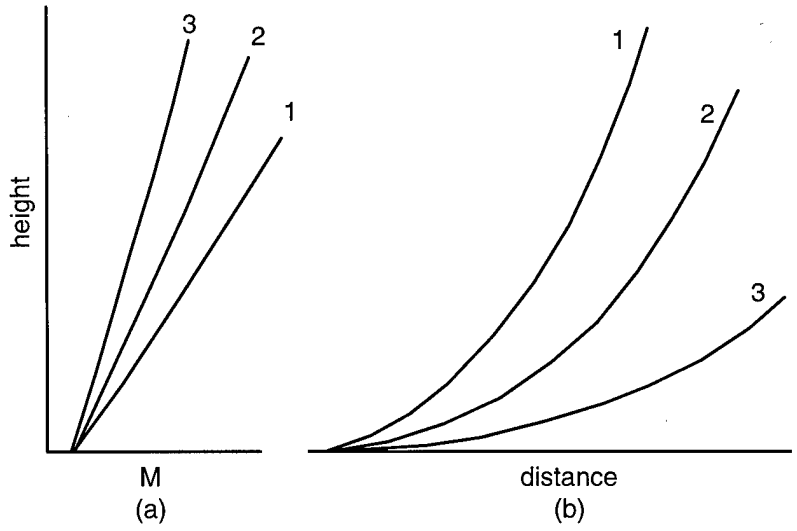

Figure 2.8 (a) 1. Substandard, 2. Standard, 3. Superstandard profiles; (b) 1. Substandard, 2. Standard, 3. Superstandard bending

beam to become zero or negative with respect to the local tangent, the anomalous form of propagation know as trapping, or ducting, can occur. A radio beam trapped in a duct can be funneled along parallel to the earth's surface for great distances, often farther than it would otherwise be able to travel under normal line-of-sight conditions. This said, ducting can occur at various altitudes and for a variety of reasons. Fundamentally, a

particular duct can be classed as one of two types: If it occurs because of an inversion at the surface, it is called a *surface duct*, or *ground-based duct*; if it is produced by an inversion some distance above the earth, it is called an *elevated* duct (see Figure 2.5). Each type is constructed and behaves differently from the other.

Recall from the previous section that a horizontal ray path is caused by an vanishing M-gradient. If the M-gradient goes negative, the ray will be bent down towards the earth. When the initial slope (i.e. near the surface) of the M-profile is negative, the result is a surface duct (see Figure 2.9). If the initial elevation angle of a particular ray launched from ground level is low enough, the beam will be bent back to the earth. Depending on the electromagnetic characteristics of the ground, the beam may be reflected only to be bent back and reflected again. In this way, the energy can be funneled along the surface for great distances. Field theory can account for this behavior using principles similar to those used in the analysis of waveguides. Kerr (1951: 18-21) determined, using waveguide theory, the maximum wavelength able to be trapped by a surface duct. It turns out the limiting factor is duct height:

$$\lambda_{MAX} = 0.014 d^{3/2}, \tag{2-17}$$

where λ_{MAX} is the *maximum trappable wavelength* in centimeters, and d, in feet, is the thickness of the layer with negative dM/dh. Hence, any surface duct higher than 500 feet will trap most microwave frequencies.

If the negative M-gradient occurs at some altitude above the surface, an elevated duct is formed (see Figure 2.10). For the most part, only those rays originating inside the duct may be trapped. The only exception is when a ray is launched above the top of the

duct at a critical angle below the horizontal. At this angle, the ray can be trapped by a very small, hence unstable, trapping layer at the top of the duct. Any other ray entering from the outside will only have its course altered by the duct. Rays launched from inside the duct may or may not be trapped, again depending on their elevation angle. A ray with a steep enough elevation angle will not be bent sufficiently to be trapped before it escapes the duct (Livingston, 1970: 105-114).

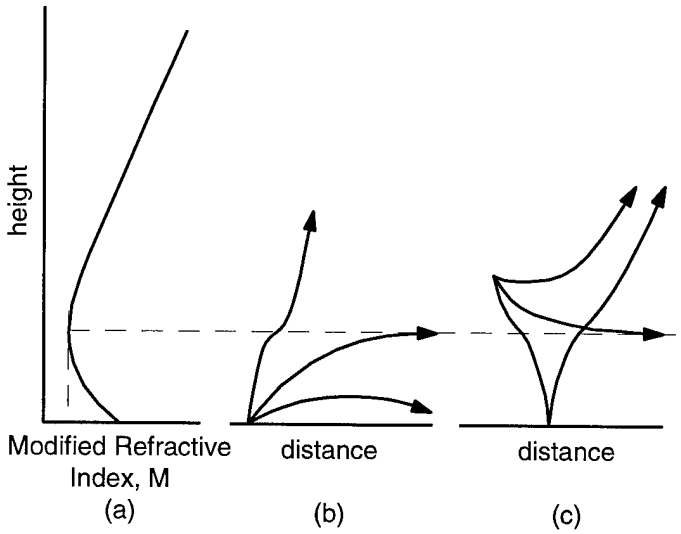

Figure 2.9 Surface duct. (a) typical profile, (b) paths of rays launched into the duct from the ground, (c) paths of rays launched from above the top of the duct (adapted from Livingston, 1970: 109)

Although the calculations involved in modeling ducting involve special techniques, we may calculate the tamer refractive behavior with considerable accuracy using the techniques of *geometric optics*, more commonly known as *raytracing* (Kerr, 1951: 41). A sister science, physical optics, based on Maxwell's equations, is also useful, but is more

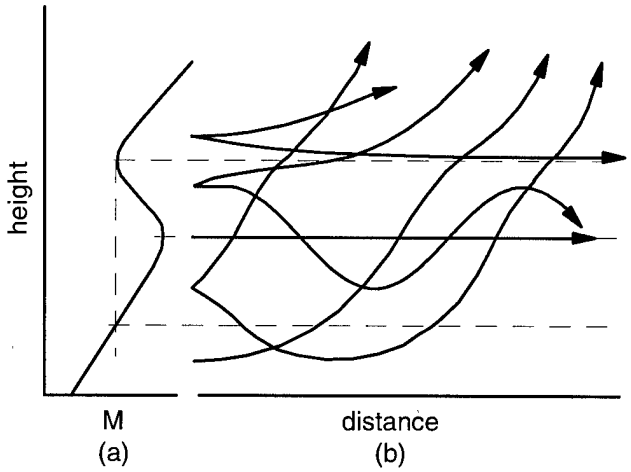

Figure 2.10. Elevated duct. (a) profile, (b) paths of rays launched at various angles both within and outside the duct (adapted from Livingston, 1970: 111-114)

often employed to determine the power losses associated with refraction. Since the goal of this thesis is to more accurately predict height and range errors, the geometrical approach will suffice as long as certain limits are kept in mind and taken into account. First, the refractive index must not vary appreciably in one wavelength; and second, neighboring rays must remain close to parallel within one wavelength (Kerr, 1951: 54), i.e. they cannot cross. It follows that these methods become more and more accurate as frequency increases. Additionally, to properly use Snell's Law, we must consider the atmosphere as a series of differentially thin spherical shells--a stratified model; and the *N*-gradient must only vary with height. Assuming these limits are satisfied, we can use the following form of *Snell's Law of Refraction* (adapted from Kerr, 1951: 48-49):

$$(a + h_1)n_1 \cos\alpha_1 = (a + h_2)n_s \cos\alpha_s \qquad (2\text{-}18)$$

where a is the earth's radius, h_1 and h_2 are the upper and lower boundaries of a given shell, n_1 and n_2 are the indices of refraction at the shell boundaries, and α_1 and α_2 are the elevation angles of the ray at the shell boundaries (Figure 2.11).

To calculate the bending, and more specifically (for the height/range error application) the location of the endpoint of the ray, we must sum the contributions of all the shells to the overall bending. So, knowing the 1) initial takeoff angle, 2) the height increment, and 3) the index of refraction as a function of height, we begin calculating the

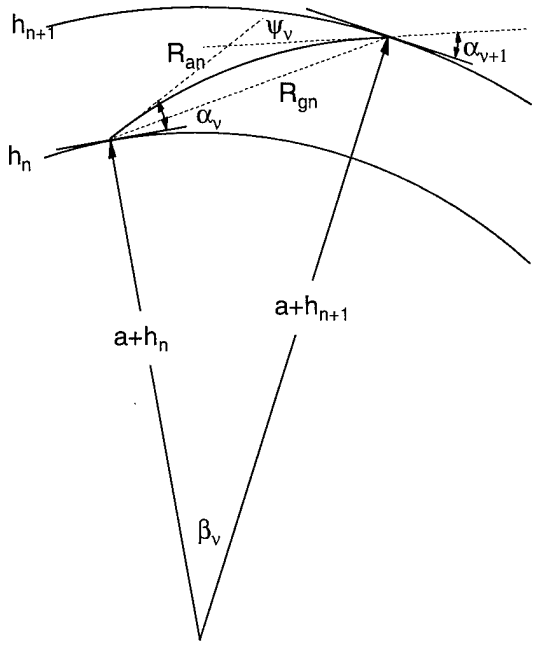

Figure 2.11. Fundamental raytracing geometry for refraction through a single shell (adapted from Bean and Dutton, 1966: 50)

effect of the first layer. First, we use Snell's Law (2-17) to solve for α_2, the elevation angle at the upper boundary of the layer. Next we calculate the total bending, ψ_1, through the layer, using a relationship derived by Weisbrod and Anderson (1958; Abel, *et. al.*, 982: 16),

$$\psi_1 = \frac{2(n_1 - n_2)\times 10^6}{\tan\alpha_1 + \tan\alpha_2} \quad . \tag{2-19}$$

Finally, the *subtense*, β_1, is calculated using the following formula (Abel, *et. al.*, 1982: 16),

$$\beta_1 = \psi_1 + \alpha_2 - \alpha_1, \tag{2-20}$$

which can be derived using the quadrilateral defined by the angles β, $\alpha_1 + 90°$, $180° - y$, and $90° - \alpha_2$. Then we simply sum the subtenses,

$$\beta_{total} = \sum_{l=1}^{L} \beta_l \tag{2-21}$$

where L is the total number of layers, to find the subtense between the ray starting and ending points. This value, along with the height of the ray ending point and the Law of Cosines, can be used to calculate the geometric (actual) range, R_g, from the ray starting point to its ending point (Abel, et. al, 1982: 16):

$$R_g = \sqrt{(a+h_i)^2 + (a+h_f)^2 - 2(a+h_i)(a+h_f)\cos\beta}\,, \tag{2-22}$$

where h_i and h_f are the initial and final heights, respectively. Further, the length of the path itself, known as the apparent range, R_a, can be approximated using the individual layer subtenses, and boundary heights to calculate the geometric range traversed within a layer, and summing:

$$R_a = \sum_{l=1}^{L} \sqrt{(a+h_l)^2 + (a+h_{l+1})^2 - 2(a+h_l)(a+h_{l+1})\cos\beta_l} \tag{2-23}$$

These calculations may be applied consistently with the raytracing limitations defined above. It should be noted that an alternate and, in fact, more succinct formula for R_a is

derived in Blake (1986: 180-182) and other places. The Abel method, however, better lends itself to the estimation and iteration process used to do point-to-point tracing.

Using these techniques in the presence of ducting, the most interesting refraction anomaly, would seem not to be sanctioned because a refractivity inversion generally violates the first raytracing condition, that is, the gradient may not change appreciably in one wavelength. However, the Navy, in the RAYS routine of their EREPS model (Patterson, 1994: 118-121), applied raytracing to the duct problem. The way they constructed the ducting profiles, along with further development of the methods used to model standard refractivity, are described and applied in chapter 3.

In order to predict the refractivity profiles that are the core element of the raytrace model, it is necessary to understand what affects tropospheric refractivity gradient and how.

Meteorological Phenomena that Affect the Refractivity Profile*

To understand the various phenomena that control tropospheric refractivity it is necessary to establish reference, or baseline conditions to which all other circumstances can be compared. For this purpose, scientists have defined a column of air that is completely mixed, or stirred, as homogeneous. In such vertically homogeneous air, the vertical variation in temperature is due solely to the change in pressure, and water vapor concentration is independent of height. Specifically, the decrease in temperature with altitude, or lapse rate, is adiabatic; that is, it represents the temperature decrease of air

* The material in this section, unless otherwise marked, is taken from Kerr, 1951: 181-293.

which rises and cools adiabatically. Although water vapor content is independent of height, the vapor pressure, dew-point, and wet-bulb temperature do vary with height because they depend upon changes in the total pressure of air. Because the temperature lapse rate is adiabatic, the air will not move vertically unless it is acted upon by some external influence. Hence, vertically homogeneous air is said to be in neutral equilibrium. Likewise, an air column with temperature that decreases with height more slowly than the adiabatic lapse rate is said to be in stable equilibrium and an air column with temperature that decreases faster than adiabatic is said to be in unstable equilibrium. The vertically homogeneous air standard is particularly useful because it is the only simple distribution that occurs often, particularly at lower altitudes. When it does occur, the layer is bounded on the top by the altitude at which condensation occurs (cloud height--on the order of 10,000 feet), and on the bottom by the top of the surface layer of air in which moisture and heat are exchanged with the ground (approximately 50 feet). Furthermore, its refractivity characteristics are close to the standard atmosphere. Drawing an analogy to 4/3 earth, well-mixed air would be approximately 6/5 (or 3.6/3) earth.

To arrive at this homogeneous state, air is mixed by three main processes, convection, eddy turbulence, and molecular diffusion. Convection, the most broad-ranging process, occurs when there is a heat source increasing the temperature of the air at the bottom of the column. When this happens, the heated air expands, becoming more buoyant, and begins to rise. Cooler air then moves horizontally to take the place of the rising air. Thus, a vertically circular air flow is established which stabilizes if an adiabatic lapse rate is achieved. In this way, the large parcels of air throughout the

column are distributed uniformly. Eddy turbulence acts within the flowing stream of air, causing random swirls and eddies to arise which distort the shape of smaller parcels of air within the stream. Molecular diffusion is the only process that does more than simply move parcels of air around. Taking place at the molecular level, it is the process by which molecules in the air (made up of water vapor and other gases) move from one parcel of air to another due to differences in concentration. It is relatively slow, but catalyzed by eddy turbulence, it is the means by which the smaller parcels of air become well-mixed. Hence, these three processes, spurred by a variety of forces, mix the air to produce a vertically homogeneous air column (Livingston, 1970: 97-98).

With vertically homogeneous air defined, we can discuss conditions that cause departures from this baseline. Perhaps the most widespread is heating from below, which can arise, for example, when the ground is heated in the morning as the sun comes up, or when a cool air mass blows out over a warm sea. The air column, then, initially in neutral or unstable equilibrium, consists of a thick lower region of cool air (arising, in the first example, from nocturnal cooling of the surface, or in the second example, the initial temperature of the cool air mass), above which the air is warmer, but decreasing in temperature adiabatically. The process starts at the surface, where the air is heated until it rises in patches through the colder air around it. As it rises, heavier, cooler air rushes in to be warmed in turn. Thus, convection develops. The warmed air rises through the cooler air until it reaches warmer air above. In this way, three regions are formed: a thin layer near the surface in which the lapse rate is greater than adiabatic, but in which turbulence is small because the air parcels are just beginning to accelerate; a thick, highly

turbulent central layer through which the rising air is accelerating rapidly; and the upper region that is stable. The process is illustrated in Figure 2.12, where the numbered curves indicate successive stages of the process either as the sun rises (as in the first example) or as the cool air mass blows farther out over the warm sea (as in the second example). The intensity of the effects of heating from below is moderated if there is cloud cover that reduces the surface heating, or winds that create so much surface turbulence they override the convective turbulence. Often, these moderating factors eliminate the homogeneous central layer altogether.

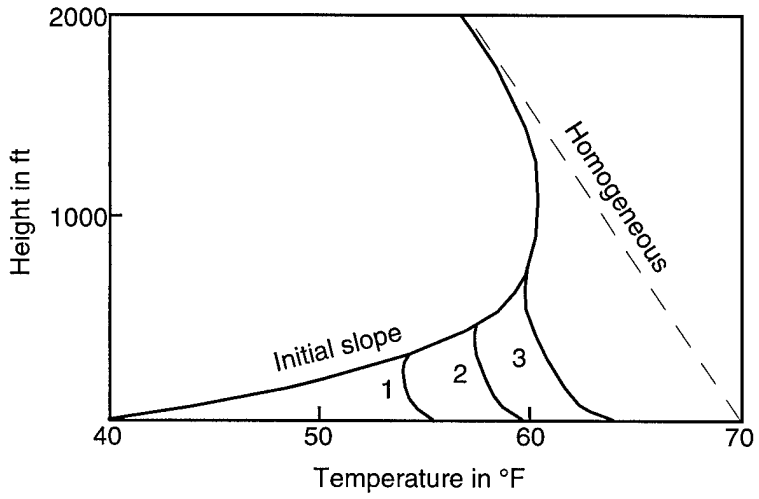

Figure 2.12. Successive temperature distributions due to heating from below. Heights and temperatures are typical, but can vary widely (adapted from Kerr, 1951: 220)

Under typical conditions, however, the central layer will be well mixed with the concomitant standard *N*-profile. The stable upper layer usually has a water vapor lapse that causes it to be superstandard, although occasionally there may be enough of a water vapor inversion to make it substandard. The surface layer is superstandard if the surface

is water or wet ground and substandard if it is dry ground. Over water especially, a large lapse in humidity often occurs resulting in an *M*-inversion and a duct. Heating from below is the foremost cause of change in neutral or unstable air.

In stable air, the primary change agent is cooling from below. This process occurs after nightfall, as heat from the air diffuses to the surface directly below it, or it can happen as a warm air mass is blown over a cool sea. Unlike heating from below, the air is not vertically turbulent, but becomes more stable. Since the air near the surface is cooled, it becomes even more concentrated and even less buoyant than it was. Further, the vertical movement that does take place is not upwards as with heating from below, but downwards, causing the temperature and humidity gradients to be concentrated near the surface. Because of this downward flow of air, the overall effects don't go as high as with heating from below, but because the cool air is building up in the bottom layer, surface inversions tend to be deeper (often, several hundred feet), and, as time progresses, they get continually deeper. Over water or wet ground, significant humidity inversions develop that can balance out the temperature inversions. Under these conditions, then, the surface layer may be superstandard, standard, or substandard. Over dry ground, the temperature inversion is acting alone, so the surface layer is superstandard. Whether over land or water, strong winds and a small temperature differential between the air and the surface will substantially increase the amount of mixing, reducing the effects of the process on the refractivity profile. Figure 2.13 is a comparison of temperature inversions under conditions of strong winds and small temperature differential, and light winds and

large temperature differential. Thus the effects of cooling from below depend on the surface type, the amount of time elapsed, the wind speed, and the temperature differential.

Another factor, which can affect both heating from below and cooling from below is wind shear. Wind shear is defined as "the variation with height of the horizontal component of the wind velocity" (Kerr, 1951: 234). Shear can be caused by a variation in the horizontal pressure gradient with height, or, more usually, by the influence of friction on the winds at the surface. Because shear causes wind speed and direction to vary with

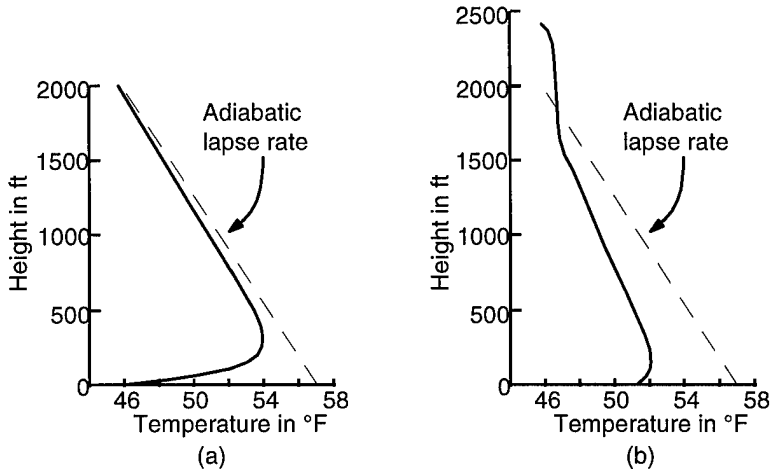

Figure 2.13. (a) Cooling from below with light winds and large temperature differential; (b) Cooling from below with strong winds and small temperature differential (adapted from Kerr, 1951: 231)

height, it can have an effect on the refractivity profile. Consider, for instance, warm, dry land air that is blown out over a cold sea. Normally, higher winds are found at the higher altitudes. So, in a given column of air over the sea, the air higher up took less time to get into position and has been over the sea for less time than the air below. For this reason it is warmer than the air below. This increases the thermal stability of the air column and under typical humidity conditions sets up a superstandard refracting layer. Another

example is that of a cool air mass blown out over a warm sea. For the same reasons, the column becomes less stable and convection is set up resulting in a homogeneous layer that is close to standard. Shear also can alter the *N*-profile over land, especially if there is a marked difference in surface characteristics. The effects are seldom as pronounced as those near the coastline, however.

At this point, at the risk of stating the obvious, it must be emphasized that the overwater modifications in the *N*-profile are never as simple as the examples so far would suggest. Factors such as shear, variations in solar radiation, variations in surface temperature, and, of course, lack of initial homogeneity of the air column, all play a part in the final condition of the air column. While the influences presented above do play major roles, they can not account for all modifications to the *N*-profile.

In addition to the forces acting on and within a particular column of air, we must consider the effects of the large air mass movements within a geographic region. One of these effects is subsidence, which is the sinking of a large air mass from a high to a low level. Subsidence is the result of dynamic causes and is generally associated with high pressure systems. As the air descends, the stable, adiabatic, or unstable nature of the air mass intensifies. Because the subsiding air mass is usually stable, its temperature is usually warmer than the air below. Similarly, the air mass is generally dryer than the air below, since it descended from a fairly high level. These two factors and others work to produce an inversion layer between the sinking air mass and the air below it. This inversion is called a *subsidence inversion*, and almost always contains a superstandard *M*-gradient. Often, there is an *M* inversion, especially over the sea. The base of a

subsidence inversion is determined by the layer of frictional influence near the surface, and can reside anywhere from one to four, or five thousand feet up. The thickness of a subsidence inversion can be several hundred feet or a several thousand feet. Obviously, an inversion this large, under the right conditions, will severely impact radio propagation. Ducting is extremely common near the great high pressure systems that occur over the oceans around the world at about 30 degrees north and south latitude. Near the southwest coast of California ducts occur on an average of 40 percent of the time, and along the coast of Japan, about 10 percent of the time (Patterson, 1994: 16). Additionally, subsidence inversions can also occur on the lee side of mountains.

When large air masses collide horizontally, they form a front. An *air mass*, by definition, is approximately uniform with regard to temperature and humidity. When two air masses traveling horizontally, come into contact with each other, the warmer air mass slides up over the cooler one. The boundary, or front, between the masses is always close to horizontal. Though its slope increases with wind speed, increasing latitude, and temperature similarity, it generally remains somewhere between 0 and 1/25. Because the upper air mass is warmer, there is then always a stable layer at the front, and often there is a temperature inversion. Ordinarily, the water vapor concentration increases with height in this layer, but not always. For this reason, the front may define a superstandard layer, a standard layer, or a substandard layer. Frontal inversions do not lend themselves to generalities. The passing of a front must also be regarded with great care because it nearly always precedes a potentially radical change in weather conditions across the

landscape and over time, which in turn causes the *M*-profile to vary with distance and time.

A frontal boundary is but one of many elements that will affect the horizontal variation of the refractivity profile. Though this thesis is primarily concerned with long term averages and climatological predictions of the vertical variations, the radar engineer must take into account all the local conditions, either current or predicted, to wisely understand how the climatological averages may vary. Consideration of the horizontal gradient is inescapable. Though coastlines probably produce the most outstanding horizontal aberrations, similar, if less intense, phenomena may be found wherever surface characteristics or weather systems change.

None of the forces described above acts independently. There are always larger influences driving theses forces, and while we can rarely predict exactly what weather conditions will occur and exactly what effect they will have on the refractivity profile, we can, by studying climatic trends, determine how geography, topology, diurnal cycles, and seasonal cycles have traditionally impacted the local weather patterns at some time of year and time of day. Here are some of the major climatic effects followed, in the next section, by a survey of worldwide climate types.

Inarguably the most regular and predictable climatic effect is the *diurnal cycle*, that is, the regular procession of day to night and back to day. Assuming no irregular influences, the cycle will proceed something like this. At midday, the atmosphere has been fully heated with all the accompanying convective mixing, so it will be homogeneous. As sunset approaches, the ground begins to cool as the sun's rays become

less and less direct. Cooling from below starts and stratification begins to develop near the surface, but the *M*-profile is probably affected only very little until after sunset. During the night, the surface cools, radiating heat. Much of this heat escapes through the atmosphere, but some of it is absorbed and reradiated by atmospheric gases, especially water vapor. For this reason, the presence of clouds reduces the amount of surface radiation considerably. At this point, cooling from below over water continues pretty much as described in that section. Cooling of the air over land, however, is more complicated both with regard to the rate and amount of cooling, and to how the air above the surface is affected. First, the temperature of land varies greatly, both with time as the night wears on, and topology, if the surface characteristics vary. Temperature variations in water are much less intense. In particular, the temperature and amount of radiation from land depend upon conductivity of the soil, which determines how fast the radiating heat is replaced from below. For example, dry sand is about three times as conductive as dry soil, and wet soil is almost three times as conductive as dry sand. Furthermore, land, unlike water, does not uniquely determine the amount of humidity at the surface, unless the ground is wet. Immediately over water, the air is saturated; but over land humidity can vary greatly. On the other hand, if the land is completely dry, there will be no humidity gradient at all, and the *M*-profile will depend solely upon temperature. Because of the variability of these factors, a variety of *M*-profiles may occur at night. Both superstandard and substandard anomalies may appear both at the surface and aloft. The superstandard behavior may produce ducts that grow in the evening just after sunset, intensify during the night, and dissipate with the sunrise. The most important

consideration, however, is that diurnal anomalies primarily occur at night. In the morning, the sun again warms the earth, heating from below begins, and through convection and turbulent mixing the atmosphere again becomes homogeneous.

The wild anomalous changes in the M-profile that occur during the diurnal cycle are generally more intense during the summer than the winter. There are three primary reasons. First, the ground is typically drier in the summer than in the winter. Since dry ground has a lower conductivity, the surface temperature changes in the summer are more dramatic than in the winter, producing stronger temperature inversions. The second reason is that the water vapor content is usually higher in the warm summer air, resulting in larger humidity gradients. Finally, the cloudiness and strong winds that moderate the diurnal cycle, are more likely to occur in winter than in summer, at least in the temperate latitudes.

Another climatological phenomenon that is widespread enough to be covered separately is the sea breeze. Since many radars operate along the coastline, what happens there is particularly important to understand. Sea breezes arise during the day when warm land air rises and is subsequently replaced by cool sea air rushing in to fill the void. In this way a circulation from sea to land is set up. When the land air has traveled some distance out to sea it subsides, often setting up a subsidence inversion depending upon the humidity distribution. This inversion may result in ducting. Similarly, at night the land cools faster than the sea causing the warm sea air to rise over the cooler land air creating a circulation in the opposite direction called a land breeze. Here again, ducting can occur because of subsidence.

Finally, it must be noted that extensive snow cover, fog, and cloudiness will all act to moderate to some extent the effects described in this section. Snow cover reduces both solar heating of the ground during the day and radiation from the ground at night, especially in the high latitudes. Cloud cover will have a similar effect because it moderates both solar heating and nocturnal radiation. When fog forms, water vapor in the air changes to liquid, reducing the vapor pressure. The humidity lapse that results tends to counteract any temperature inversions that exist, preventing extreme superstandard behavior (Bean and Dutton, 1966: 135).

Climate Survey

While the meteorological effects described in the last section determine the anomalous characteristics of the *M*-profile, the value of *N* at the surface and the initial N-gradient apart from anomalous influences are determined primarily by climate, that is geography and time of year. Based on over two million weather observations taken at 45 weather stations across the continental United States, the average value of refractivity at the surface, N_S, is 313, according to Bean and Thayer (1959). Using Bean and Thayer's CRPL standard atmosphere (2-10), we can calculate the initial gradient, ΔN, to be approximately -41.94. These numbers represent the average. However, seasonal changes and the vast array of topographies across the United States give us surface values that vary widely from these. When the scope of observation is expanded worldwide, the variations become even more expansive.

Bean and Dutton (1966: 89-109) conducted a study of how surface refractivity varies with climate using long terms means of temperature, pressure, and humidity given in the United Nations monthly publication *Climate Data for the World.* They examined five years of records for each of 306 stations worldwide from the period 1949-1958. This section contains a summary of their most significant findings.

Most of Bean and Dutton's conclusions concerned the annual range of variation of surface values of N. N_S varies with the diurnal cycle, with season, and, of course, with topology. Table 2. 2 contains the annual means and ranges of N_S for six different climate types which are defined and typified. From the data presented there, the

Table 2. 2. Characteristics of climatic types (Bean and Dutton, 1966: 103)

Type	Location	Annual mean N_S (N units)	Annual range of N_S (N units)	Characteristics
I. Midlatitude-coastal	Near the sea or in lowlands on lakes and rivers, in latitude belts between 20° and 50°.	300 to 350	30 to 60	Generally subtropical with marine or modified marine climate.
II. Subtropical-Savanna	Lowland stations between 30°N and 25°S, rarely far from the ocean.	350 to 400	30 to 60	Definite rainy and dry seasons, typical of Savanna climate.
III. Monsoon-Sudan	Monsoon--generally between 20° and 40°N, Sudan--across central Africa from 10° to 20°N	280 to 400	60 to 100	Seasonal extremes of rainfall and temperature.
IV. Semiarid-Mountain	In desert and high steppe regions as well as mountainous regions above 3,000 ft.	240 to 300	0 to 60	Year-round dry climate.
V. Continental-Polar	In middle latitudes and polar regions. (Mediterranean climates are included because of the low range resulting from characteristic dry summers).	300 to 340	0 to 30	Moderate or low annual mean temperatures.
VI. Isothermal-equatorial	Tropical stations at low elevations between 20°N and 20°S, almost exclusively along seacoasts or on islands	340 to 400	0 to 30	Monotonous rainy climates.

following observations can be made: Generally, N_S decreases with increasing latitude. Surface refractivity values in purely maritime regions such as the west coasts of North

America and Europe are low and undergo relatively little variation due to the constant onshore advection of cool, moist sea air. Continental areas like central North America generally have surface refractivity lower than the adjacent maritime areas, but with more variation. The variation comes from the changes in radiative heating from day to night, and summer to winter, which are not modified by air from the ocean. Regions similar to the east cost of the United States have a combined maritime and continental influence, in which a variety of air mass types interact to produce a moderate amount of variation throughout the year. Mountainous places generally have lower values of N_S because of the fundamental changes in temperature, pressure, and humidity with altitude. The refractivity variation is typically moderate in the mountains. Larger ranges are found in places like Australia, the African plateau near the Cameroons, and in the Great Basin of the southwestern United States where there are wide ranging temperature variations throughout the year, but relatively little humidity to act as a moderating factor. Some of the largest ranges in the world are found in the African Sudan and in areas influenced by the unique characteristics of the Indian monsoon.

Of course, this has been an extremely broad look at world climate types. Studies of local patterns in a given region would, of course, provide more insight into the refractive effects playing in that area. Indeed, Bean and Dutton (1966: 110-131) include a fairly detailed overview of refractivity in the continental United States that may be of interest to the radar engineer involved in refractivity prediction.

With a detailed knowledge of worldwide climate, a solid grasp of the various forces that can alter the M-profile, and a thorough understanding of the mathematics of N-refractivity and raytracing, one may construct a model that can predict, with some accuracy, how much the atmosphere will bend an electromagnetic radar wave launched into the atmosphere at a given elevation angle. Accuracy, here, is relative and must be compared to what has gone before. Previous radar range performance models have relied on four-thirds earth, or at best, a standard refractive profile based on the United States average surface refractivity value, N_S=313. Climatology and raytracing can put us closer.

III. Methodology

Construction of a refractivity profile depends on how much knowledge there is of the prevailing atmospheric conditions. Over the past 150 years, sailors, scientists and engineers have collected a wealth of climatological data fit for making educated guesses about what atmospheric conditions will be like at a given place and time. A profile built up from this type of data is all that is needed to compute a close approximation to the most direct path from a given radar to a given target on a given day in a particular location.

Specifically, geometric optics (raytracing) is used to calculate the path of a single ray of energy leaving the radar at some takeoff (initial elevation) angle. The only problem is determining which takeoff angle will put the endpoint of the ray on the target. Since the raytrace is not a closed-form solution, there is no way of working backward to the answer. Hence, a trial-and-error iterative approach is employed: First, an initial takeoff angle is estimated and the ray is traced through the atmosphere until it reaches the target height. Next, the subtense of the trace endpoint (i.e. the angle defined by the radar, the earth's center and the endpoint of the trace) is compared with the subtense of the target, and a new takeoff angle is estimated based on the magnitude and direction of the difference. The process is repeated until the trace ends at the target subtense (Figure 3.1).

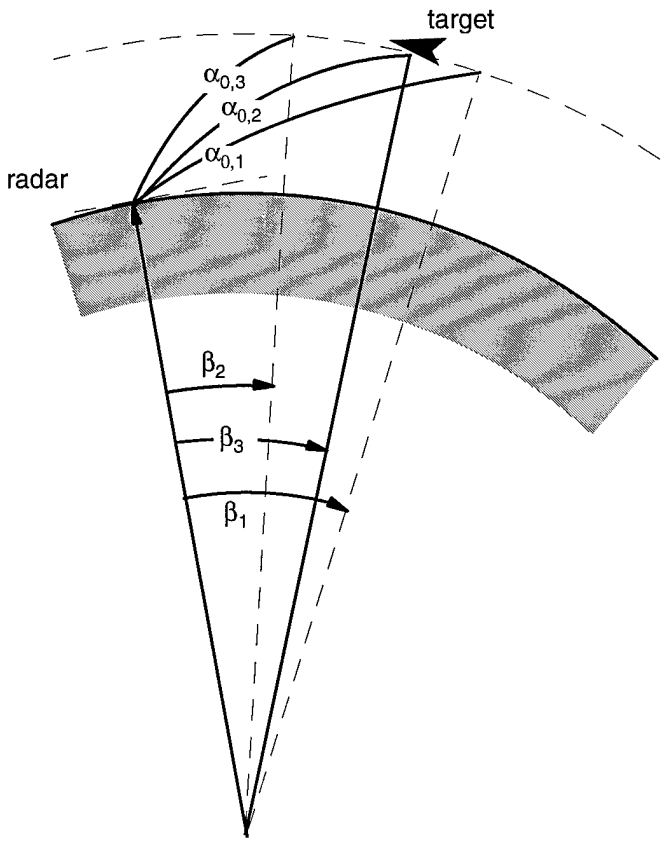

Figure 3.1 Initial takeoff angle, α_1, estimated; trace 1 goes beyond target. New angle, α_2, estimated; trace 2 undershoots. Endpoint of trace 3, using angle, α_3, finds target.

Finally, the initial elevation and the path length (or apparent range) are used to calculate the apparent height, which, when compared with the actual height, yields the height error. Similarly, the trace length (apparent range) compared with the actual geometric (or straight line) range provides the range error.

This chapter details the above process. First, the database is described. Following that is a step-by-step discussion of how the model developed for this project works. Note that throughout the discussion, the symbols used for the variables involved match as

closely as possible those used in the MATLAB® code itself. Also note that the important capabilities and limitations of the model are specifically discussed in Chapter 5, Findings and Conclusions. Also, a complete listing of the MATLAB® source code is included in Appendix A.

Climatology Database

The fuel for this climatology-based radar propagation prediction model is a the Historical Electromagnetic Propagation Condition (HEPC) Database. Compiled by the U.S. Navy, the HEPC database contains statistical climatological data for 921 radiosonde stations distributed worldwide and is an integral part of the Navy's Advanced Refractive Effects Prediction System (AREPS) propagation model. The statistics it contains are derived from two meteorological databases: GTE Sylvania's Radiosonde Data Analysis II, and the National Climatic Data Center's Duct63 database. The former is a "large scale analysis of approximately three million worldwide radiosonde soundings from 1966 to 1969 and 1973 to 1974." The latter consists of mostly marine surface observations spanning 15 years. These observations were taken from ship logs, ship weather reporting forms, published ship observations, automatic buoys, teletype reports, and card decks purchased from foreign meteorological services (Patterson, 1987: 1-3,9).

The HEPC database is public domain, available on the Space and Naval Warfare Systems Center webpage, and is encoded in .dbf format which, with the exception of a header and some delimiters, is ASCII text.

Each record in the database contains the statistics for a single radiosonde station. The first seven fields in a record are station information. The next twelve each contain monthly mean refractivity parameters. The fields are defined as follows (Figure 3.2):

MSQ - Marsden Square containing the station. A Marsden Square is a 10° lat. by 10° long. portion of the Earth's surface

WMO - World Meteorological Organization station number

Name - station name

Inland/Coast - Indicator (L=inland, C=coast)

Latitude - sign is negative for south, positive for north

Longitude - sign is negative for east, positive for west

Station Elevation - above mean sea level (meters)

Monthly Data (one field for each month) - Each contains the following:

Number of 1200Z observations

Number of 0000Z observations

Surface N-unit value

Surface to 1000 meter M-unit gradient

Surface-based duct M-unit gradient

Sfc-based duct optimum height (layer base) (meters)

Surface-based duct thickness (meters)

Surface-based duct M-unit deficit

Surface-based duct trapping frequency (MHz)

Sfc-based duct 1200Z percent occur

Sfc-based duct 0000Z percent occur

Elevated duct M-unit gradient

Elevated duct optimum height (layer base) (meters)

Elevated duct thickness (meters)

Elevated duct M-unit deficit

Elevated duct trapping frequency (MHz)

Elevated duct 1200Z percent occur

Elevated duct 0000Z percent occur

Probability of > 1 elevated duct (%×100)

Probability of sfc-based and elevated ducts (%×100) (Patterson, 1993)

Statistical data on surface conditions and the significant ducting parameters is listed this way for every month of the year for virtually every place in the world inhabited by human beings (and some that are not). Sadly, the database contains only mean values for each parameter. There is no variation data. This omission certainly obscures the true climatological picture, but as no other data set is as complete and usable, the partial view must be accepted.

Each data-element described above is used in CLIMAREF at some point. Indeed, the database is consulted throughout the model, from the initial stages of determining the most appropriate radiosonde station to use, to the construction of the refractivity profile before the final raytracing.

- Each record consists of a header and 12 month-fields:

(Header)

MSQ	WMO	Name	Inland/Coast indicator (L=inland, C=coastal)	Latitude	Longitude	Elevation
062	48354	Udorn Thani, Thailand	L	17.37	-102.80	178

(Jan month field - 1 exists for each month of the year)

105	119	322	120	119	86	172	18	526	4	1	123	2316	121	4	345	41	41	670	134
Number of 1200Z observations	Number of 0000Z observations	Surface N-unit value	Surface to 1000 meter M-unit gradient	Surface-based duct M-unit gradient	Sfc-based duct optimum height (layer base)	Surface-based duct thickness	Surface-based duct M-unit deficit	Surface-based duct trapping frequency	Sfc-based duct 1200Z percent occur	Sfc-based duct 0000Z percent occur	Elevated duct M-unit gradient	Elevated duct optimum height (layer base)	Elevated duct thickness	Elevated duct M-unit deficit	Elevated duct trapping frequency	Elevated duct 1200Z percent occur	Elevated duct 0000Z percent occur	Probability of >1 Elevated Duct (%x100)	Probability of sfc-based and elevated (%x100)

Figure 3.2 Fields contained in one record of the HEPC database

CLIMAREF Detailed Description

CLIMAREF, the model constructed for this thesis, was written in MATLAB®, Version 5.2.0.3084. There are nine modules, or in MATLAB® terminology, "functions." (see Appendix A). The first module calls the other eight and performs various display and plotting functions. This module (and possibly module 2, the input routine) may be tailored or replaced in order to integrate CLIMAREF into a larger application without having to modify the other eight modules.

The remainder of the chapter contains a theoretical description of how CLIMAREF works. While the operation of every module is covered, there is no attempt

made beyond this point to delineate where one module leaves off and another begins. The MATLAB® routines are internally documented fairly well, and are included in the Appendix A.

Initial Data Entry. The input data the model requires are month of operation, *MON*, whether operation will be during the day or night, *DYNT*, the latitude and longitude of the radar, *RLAT*, *RLONG*, the elevation of the radar above ground level, *REL*, the direction the radar is pointing in degrees, *RAZ*, the height of the target above ground level, *THT*, and the range of the target, *TRG*.

Two important qualifications regarding this data must be made. First, all heights and ranges must be converted to kilometers before they are used in the program. The data may be entered in feet or nautical miles, but it must be converted. Second, all heights are measured from ground level, defined as the elevation above sea level of the radiosonde station whose data is used to construct the N-profile. It is assumed the radar will be near enough to the station that surface elevation of the two locations will be fairly similar. If not the, station selected may not be the best station for the purpose even if it is the nearest. More will be discussed on this subject later.

Choosing station(s) to use for calculation. Given the radar latitude and longitude, CLIMAREF finds the ten nearest radiosonde stations to the radar site. The user, given the list, is then prompted to choose the best station for the purpose. To identify the nearest stations, CLIMAREF takes advantage of the Marsden Square method of organizing the stations.

Each radiosonde station in the HEPC database is labeled with a WMO number and a Marsden Square number. The WMO number is simply for identification. The MSQ number, however, locates that station in a square, so to speak, bordered by parallels and meridians evenly divisible by ten, e.g. Dayton is in MSQ 117, bordered by the 30th and 40th parallels and the 80th and 90th west meridians. Further, there are limits to MSQ coverage. There are no MSQs defined north of 80° N or south of 70° S. Within that area, the radiosonde stations are most concentrated near populated areas, especially in the more developed countries.

Using the MSQ numbering rules (Patterson, 1987: 10) and a look-up table of the MSQs adjacent to, and west of, the prime meridian, CLIMAREF determines the number of the MSQ where the radar is located and the number of each of the surrounding MSQs (Figure 3.3). Next, using pointers collected from a reference file called MSQLIST, CLIMAREF identifies all the stations located within those nine MSQs and gathers location data for each station. MSQLIST was created for this project as a quick-reference companion file to the main database.

To determine which stations of those within the nine MSQs are the nearest to the radar, a spherical coordinate system is assumed at the origin of the earth and the position of each of the stations is determined based on the latitude complement, the longitude, and the local earth radius of curvature (Figure 3.4). The latter is calculated (Abel, 1982: 18-19):

$$RC = \frac{A^2}{B(1+C\cos^2\phi)^{1/2}(1+C\cos^2\phi\cos^2\theta)} \quad , \tag{3-1}$$

where,

A = semimajor (equatorial) radius (6378.139 km)

B = semiminor (polar) radius (6356.750 km)

$C = A^2 / B^2 - 1$

ϕ = latitude

θ = radar azimuth

The local radius of curvature is used because the earth more closely approximates an oblate spheroid than a true sphere. Of course, the curve of the local earth surface is the important factor in the path calculations, not the actual radius.

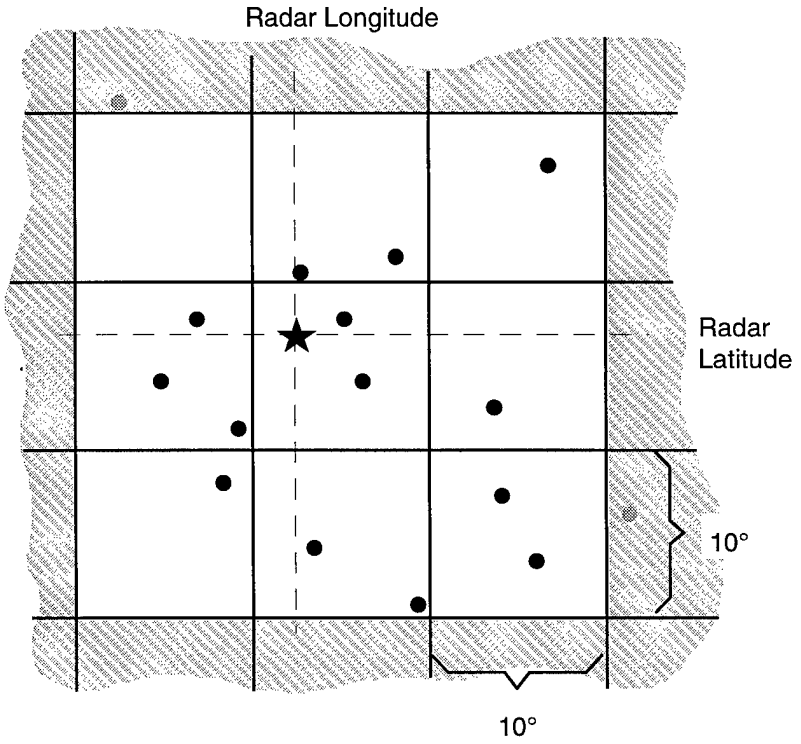

Figure 3.3 Radar (star) and surrounding radiosonde stations (circles) within the nine-MSQ group

Then, the spherical coordinates are converted to three-dimensional rectangular using the standard formulas:

$$x = RC\sin(RLONG)\cos(90 - RLAT) \ , \tag{3-2}$$

$$y = RC\sin(RLONG)\cos(90 - RLAT) \ , \tag{3-3}$$

$$z = RC\cos(RLONG) \ . \tag{3-4}$$

If we follow the same procedure to determine the coordinates of the radar, we can compare each station vector to the radar vector to get the subtense angle,

$$\cos\beta_{RS} = \frac{x_S x_R + y_S y_R + z_S z_R}{RC^2} \tag{3-5}$$

where,

x_S, y_S, z_S = station coordinates
x_R, y_R, z_R = radar coordinates
β_{RS} = subtense between radar and station

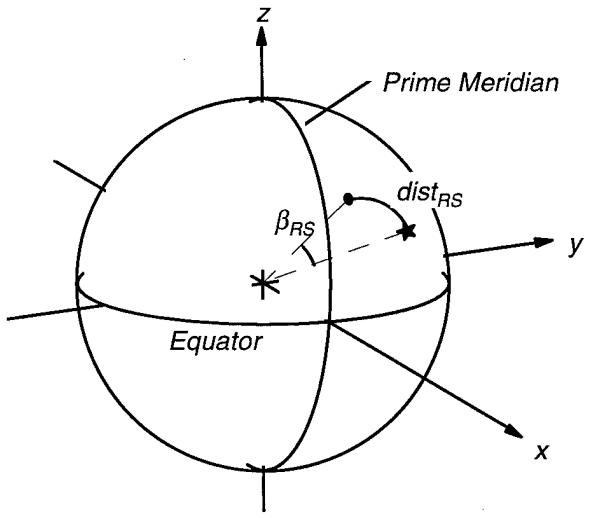

Figure 3.4 Calculating the distance between the radar and a nearby radiosonde station

and then the actual surface distance between them is:

$$dist_{RS} = \beta_{RS} \times RC. \tag{3-6}$$

There is some small inaccuracy in this calculation since the earth only approximates an oblate spheroid, but for these purposes it is quite acceptable.

Once the distance to every station within the nine-MSQ region is calculated the list of stations is sorted by distance and truncated after ten stations. Ten is an arbitrary cutoff with no special significance so five or some other number might work just as well. The important thing is that there be enough stations listed to allow the user some flexibility in his choice.

The final step in the station selection process is to display these ten nearest stations along with the elevation, and distance from the radar for each, allowing the user to choose one or more stations with which to approximate the atmospheric conditions local to his radar. Normally, the user will choose the nearest station. If, however, the radar is situated in the midst of two or three stations which all contain relevant data, the user may select both or all of them and let the model interpolate the data (though at present the model will not interpolate ducting data -- only surface parameters). In many cases this will be the most accurate option. Care must be taken, however, whether choosing a single station or interpolating, that the climate of the radar and the climate of the station(s) are similar. For instance, consider a radar at 1000 feet above mean sea level (MSL); the nearest station is 150 km away at 500 feet MSL; and the next station is 180 km away at 900 feet MSL on the same plateau as the radar. In this case it is a bad decision to choose the nearer station because of the altitude difference. The second

station will likely have a climate more closely approximating that of the radar. This same reasoning will apply when choosing two or three stations for interpolation. Interpolating, for example, between an off-coast (fixed ship) station, and an inland site is hardly a wise idea. Because of the abstract nature of this final decision, it is left to the user to make.

Constructing the Refractivity Profile. When the decision is made, and the user selects the indices of one, two, or three stations, CLIMAREF will retrieve the data from the database, interpolate if necessary, and calculate the refractivity profile, *N(h)*, from the surface to the highest significant altitude.

For each station selected, CLIMAREF, retrieves the surface refractivity, *NS*, and the modified refractivity gradient up to 1000 meters, *ΔM1K*. This quantity is converted to N-units (Patterson, 1987: 14),

$$\Delta N1K = \Delta M1K - \frac{10^6}{a_e} = \Delta M1K - 156, \tag{3-7}$$

where a_e is the mean radius of the earth, and used to compute the refractivity at 1000 meters:

$$N1K = NS + \Delta N1K. \tag{3-8}$$

These two parameters, *NS*, and *N1K*, are the basis for construction of the refractivity profile and must be obtained for each of the one, two, or three stations selected.

Additionally, a surface duct or an elevated duct may be included in the refractivity profile. If the decision is made not to interpolate and a single station is selected, the ducting statistics are retrieved from the database and displayed along with a query requiring the user to select "Surface duct, Elevated duct, or No duct." The user may

make his selection based on the displayed "Percent of time duct occurs" and the heights and thicknesses associated with the duct. Remember again, that these parameters are only mean values. Anomalous propagation effects are highly unpredictable and the mean parameters are certainly nothing to be counted on. Nonetheless, some users may want to include ducting to get an idea of the effects a duct would have if present. The extent to which ducting is successfully modeled is discussed in the next two chapters.

If the user chooses more than one station so as to arrive at an interpolated profile, he will forego ducting by default. There are two interpolation routines, one for the two-station scenario, and one for the three-station scenario. For the purposes of this paper, the former will be called linear-interpolation, and the latter, planar-interpolation. Both compute new values of *NS*, and *N1K*. Both of these algorithms were custom-built, so to speak, for this project, and will be derived in some length here.

The linear-interpolation algorithm is simple as interpolations go (Figure 3.5a).

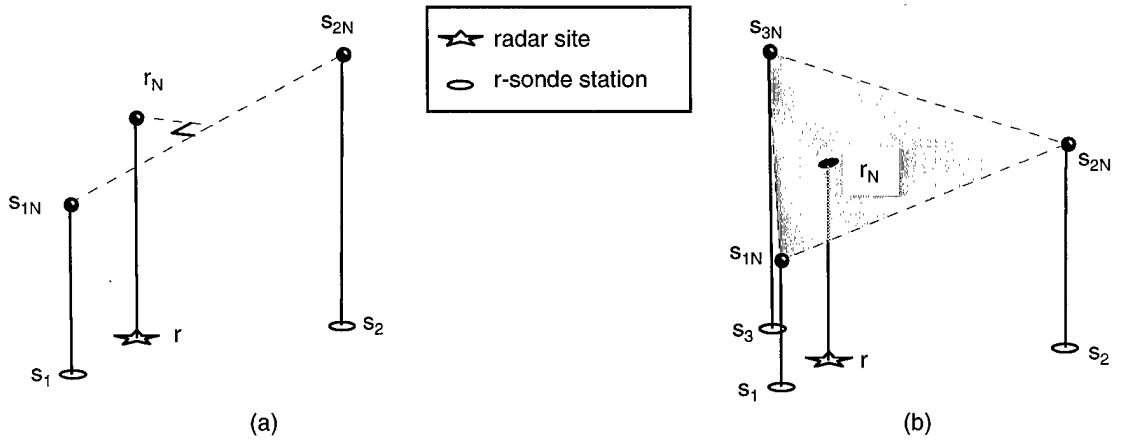

Figure 3.5 (a) Linear and (b) Planar interpolation methods

First, the distance between the two stations is calculated in the same way the distances between the radar and the stations were calculated. Then, a triangle is constructed using the distances between the three sites (i.e. radar, station 1, station 2): The radar, point r, is placed on the Cartesian x-y plane at (0,0), and station 1, point s1, at (d_1,0), d_1 being the distance between the radar and station 1. The coordinates of station 2, point s2, are calculated using the other two distances (Figure 3.6):

$$x_2^2 + y_2^2 = d_2^2 \tag{3-9}$$

and

$$(d_1 - x_2)^2 + y_2^2 = d_{12}^2 \tag{3-10}$$

hence,

$$x_2 = \frac{d_2^2 - d_{12}^2 + d_1^2}{2d_1} \tag{3-11}$$

$$y_2 = \sqrt{d_2^2 - x_2^2}\ . \tag{3-12}$$

Note it doesn't matter whether station 2 is placed in the positive or the negative y-halfplane.

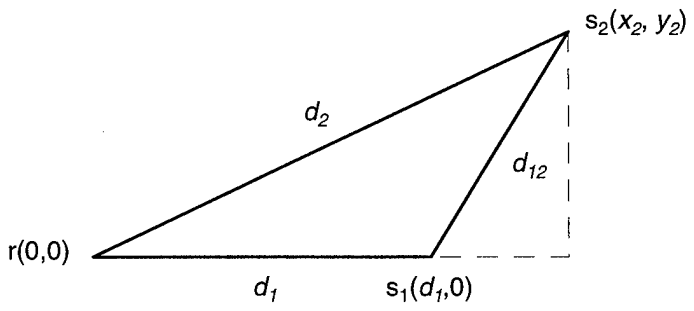

Figure 3.6 Geometry for x-y placement during linear interpolation

The z-coordinates of each station will be *NS*, and then *N1K*, depending upon which value is being interpolated. First, however, these values must be normalized to sea level and sea level + 1km, respectively, since the elevations of the two radiosonde stations will probably be different. In other words, we must find a common height at which to interpolate the refractivity values. This is done using the bi-exponential refractivity model (see eq. 2-8, 2-9):

$$c_e = \ln \frac{N_S}{N_{1km}} \tag{2-9}$$

$$N = N_S \exp\{-c_e(h - h_S)\}, \tag{2-8}$$

$$N_{MSL} = N_S \exp\{-c_e[a_e - (a_e + SEL)]\} = N_S \exp\{-c_e[-SEL]\}, \tag{3-13}$$

where h is the height at which we want to find N, h_S is the surface height, a_e is the mean earth's radius, and *SEL* is the station elevation. Thus we have two points, s_{1N} and s_{2N}, in three-dimensional space representing the locations and N-values of the two stations, and a set of x-y coordinates, r, representing the location of the radar site.

To perform the interpolation itself, a line is constructed between s_{1N} and s_{2N}:

$$\frac{x - x_1}{a} = \frac{y - y_1}{b} = \frac{z - z_1}{c} \ , \tag{3-14}$$

where,

$$a = x_2 - x_1 \qquad b = y_2 - y_1 \qquad c = z_2 - z_1 \ . \tag{3-15}$$

Next, we consider the projection of the line onto the x-y plane, and find the slope of the projection to be $m = b/a$. We want to find the value of N (surface or 1K) at the point, p, on the line nearest to the radar (Figure 3.7). So, we construct a perpendicular line ($m = -a/b$) from line s_1-s_2 to the radar location, point r.

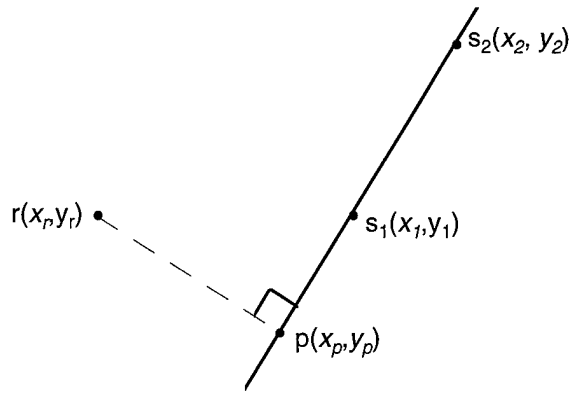

Figure 3.7 Construction of perpendicular during linear interpolation

Since,

$$\frac{y_p - y_r}{x_p - x_r} = -\frac{a}{b} \quad \text{and} \quad \frac{x_p - x_1}{a} = \frac{y_p - y_1}{b} \ , \tag{3-16}$$

$$x_p = \frac{\frac{a}{b}x_r + \frac{b}{a}x_1 - y_1 + y_r}{\frac{b}{a} + \frac{a}{b}} \tag{3-17}$$

As it turns out, we need not calculate y_p. To get our interpolated value we simply calculate z_p , the height value of line s_1-s_2 at point p:

$$\frac{z_p - z_1}{c} = \frac{x_p - x_1}{a} \quad \Rightarrow \quad z_p = \frac{c}{a}(x_p - x_1) + z_1 = N_{\text{interp}} \ . \tag{3-18}$$

Finally, the radar surface elevation is interpolated from the station heights and the interpolated values of *NS* and *N1K* (at sea level) are de-normalized to the interpolated elevation using equations 3-13 and 3-14.

The three-station, or planar, interpolation is similar to the two-station case except that a plane is constructed between the stations instead of a line (Figure 3.5b). First a

triangle is constructed as in the two-station case between points r, s_1, and s_2 (Figure 3.8). Then x_3 and y_3 are computed the same as x_2 and y_2 (equations 3-11, 3-12).

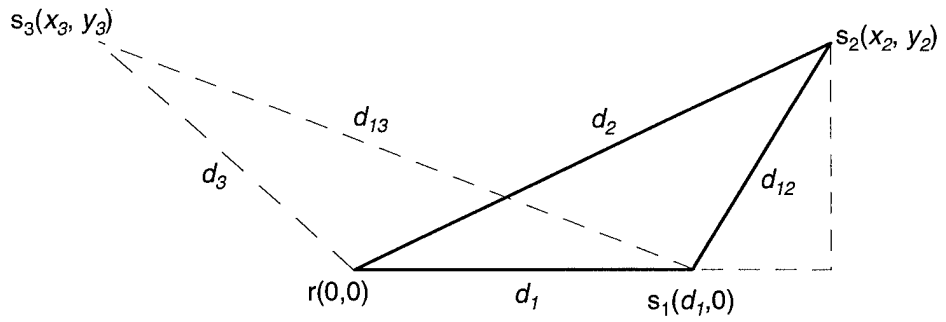

Figure 3.8 Geometry for x-y placement during planar interpolation

Again, y_2 is considered positive as a matter of convenience. To determine the sign of y_3, however, d_{23} must be calculated using a positive and a negative y_3 and compared to the actual distance between stations two and three. That is,

$$d_{23}^{+} = \sqrt{(x_2 - x_3)^2 + (y_2 - y_3^{+})} \quad \text{and} \quad d_{23}^{-} = \sqrt{(x_2 - x_3)^2 + (y_2 - y_3^{-})} \; . \qquad (3\text{-}19)$$

CLIMAREF uses the y_3 value yielding the d_{23} that matches the actual distance between stations two and three. Once again, *NS* and *N1K* values for the three stations are normalized to sea level and used as the z coordinates.

The equation describing the plane containing points s_{1N}, s_{2N}, and s_{3N} is

$$A(x - x_1) + B(y - y_1) + C(z - z_1) = 0 \qquad (3\text{-}20)$$

where A, B, and C are the direction numbers of a line perpendicular to the plane. Two vectors lying in the surface of the plane are:

$$\vec{u}_{12} = (x_2 - x_1)i + (y_2 - y_1)j + (z_2 - z_1)k \tag{3-21}$$

and $$\vec{u}_{13} = (x_3 - x_1)i + (y_3 - y_1)j + (z_3 - z_1)k \tag{3-22}$$

and a vector perpendicular to the plane is given by $\vec{u}_{12} \otimes \vec{u}_{13}$, so that

$$\begin{aligned} A &= (y_2 - y_1)(z_3 - z_1) - (z_2 - z_1)(y_3 - y_1) \\ B &= (z_2 - z_1)(x_3 - x_1) - (x_2 - x_1)(z_3 - z_1) \\ C &= (x_2 - x_1)(y_3 - y_1) - (y_2 - y_1)(x_3 - x_1) \, . \end{aligned} \tag{3-23}$$

Setting

$$D = -Ax_1 - By_1 - Cz_1 \ , \tag{3-24}$$

the plane is defined by

$$Ax + By + Cz + D = 0 \ . \tag{3-25}$$

Since the interpolated N-value is the point on the plane directly above point r,

$$z_r = \frac{-Ax_r - By_r - D}{C} = N_{\text{interp}} \ . \tag{3-26}$$

As before, CLIMAREF de-normalizes the interpolated values to the interpolated radar elevation to complete the interpolation process.

Once the refractivity parameters are in hand, the profile is constructed. To do this, the atmosphere is sliced horizontally into layers *dh* thick. Then the refractivity *N(h)* is calculated for every layer boundary from the surface up to a maximum altitude five kilometers higher than the radar height or the target height, whichever is higher. The five kilometers is a buffer to provide for circumstances in which the trace itself actually goes higher than either endpoint (This could occur in a duct).

If the user selects not to include ducting in the profile, the calculations are simple, again using equations 2-8 and 2-9:

$$N(h) = N_S \exp\{-c_e(h - h_S)\}, \tag{2-8}$$

where

$$c_e = \ln\frac{N_S}{N_{1km}} = \ln\frac{N_S}{N_S + \Delta N}. \tag{2-9}$$

If ducting is to be included, however, every unique level of the duct must be taken into account when building the profile.

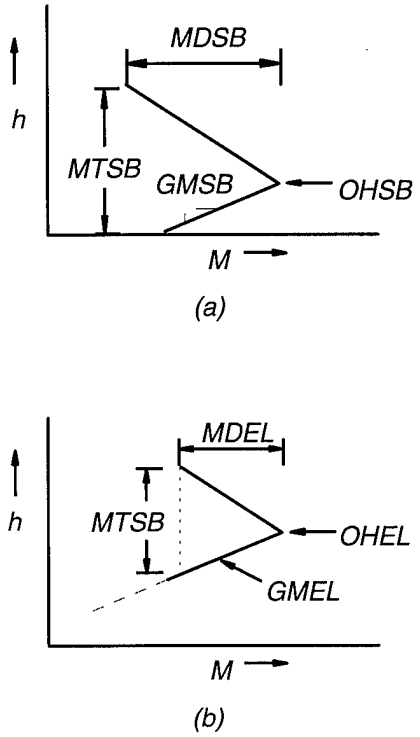

Surface-Based Duct Parameters	
GMSB	M-unit gradient
OHSB	optimum height
MTSB	thickness
MDSB	M-unit deficit
MFSB	trapping frequency
PSB12	1200Z % occur
PSB00	0000Z % occur
Elevated Duct Parameters	
GMEL	M-unit gradient
OHEL	optimum height
MTEL	thickness
MDEL	M-unit deficit
MFEL	trapping frequency
PEL12	1200Z % occur
PEL00	0000Z % occur
P2EL	possibility of >1 elevated duct
PSBEL	probability of surface-based and elevated ducts

Figure 3.9 Duct parameters: (a) Surface duct, (b) Elevated duct (figure adapted from Patterson, 1987)

Figure 3.9 illustrates how each duct is built up from the parameters in the database.

Before the *N(h)* values are computed, CLIMAREF calculates the profile height, *ph*, and

refractivity, pM, at each of the significant levels in the duct using the following formulas derived from the figure:

Surface Duct:

surface: $ph_1 = 0 \qquad pM_1 = NS$ (3-27)

opt coupling ht: $ph_2 = OHSB \qquad pM_2 = NS + GMSB \cdot OHSB$ (3-28)

top of duct: $ph_3 = MTSB \qquad pM_3 = pM_2$ - MDSB (3-29)

1 km above duct: $ph_4 = ph_3 + 1km \quad pM_4 = pM_3 + (M1K - NS)$ (3-30)

Elevated Duct:

surface: $ph_1 = 0 \qquad pM_1 = NS$ (3-31)

opt coupling ht: $ph_2 = OHEL \qquad pM_2 = NS + GMEL \cdot OHEL$ (3-32)

top of duct: $ph_3 = OHEL - \frac{MDEL}{GMEL} + MTEL \qquad pM_3 = pM_2 - MDEL$ (3-33)

1 km above duct: $ph_4 = ph_3 + 1km \quad pM_4 = pM_3 + (M1K - NS)$ (3-34)

All the heights given here are measured with respect the surface.

Once the program arrives at the M-values, it converts them to N-values using

$$N(h) = M(h) - 156h, \tag{3-35}$$

where h is the height above the surface, following the convention of the database (Patterson, 1987, 14) (see also eqs. 2-14, 2-15) . Above the top of the duct, CLIMAREF calculates the profile using pN_3, pN_4 as NS and $N1K$, respectively, in equations 2-8 and 2-9. With the profile set up, the stage is set for raytracing.

Raytracing. Raytracing, as the term is used generally in this paper, is the process of computing the single most direct (or shortest) path from the radar to the target as it is

constrained by the prevailing refractive effects of the atmosphere. This path, due to refraction, will not be a straight line; neither will it be a function with a closed solution. Hence, the only way this path can be computed, in the general case, is by breaking the atmosphere into exceedingly thin concentric shells around the earth, determining the index of refraction for each layer, launching a ray into space at some initial takeoff angle from the radar antenna, and calculating how much the ray bends as it passes through each successive layer. The fulcrum upon which the whole process turns is Snell's Law, as shall be seen.

Unfortunately, the only way of putting the endpoint of the ray squarely upon the target is the process of estimation, approximation and iteration described in the first paragraphs of this chapter. The details will be described presently. First, however, it is important to define the fundamental types of paths that can be produced by such a process.

When no ducting is present, there are three path types. The simplest occurs when the radar elevation angle is positive (Figure 3.10a). The energy travels upwards with a gradual bend toward the earth until it reaches the target. On the other hand, if a ray is launched at a negative angle it will travel towards the earth, bending gradually towards the earth and eventually either strike the surface (and be reflected or absorbed) or pass close to the surface at some minimum height (the tangent point) only to continue on into space. From this scenario, two path types arise: the short path (Figure 3.10b), on which the ray reaches the target before hitting the earth or passing through the tangent point; and the long path (Figure 3.10c), on which the ray only reaches the target after it has passed

through the tangent point. The ducted path, will either be a distorted variant of one of the three non-ducted paths, or it will be a path fully contained within the duct. This last path type will only occur if the radar and the target are in the duct together.

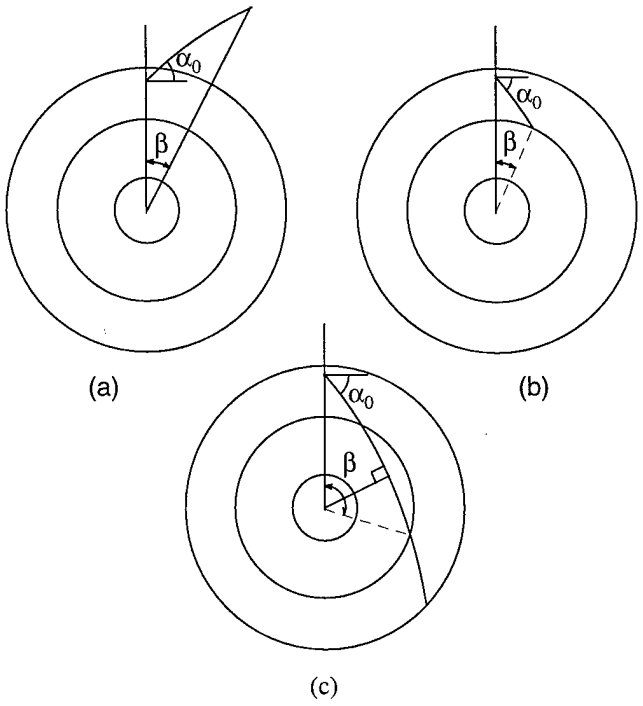

Figure 3.10 Basic path types: (a) upward, (b) downward-short, (c) downward-long (figure adapted from Abel, 1982: 5)

Of course, these paths are only realized if CLIMAREF can put the ray endpoint on the target. Mathematically the problem is this: For a given radar height, target height, target range and refractive profile, a ray launched at an initial elevation (takeoff) angle, α_0, will cause the ray to pass through the target height at an estimated subtense, $\beta_\varepsilon(\alpha_0)$ (Figure 3.1). That subtense will be correct when,

$$\beta_e(\alpha_0) = \beta_t \ , \quad \text{or} \quad \beta_e(\alpha_0) - \beta_t = f(\alpha_0) = 0 \tag{3-36}$$

where β_t is the target subtense calculated from the target range, target height, earth's radius, and the surface elevation. The algorithm used for this thesis project is taken from USAFETAC Technical Report, TN-82/005, "The Theory and Use of a Raytracing Model Developed at USAFETAC," by Capt Michael D. Abel, *et. al.*, published in 1982. Abel's method is an example of a simple iterative technique for approximating a root known as the Newton-Raphson method of numerical approximation. The Newton method is summarized:

$$\alpha_{0_n} = \alpha_{0_{n-1}} - \frac{f(\alpha_{0_{n-1}})}{f'(\alpha_{0_{n-1}})} \quad . \tag{3-37}$$

In the simplest cases, f', is known. However, in this case, because $f(\alpha_0)$ cannot be put in closed form, it must be numerically approximated on the fly as will be shown.

Using the Newton-Raphson Method, then, the first step is to determine an initial estimate for the takeoff angle. To do this CLIMAREF uses 4/3-earth standard refraction, an idea suggested by Abel (1982: 21) though unaccompanied by any algorithms. Hence, the algorithm for making this initial guess is derived here. Enlarging the radius of the earth by 1/3 (Figure 3.11) and keeping the radar height, target height (for this derivation surface elevation is disregarded for simplicity), and surface range constant under 4/3-earth refractive conditions causes the radio path to flatten into a line, and the radar-to-target subtense to decrease by 1/4, i.e.

$$\beta_{4/3} = \beta_t \frac{a}{a_{4/3}} = \beta_t \frac{3}{4} \, . \tag{3-38}$$

The 4/3-earth model and the Law of Cosines show the apparent range (path length) to be

$$TRG_{app} = \sqrt{(a_{4/3} + REL)^2 + (a_{4/3} + THT)^2 - 2(a_{4/3} + REL)(a_{4/3} + THT)\cos\beta_{4/3}} \quad , \tag{3-39}$$

allowing the law of sines to be used to find our initial estimate:

$$\alpha_0 = \cos^{-1}\left(\frac{(a_{4/3} + THT)\sin\beta_{4/3}}{TRG_{APP}}\right). \tag{3-40}$$

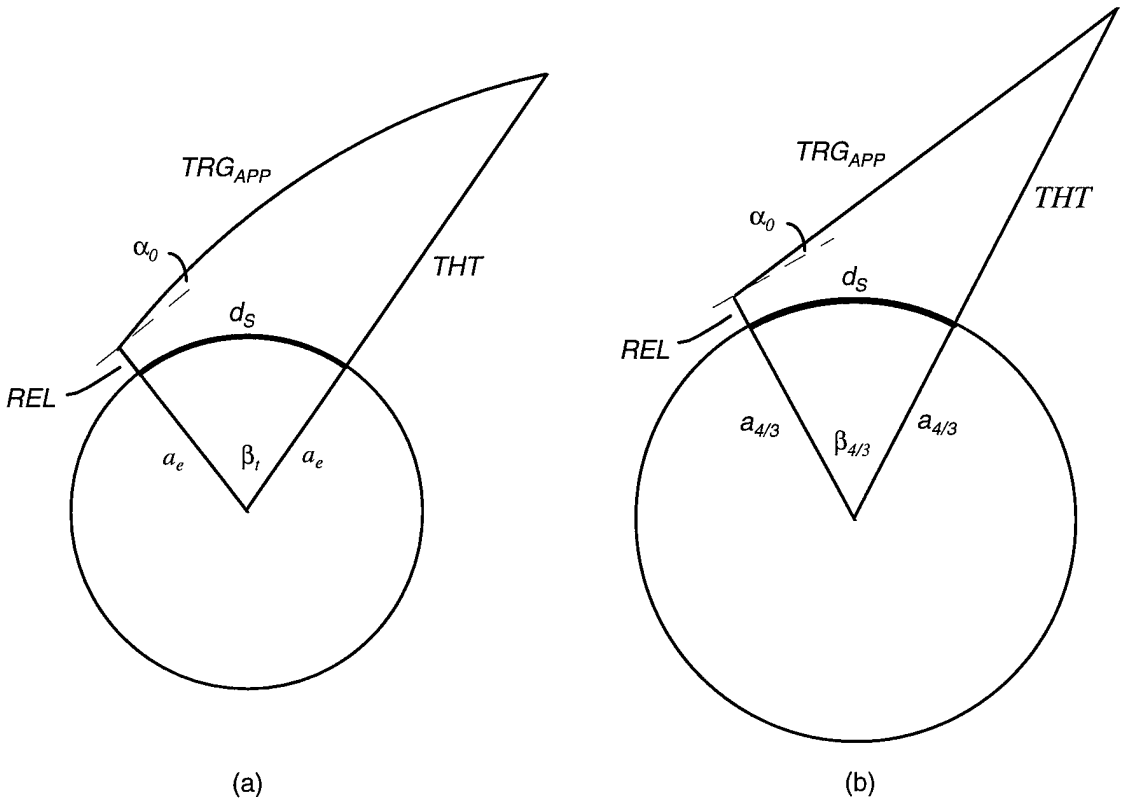

Figure 3.11 4/3 earth estimation of initial takeoff angle; (a) earth actual size, refracted ray path (b) earth enlarged to 4/3 actual, ray path subsequently flattened

CLIMAREF now uses this initial estimate of the ray takeoff angle to begin the first raytrace. Since the basic raytrace process is discussed in some detail in chapter two, only the equations are given here using the variable names used in CLIMAREF.

Following those we shall examine the somewhat complex estimation and approximation techniques.

Beginning at the radar and ascending or descending to the target, the bending of the ray must be calculated over every layer. As the ray approaches a layer, the known parameters are the initial elevation, α_1, the thickness of the layer, *dh*, and the refractivities, N_1 and N_2, at boundary 1 and boundary 2 of the layer. The program will compute the elevation angle of the ray as it approaches boundary 2, α_2, the amount of bending, Ψ_1, through the layer, and finally, the subtense, β_1, of the ray path through the layer. These are calculated like so (eq 3-41, 3-42, 3-43 are from Abel, 1982, 15-16):

$$\cos\alpha_2 = \left[1 + (N_1 - N_2)\times 10^{-6} - \frac{dir \cdot dh}{r_0 + h_1}\right]\cos\alpha_1 \qquad (3\text{-}41)$$

(where *dir* is the direction of the ray through the layers: 1 indicates up -1 indicates down)

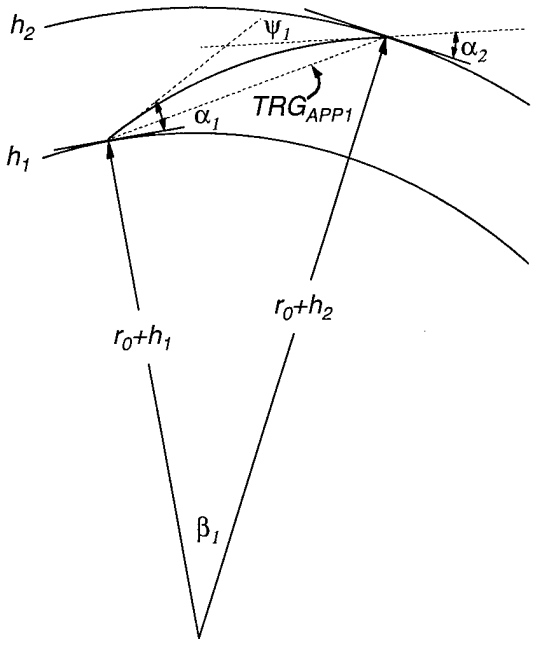

Figure 3.12 Basic raytracing geometry

$$\Psi_1 = \frac{2(N_1 - N_2)\times 10^6}{\tan\alpha_1 + \tan\alpha_2} \tag{3-42}$$

$$\beta_1 = \Psi_1 + \alpha_2 - \alpha_1 \tag{3-43}$$

TRG_{APP1} is calculated using the Law of Cosines as,

$$TRG_{APP1} = \sqrt{(r_0 + h_1)^2 + (r_0 + h_2)^2 - 2(r_0 + h_1)(r_0 + h_2)\cos\beta_1} \tag{3-44}$$

Note that this length is approximated as the secant of the actual path over the layer. Next, β_1 is accumulated into the total estimated subtense, β_ε, and TRG_{APP1} is accumulated into the total apparent range, TRG_{APP}. The next step is to calculate $\delta\beta_1/\delta\alpha_0$ over the layer:

$$\frac{\delta\beta_1}{\delta\alpha_0} = \frac{\tan\alpha_0}{\tan\alpha_1} - \frac{\tan\alpha_0}{\tan\alpha_2} - \frac{\Psi_1 \tan\alpha_0}{\tan\alpha_1 + \tan\alpha_2}\left(\frac{1}{\cos\alpha_1 \sin\alpha_1} + \frac{1}{\cos\alpha_2 \sin\alpha_2}\right) \tag{3-45}$$

This result is accumulated and used to estimate the next initial takeoff angle. Finally, CLIMAREF updates the heights, boundary 1 elevation angle, and the refractivity values, then loops back and performs the calculations for the next layer.

In the case of a downward long path or a ducted path the trace will pass through a height extrema, i.e. a point at which the ray is tangent to the earth's surface. When $\cos\alpha_2$ (eq. 3-41) comes out to be greater than one, CLIMAREF knows an extrema has been hit and that special treatment is required (Abel, 1982: 23-29). First, the extrema height, which generally will not fall on one of the predetermined height levels, must be calculated as (Abel, 1982: 23-24):

$$h_m = h_1 + dir \cdot \Delta z = h_1 + dir \cdot \left| \frac{|B| - \sqrt{B^2 - AC}}{A} \right| , \tag{3-46}$$

where,

$$A = \frac{1}{r_0 + h_1}\frac{\delta n}{\delta h} \tag{3-47}$$

$$B = \frac{1}{2}\left(\frac{1}{r_0 + h_1} + \frac{\delta n}{\delta h}\right) \tag{3-48}$$

$$C = 1 - \cos\alpha_1 \ . \tag{3-49}$$

Also, $\delta\beta_1/\delta\alpha_0$ is calculated differently for the tracing steps on either side of the extrema. The value prior to the extrema is (Abel, 1982, 29):

$$\frac{\delta\beta_1}{\delta\alpha_0} = \frac{-\tan\alpha_0}{\tan\alpha_1} + \frac{2n_0 r_0 \sin\alpha_0}{\tan\alpha_1\left(\frac{n_2}{\gamma} + r_0 + h_2\right)} - \frac{\Psi_1 \tan\alpha_0}{\sin^2\alpha_1} \tag{3-50}$$

The value for the step following the extrema, by symmetry, must be the same, although Abel has two separate formulas for the two steps. (Note: The first term in equation 44 in Abel should have a negative sign in front of it, and the second formula does not result in the same value as the first as it should for reasons undiscovered by this author.) Once the extrema height has been established, the rest of the layer calculations proceed as usual.

Generally speaking, the trace should stop when it reaches the target height, and for the upward path this simple logic is all that is required. However, for downward paths and paths where ducting is present, a more involved set of rules is required to tell the program when to stop a given trace and reestimate if necessary. To wit, nine unique stopping cases have been defined: The trace will stop if:

Case 1: Radar and target not in duct together, α_0 positive, trace is ducting

Case 2: Radar and target not in duct together, α_0 positive, target height reached

OR

Radar and target are in duct together, α_0 positive, target height reached, then trace leaves duct

Case 3: Radar and target not in duct together, α_0 negative, trace is ducting

Case 4: Radar and target not in duct together, α_0 negative, target is higher than radar, target height reached

OR

Radar and target are in duct together, α_0 negative, target is higher than radar, trace leaves duct, target height reached

Case 5: Radar and target not in duct together, α_0 negative, target is lower than radar, target height reached twice (long path)

OR

Radar and target not in duct together, α_0 negative, target is lower than radar, target height reached once and trace reached the surface of the earth (short path)

OR

Radar and target are in duct together, α_0 negative, target is lower than radar, trace leaves duct, target height reached twice (long path)

OR

Radar and target are in duct together, α_0 negative, target is lower than radar, trace leaves duct, target height reached once and trace reached the surface of the earth (short path)

Case 6: Radar and target are in duct together, trace remains in duct, trace endpoint is beyond target, target height reached

OR

Radar and target are in duct together, α_0 positive, trace passes through target eight, reaches maxima, trace reaches surface of earth on downslope

Case 7: α_0 negative, trace reached surface of the earth, and no other stop situation exists

Case 8: Radar and target not in duct together, α_0 negative, target is lower than radar, trace reaches height minima at a point higher than target

Case 9: Radar and target are in duct together, trace is ducting without reaching target height (i.e. amplitude of oscillating duct path not large enough to reach target)

Some stop cases will trigger CLIMAREF to check for endpoint on target, some will not. If the endpoint of the ray is not on target, a new estimate for α_0 is computed. How that is done depends directly on the reason for stopping the previous trace.

If the trace is stopped because of cases 2, 4, 5 or 6, the program checks to see if the ray subtense matches the target subtense for any of the points where the trace passed through the target height. Here "points" is plural because for both the downward path and the ducted path, the trace may pass through the target height more than once. The tolerance for a subtense match is set to $\pm 10^{-6}$ radians, which corresponds to a range tolerance of about $\pm$ 6 meters at the earth's surface. For simple, non-ducting scenarios, CLIMAREF usually beats this tolerance in two to four iterations. The maximum allowable iterations is currently twenty. There are cases in which the program needs the extra iterations to zero in on a radio hole or overcome distortion in the trace caused by a

duct. For some scenarios, ducting causes enough ambiguity to completely baffle the estimating routines and the iteration limit is reached forcing an error message. The next two chapters cover these limitations in more detail.

If the trace misses the target, α_0 is used in the next estimation and either discarded or, if it puts the trace closer to the target than any previous angle, stored as a limiting takeoff angle for either the high side or low side of the target subtense. This puts a bound on any future estimated takeoff angles to guard against wild estimations, which, under certain ducting conditions, can easily occur. Unfortunately, it is not a perfect defense against a diverging approximation.

Cases 1, 3, 7, 8, and 9 do not require a target-reached check since they represent traces aborted for reasons other than target-height-reached.

If CLIMAREF determines that the ray endpoint is not yet on the target, it estimates a new α_0 based on everything it knows about the situation. Generally, the Newton-Raphson method will be used to make the new estimation, that is, from eq. 3-38 (Abel, 1982: 27),

$$\alpha_0' = \alpha_0 + \frac{\beta_t - \beta_e}{\delta\beta / \delta\alpha_0} \tag{3-51}$$

where α'_0 is the new takeoff angle estimate, α_0 is the old estimate, β_t is the target subtense, β_e is the subtense of the endpoint of the last raytrace and $\delta\beta/\delta\alpha_0$ is the accumulated estimate of how β_e changes with α_0 as described above.

Depending on the stopping case, this estimate may be augmented or replaced by other estimating techniques designed to keep the tracing out of trouble. Here are the estimation procedures for each stopping case:

Case 1: a) If every trace so far has been in the duct, multiply last takeoff angle by 1.5 to break out of the duct

b) If a previous trace was not ducted, estimate α_0 by splitting the difference between the lowest out-of-duct takeoff angle and the highest ducted takeoff angle in order to get out of the duct without going too high. Note: The out-of-duct trace was too high since otherwise the estimator would not have gone lower causing the ray to be ducted again (Figure 3.13).

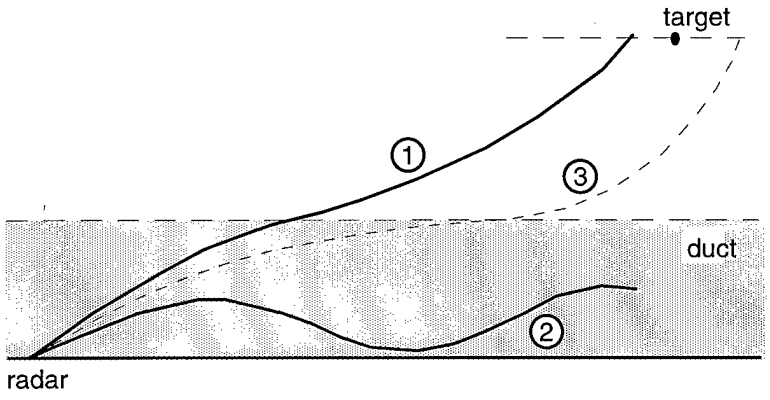

Figure 3.13 Takeoff angle estimation (flat earth representation) - Case 1

Case 2: Standard Newton-Raphson estimation

Case 3: a) If every trace so far has been in the duct, multiply last takeoff angle by 1.5 to break out of the duct

b) If a previous trace was not ducted, estimate α_0 by splitting the difference between the highest out-of-duct takeoff angle and the lowest ducted takeoff angle in order to get out of the duct without going too low. Note: Similar to Case 1, except α_0 is negative.

Case 4: Standard Newton-Raphson estimation

Case 5: Standard Newton-Raphson estimation

Case 6: a) Standard Newton-Raphson estimation

b) If the resulting takeoff angle is lower than the last angle that was too low to allow the ducted ray to reach the target height, multiply the estimated angle by 1.2 to increase its magnitude (Figure 3.14).

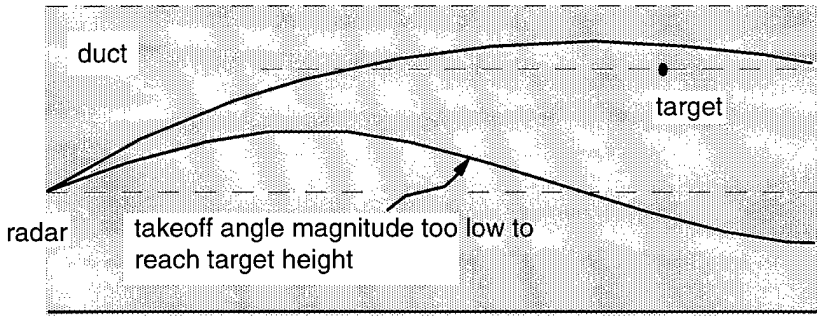

Figure 3.14 Takeoff angle estimation - Case 6

Case 7: a) If all traces have hit the ground and target is higher than radar, force a positive elevation angle 0.25 the magnitude of the last takeoff angle. This will get the trace out of the dirt and force the approximation to converge down to the proper angle

b) If all traces have hit the ground and the target is lower than the radar, multiply the last α_0 by 0.75 to eventually get it out of the dirt.

c) If a previous trace did not hit the ground, split the difference between the highest takeoff angle that hit the ground and the lowest angle that did not hit the ground. The logic is similar to Case 1, b.

Case 8: a) If no trace has yet reached down to the target height, multiply last α_0 by 1.2

b) If a trace has reached down to the target height, split the difference between highest trace that reached target height and the lowest that did not (Figure 3.15).

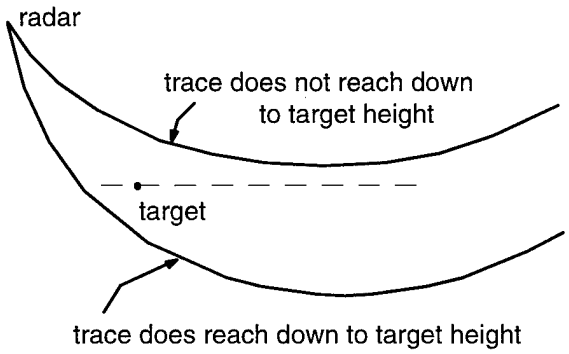

Figure 3.15 Takeoff angle estimation - Case 8

Case 9: Multiply takeoff angle, α_0, by 1.2 to allow trace to reach target height

Note that in any case, if the target height has been reached more than once, the β_e used in the estimation must be the one nearest to the target, naturally. All these conditional adjustments to the standard approximation are necessary to cover situations that are outside the simple paradigm assumed by the Newton-Raphson method.

Once a new α_0 has been estimated, CLIMAREF compares it to the previous takeoff angles that put the trace endpoint nearest the target -- one for the high side and one for the low. If the new angle is outside these limits, it is recalculated as the bisection of the two limiting angles. This bisection method is simpler and not as efficient as Newton-Raphson, but because ducting effects sometimes cause the latter method to malfunction, bisection is useful as a backup and a check. When the new takeoff angle is finalized, a new trace is performed. This process will repeat itself until the trace endpoint lands squarely on the target, indicating the most direct path to the target has been found.

When the raytracing is complete with the trace endpoint on the target, all that is left to do is calculate the range and height error, which are the fundamental output of the model. First, the geometric elevation angle, α_g (the elevation angle at the radar of the straight line path to the target), of the target is computed.

$$\alpha_g = \pm \operatorname{asin}\left(\frac{(r_0 + THT)\sin\beta_t}{TRG}\right) - \frac{\pi}{2} \tag{3-52}$$

To determine the sign of α_g we must use it in the Law of Cosines to calculate the radius to the target, then compare that with the known target radius, r_0+THT.

$$r_t = \sqrt{r_0^2 + TRG^2 - 2r_0 TRG\cos(\alpha_g + \pi/2)} \tag{3-53}$$

Whichever α_g causes r_t to come closest to r_t=r_0+THT, is the one used for the remaining calculations.

Next, the apparent (or measured) target height, THT_{APP}, is computed.

$$THT_{APP} = \sqrt{r_0^2 + TRG_{APP}^2 - 2r_0 TRG_{APP}\cos(\alpha_0 + \pi/2)} - r_0 \tag{3-54}$$

With these parameters in hand, CLIMAREF can calculate the errors:

$$THTERR = THT_{APP} - THT \tag{3-55}$$

$$THTERR_{100} = \frac{THTERR}{THT} \times 100 \tag{3-56}$$

$$TRGERR = TRG_{APP} - TRG \tag{3-57}$$

$$TRGERR_{100} = \frac{TRGERR}{TRG} \times 100 \tag{3-58}$$

Actually, the absolute error is probably more important than percent error for air traffic considerations, but both are calculated as a matter of course.

Display Data. Of course the last step is to display this data for the user. Actual height and range, apparent height and range, and the height and range errors are all displayed. In addition, the actual path, the geometric (straight-line) path, and the apparent path are plotted in one of two representations: curved earth (Figure 3.16) or flat earth (Figure 3.17). In neither representation does the height axis match the range axis. If the plots were to scale, no distinction could be made between the various curves. They would be so close as to be on top of each other.

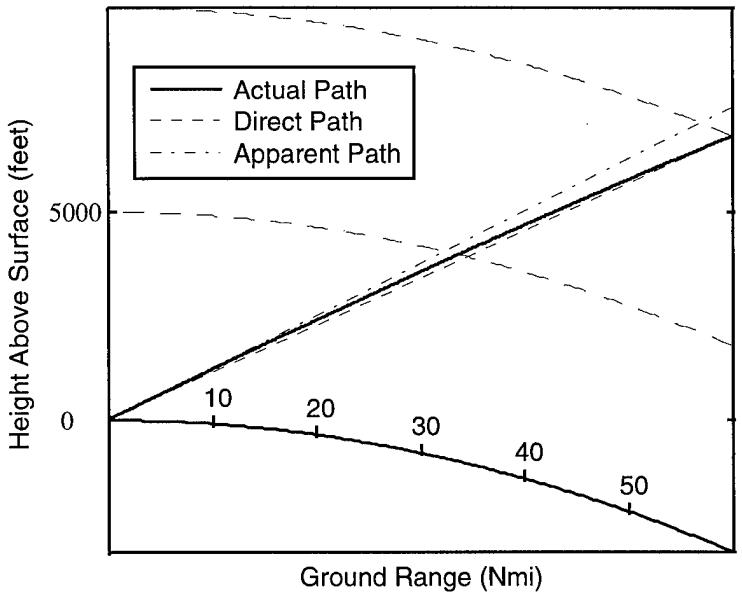

Figure 3.16 Sample output plot -- curved earth

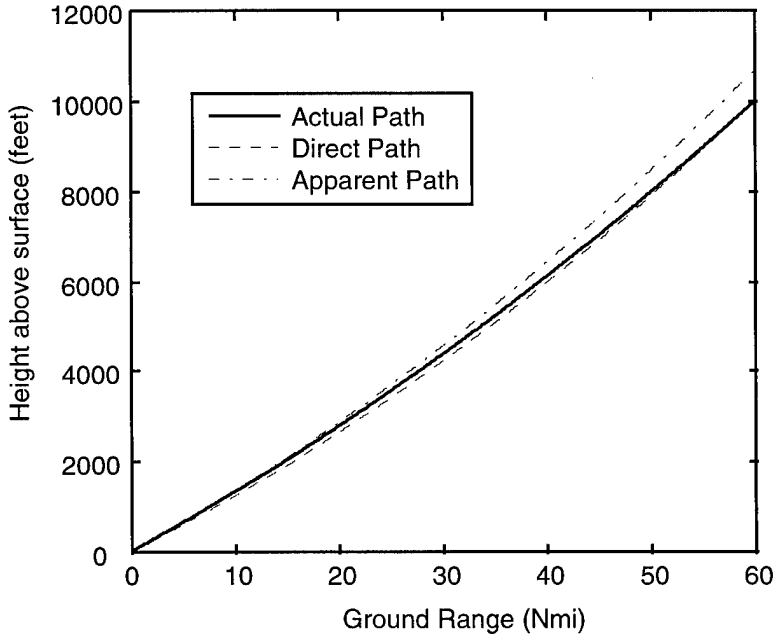

Figure 3.17 Sample output plot -- flat earth

So, using Snell's Law-based raytracing techniques driven by climatologically predicted refractive profiles, CLIMAREF predicts radar height and range error for any time of year at nearly any location in the world. The following chapters contain the results and analysis of a variety of proof tests demonstrating the usefulness of CLIMAREF for its intended purpose. Additionally, some of the program's capabilities and limitations are presented.

IV. Data and Analysis

The CLIMAREF model was developed for this thesis as a new approach to height error prediction, replacing the old four-thirds earth and exponential standard atmosphere techniques. The purpose of this chapter is to demonstrate the model's validity, to present sample data as evidence of the model's usefulness, and to show where the algorithm breaks down. First, CLIMAREF output is compared to a height-range-angle chart derived in Blake (1986: 185) and to RAYS, a submodule of the Navy's EREPS software. Next, a validation test of the interpolation routines demonstrates the accuracy of the geographical calculations involved. And then, the problem of a minimum initial ray elevation angle is explored. After that, a survey of climate variation in terms of height error is presented. And, finally, an inside look at CLIMAREF's workings provides insight into tracing scenarios where the estimation algorithm breaks down. Chapter 5 contains conclusions suggested by the results presented in this chapter.

Validation: CLIMAREF vs. Blake and CLIMAREF vs. RAYS

The best way to validate CLIMAREF would be to compare its results with statistics derived from an actual radar-target-atmosphere system. Such a comparison was impossible in this case due to time and resource constraints. As a substitute, the performance of the raytracing algorithms used in CLIMAREF was compared to the height-range-angle chart in Blake (1986: 185) and to EREPS RAYS.

The height-range-angle chart in Blake allows determination of the proper takeoff angle for a given target height and range. It is based on a closed-form geometrical optics solution. The height selected was 30,000 feet, and the range, 80 nautical miles. The required takeoff angle given by Blake was 3.0 degrees as close as it could be read on the chart. CLIMAREF was modified to display the final takeoff angle and run using the standard atmosphere option. The final takeoff angle given by CLIMAREF was 3.0027 degrees.

The second test was also fairly simple. . RAYS "traces the paths, in height and range, of electromagnetic rays based upon a linearly segmented refractivity-versus-altitude profile(s)..." The software was developed and is used by the Naval Command Control and Ocean Surveillance Center. (Patterson, *et. al.*, 1994: 35). To make comparisons with RAYS, a program called RAYSD was developed using the same tracing mathematics used in CLIMAREF. RAYSD differs from CLIMAREF in that no target is involved. The user selects a radar height and a ray takeoff angle and the ray is traced to a maximum height or range, whichever comes first. The program simply computes the path of a given ray through a given atmosphere. EREPS RAYS does much the same thing. Unfortunately, RAYS is a DOS program and the output is to the screen only – there is no data output. Nevertheless, using a screen capture program and overlaying the RAYS and RAYSD plots, the degree of correspondence between the two models can be reasonably ascertained.

The test was performed first using a surface duct and then an elevated duct scenario. The elevation and M-values in Table 4.1 were used in both programs to

construct the refractivity profiles. For the surface duct test, the radar height was 3 feet and traces were launched using takeoff angles: 0.05, 0.1125, 0.175, 0.2375, and 0.3 degrees. For the elevated duct test, radar height was 2500 feet and the ray takeoff angles were -0.5, -0.3, -0.1, 0.1 and 0.3 degrees. The results are plotted in Figure 4.1 and Figure 4.2.

In both scenarios, the RAYSD plots match the RAYS plots perfectly as well as can be detected given the plot resolution. There is no discernible difference between the curves.

Table 4.1 Height and Modified IOR Parameters for RAYSD-RAYS Validation Tests -- Surface Duct, and Elevated Duct Respectively

Altitude Above Surface		Modified IOR, M	Altitude Above Surface		Modified IOR, M
feet	meters		feet	meters	
0	0	323	0	0	330
174	53	329	2369	722	414
463	141	320	2740	835	406
3743	1141	435	3281	1835	499

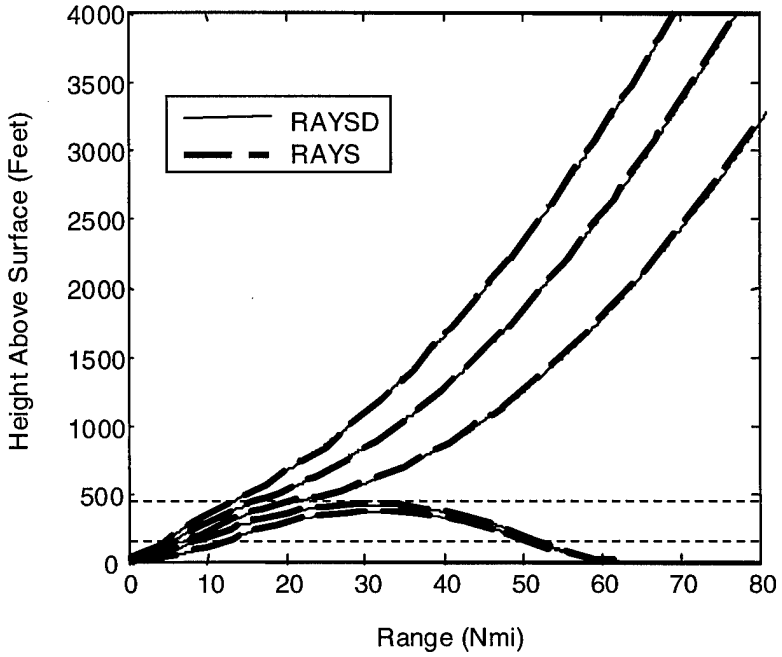

Figure 4.1 RAYSD vs. RAYS discrepancies -- Surface Ducts

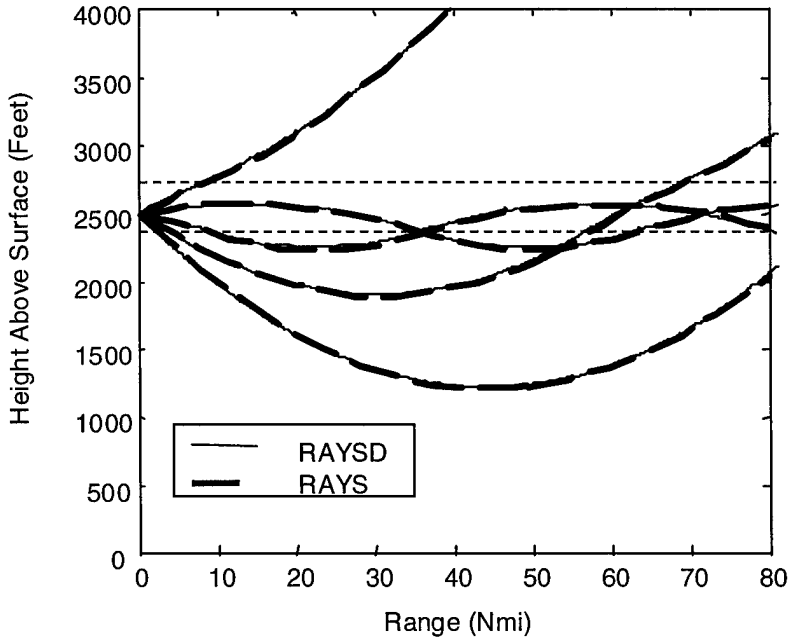

Figure 4.2 RAYSD vs. RAYS discrepancies -- Elevated Duct

Interpolation Check

Two interpolation routines, referred to as the linear algorithm and the planar algorithm, were developed as a part of CLIMAREF to find the refractivity values near or at the radar site using data from two or three nearby radiosonde stations. To verify the accuracy of these routines, a test was performed.

Linear algorithm. To test the linear routine, two radiosonde stations, Pittsburgh

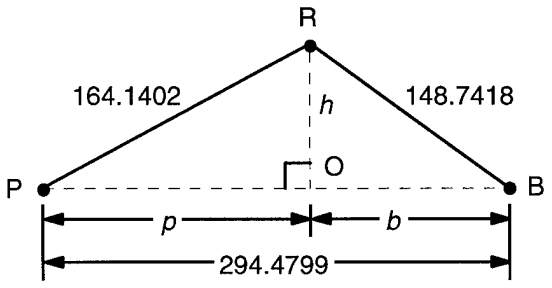

Figure 4.3 Geometry for test of linear interpolation

and Buffalo, were chosen, with a radar located off center somewhere in between (40°N, 80°W) so that the three sites were configured as shown in Figure 4.3. The surface distances, in kilometers, between the stations were obtained from the distance-finding algorithm in the CLIMAREF module, CR4calcdist (which was also checked for reasonable accuracy against a map). Distances *p, b,* and *h* were found using the Pythagorean Theorem: $p = 155.42$, $b = 139.06$, and $h = 52.79$. Since *NS* and *N1K* at Buffalo are 314.2348 and 278.7399, respectively, and *NS* and *N1K* at Pittsburgh are 313.9588 and 279.0745 respectively, a manual interpolation along line PB at point O, yields:

$$\frac{139.06}{294.48} = \frac{313.9588 - NS_O}{313.9588 - 313.2348} \quad \Rightarrow \quad NS_O = 314.09 \ ,$$

which is used as *NS* at the radar site. Using the same site locations in CR7interp, the output was *NS* = 314.05. The difference is negligible for our purposes. Similarly, the manual computation yielded *N1K* = 278.92, which exactly matches the CR7interp *N1K* value.

Planar algorithm. To test the planar interpolation, a third station, Flint-Bishop, Michigan, was selected. The radar and the other two stations were left alone. The distances between the stations and the radar were again derived from CR4calcdist and are given in Figure 4.4.

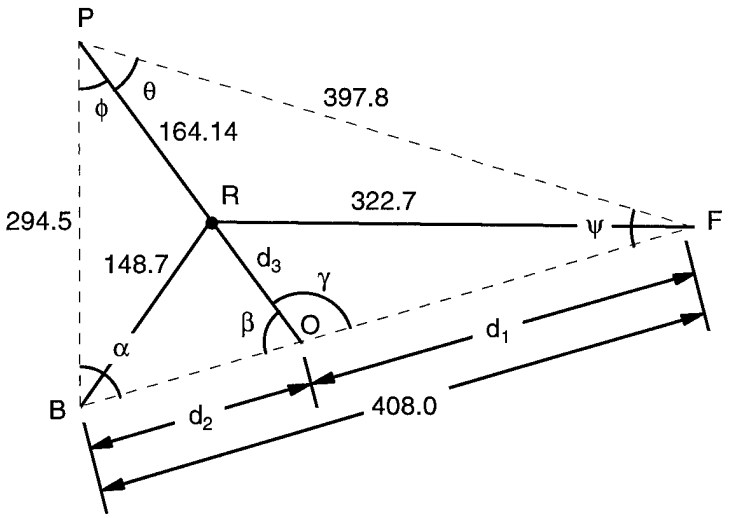

Figure 4.4 Geometry for test of planar interpolation

This interpolation is a bit more complicated: First, ϕ, θ, and ψ were found using the Law of Cosines. Next, α and β were derived from ϕ, θ, and ψ. Then, d_1=313.14, d_2=94.86,

and d_3=107.34 were found using the Law of Sines. Using these values and knowing from CLIMAREF that *NS* at Buffalo and Flint are 313.9588 and 312.6295 respectively, *NS* at point O was linearly interpolated as 313.65. Using that value and the value of *NS* at Pittsburgh, 314.2348, the *NS* at the radar site was interpolated to be 313.88. CLIMAREF computed the same value. Similarly, the manual method and CLIMAREF yielded the same value for *N1K* at the radar site, 278.7437.

These two tests, then, demonstrate the validity of the interpolation algorithms developed for CLIMAREF.

Run-Time Test

A test was performed to determine the amount of processing time CLIMAREF requires in its non-compiled MATLAB® coded form. The test was run on three different computers, a 66 MHz 486 IBM PC compatible, a 166 MHz Pentium, and a SUN Microsystems Sparcstation 20. The MATLAB® *tic* and *toc* commands were placed in CR1main before and after, respectively, the call to CR9raytrace in order to time the tracing only. The results are listed in Table 4. 2.

Table 4. 2 Run-time results for three targets in standard atmosphere refraction

Radar El (ft)	Targ. Ht (ft)	Target Rng (Nmi)	# Iterations Req'd	486 66	Pentium 166	Sparc 20
30	2000	5	3	35.2	2.5	8.0
30	10,000	30	3	246.2	21.0	66.0
30	40,000	150	3	out of mem	209.7	456.0

Minimum Elevation Angle

On rare occasions, the initial elevation angle for a CLIMAREF trace is so small that problems occur. If the angle is too small and negative, the first subtense calculated blows up to an unrealistically large value. If it is too small and positive, either the subtense blows up or the estimation routine has hard time finding the correct angle. Although CLIMAREF handles these errors gracefully (if not completely satisfactorily) it is important to understand the nature of the problem. Hence a test was performed.

Small Negative Angles. To examine the raytracing response to a small negative angle, CLIMAREF was run using standard atmosphere refraction and various target ranges and heights until the small, negative angle response was observed. The particular scenario was radar elevation = 0.3 km (984 ft), target height = 0.305 km (1001 feet), and target range = 10 km (5.4 Nmi).

Everything went wrong on the first tracing step. CLIMAREF chose an initial elevation angle, $\alpha_0 = -5.65350\times10^{-5}$ radians. That is, it expected to trace a downward path that would reach a tangent point, and find the target as it moved away from the earth. The first level height, h_1, was of course the radar height. The second level height, then was h_2=0.299 km. Since $\cos(\alpha_1)$=0.999999998401, and using

$$\cos\alpha_2 = \left[1+(N_1-N_2)\times10^{-6}-\frac{dir\cdot dh}{r_0+h_1}\right]\cos\alpha_1 \qquad (3\text{-}41)$$

together with the appropriate values for N_1, N_2, *dir*, *dh*, and r_0, $\cos(\alpha_2)$ was calculated as 1.00000011240. To the raytracing routine, a result greater than one indicates an

extrema has been reached, in this case a minima. So α_2 is set equal to zero and the bending, ψ_1 , over the layer is computed using:

$$\psi_1 = \frac{2(n_1 - n_2) \times 10^6}{\tan\alpha_1 + \tan\alpha_2} \quad . \tag{2-19}$$

Since α_1 was so small and α_2 was zero, ψ_1 blew up. In turn, β_1,

$$\beta_1 = \psi_1 + \alpha_2 - \alpha_1 \quad , \tag{2-20}$$

blew up causing the extreme results described above.

The problems disappeared when the target was raised to 0.306 km and when it was lowered to 0.300.

Small Positive Angles. When the target was at 0.306 km, a single raytrace worked fine using a positive angle of 2.655×10^{-5}. Further testing was precluded for lack of time.

Climate variation

The primary concern of the project sponsor, NAIC, is finding a technique for ray path prediction and height error prediction that is better than the traditional four-thirds earth or standard atmosphere solutions. To demonstrate the added value of CLIMAREF, a test was conducted in which the ray path was computed for a sample target under varying conditions. The height error was calculated for each scenario and plotted with reference to the standard atmosphere height error, which was 804 feet.

The sample target and radar positions were held constant throughout the test. The radar was 30 feet above the surface, the target was 10,000 feet above the surface, and

the two were 60 nautical miles apart. The variables were month: January, April, July, and October; duct type: no ducting, surface, duct, elevated duct; and location: seventeen locations representing a variety of North American and world climate types (see tables below). Fifteen of the seventeen locations were chosen to correspond to locations used by Bean and Dutton in *Radio Meteorology* (1966: 109-131). Where the database was lacking, substitutions were made, i.e. Cape Kennedy was used instead of Cocoa, FL; Howard AB was used instead of Balboa, Panama; Port Hardy, Canada was used instead of Tatoosh Is, WA; and Wheelus, Libya was used instead of Tripoli, Libya. All substitutes are close in climate and proximity to the originals. The other two of the seventeen stations, Jodhpur, India and Fort Lamy in the Sahara Desert, were chosen because Bean and Dutton noted those areas as having the largest ranges of surface N-units (1966: 102). The results are tabulated in, Table 4.3, Table 4.4 and Table 4.5 and shown plotted in Figure 4.5 through Figure 4.11. Table 4.6 holds some statistics derived from the climate variation test.

Table 4.3 Height Error (feet) -- No Ducting
(*REL*=30 feet, *THT*=10000 feet, *TRG*=60 Nmi)

Location	JAN	APR	JUL	OCT
Portland, ME	677.3	695.7	989.1	806.2
Washington, DC	695.7	695.9	990.2	788.1
Hatteras, NC	788.4	951.1	1257.6	1006.9
Cape Kennedy, FL	917.9	989.3	1224.3	1010.0
Miami, FL	882.8	901.0	1154.0	1028.6
Howard AB, Panama	1064.4	1047.5	1084.3	1084.0
Brownsville, TX	826.3	1133.3	1222.5	955.6
Columbia, MO	695.1	695.6	917.8	732.2
Bismarck, ND	748.7	638.7	787.2	675.6
Denver, CO	634.4	579.6	745.9	598.0
San Diego, CA	931.3	1019.7	1463.0	1211.8
Oakland, CA	860.5	914.2	1394.8	1142.8
Port Hardy, Canada	732.9	769.7	844.0	806.9
Churchill, Canada	878.9	768.9	806.3	732.5
Jodhpur, India	675.7	675.8	920.0	824.0
Fort Lamy, Chad	747.4	711.2	1116.1	1110.7
Wheelus, Libya	806.0	1263.3	1713.0	1165.0

Table 4.4 Height Error (feet) -- Surface Ducting
(*REL*=30 feet, *THT*=10000 feet, *TRG*=60 Nmi)

Location	JAN	APR	JUL	OCT
Portland, ME	835.4	851.1	1179.7	1032.7
Washington, DC	867.6	922.4	1187.0	999.3
Hatteras, NC	1015.9	1187.0	1595.0	1313.1
Cape Kennedy, FL	1141.5	1183.2	1504.4	1195.6
Miami, FL	1468.8	1555.6	1411.0	1364.0
Howard AB, Panama	1253.0	1177.9	1161.5	1136.0
Brownsville, TX	1313.7	1421.1	1430.7	1157.2
Columbia, MO	798.7	939.0	1106.8	1077.1
Bismarck, ND	904.5	898.6	1101.3	817.4
Denver, CO	810.3	770.8	1018.7	799.0
San Diego, CA	1118.3	1205.4	1905.6	1583.8
Oakland, CA	1048.0	1172.8	1615.2	1366.2
Port Hardy, Canada	949.2	989.7	1003.7	969.3
Churchill, Canada	1057.3	911.9	1021.4	945.7
Jodhpur, India	--	1453.3	1858.2	1029.7
Fort Lamy, Chad	1250.8	923.9	1590.4	1493.1
Wheelus, Libya	1085.5	1641.8	2256.0	1478.8

Table 4.5 Height Error (feet) -- Elevated Ducting
(*REL*=30 feet, *THT*=10000 feet, *TRG*=60 Nmi)

Location	JAN	APR	JUL	OCT
Portland, ME	714.4	693.4	832.3	1032.6
Washington, DC	690.8	728.1	862.9	809.9
Hatteras, NC	862.9	945.2	1256.6	1010.5
Cape Kennedy, FL	931.1	1020.1	1235.4	1004.8
Miami, FL	920.4	996.0	1109.5	950.0
Howard AB, Panama	961.2	920.5	1002.9	868.9
Brownsville, TX	951.7	1186.6	1233.0	944.2
Columbia, MO	776.0	783.1	899.1	720.6
Bismarck, ND	787.4	667.7	792.2	761.4
Denver, CO	681.2	700.0	678.0	701.4
San Diego, CA	1028.9	1094.7	1596.2	1287.5
Oakland, CA	887.3	1004.0	1502.0	1162.2
Port Hardy, Canada	801.6	762.6	870.6	769.5
Churchill, Canada	915.0	809.6	801.8	945.7
Jodhpur, India	530.8	258.7	887.0	608.8
Fort Lamy, Chad	-1973.1	460.55	1073.2	101.2
Wheelus, Libya	788.5	1323.7	1643.9	957.3

Table 4.6 Height Error Statistics (*REL*=30 feet, *THT*=10000 feet, *TRG*=60 Nmi)
Note: Std Atm Ht Err = 804.1 feet

units=feet	Mean	Std Dev	Dev from Std Atm	Max	Min
No duct	916.5	222.6	249.3	1713.0	579.6
Surface duct	1183.9	299.5	483.7	2256.0	675.7
Elevated duct	860.6	431.5	435.1	1643.9	101.2
Overall	987.0	358.3	402.3	2256.0	101.2

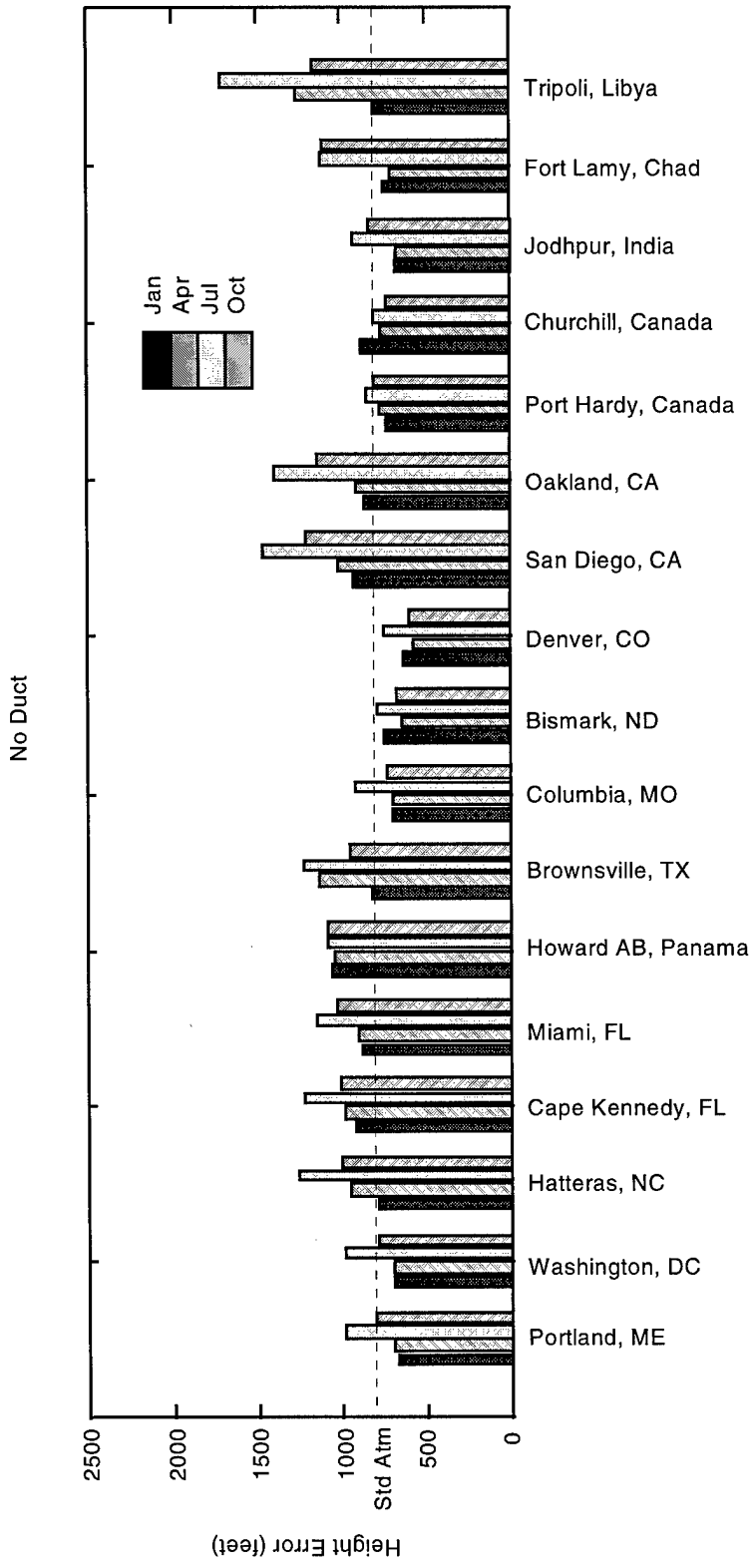

Figure 4.5 Climate variation -- No Ducting, Seasonal Comparisons

Minimum Elevation Angle

On rare occasions, the initial elevation angle for a CLIMAREF trace is so small that problems occur. If the angle is too small and negative, the first subtense calculated blows up to an unrealistically large value. If it is too small and positive, either the subtense blows up or the estimation routine has hard time finding the correct angle. Although CLIMAREF handles these errors gracefully (if not completely satisfactorily) it is important to understand the nature of the problem. Hence a test was performed.

Small Negative Angles. To examine the raytracing response to a small negative angle, CLIMAREF was run using standard atmosphere refraction and various target ranges and heights until the small, negative angle response was observed. The particular scenario was radar elevation = 0.3 km (984 ft), target height = 0.305 km (1001 feet), and target range = 10 km (5.4 Nmi).

Everything went wrong on the first tracing step. CLIMAREF chose an initial elevation angle, $\alpha_0 = -5.65350\times10^{-5}$ radians. That is, it expected to trace a downward path that would reach a tangent point, and find the target as it moved away from the earth. The first level height, h_1, was of course the radar height. The second level height, then was h_2=0.299 km. Since $\cos(\alpha_1)$=0.999999998401, and using

$$\cos\alpha_2 = \left[1 + (N_1 - N_2)\times10^{-6} - \frac{dir \cdot dh}{r_0 + h_1}\right]\cos\alpha_1 \qquad (3\text{-}41)$$

together with the appropriate values for N_1, N_2, *dir*, *dh*, and r_0, $\cos(\alpha_2)$ was calculated as 1.00000011240. To the raytracing routine, a result greater than one indicates an

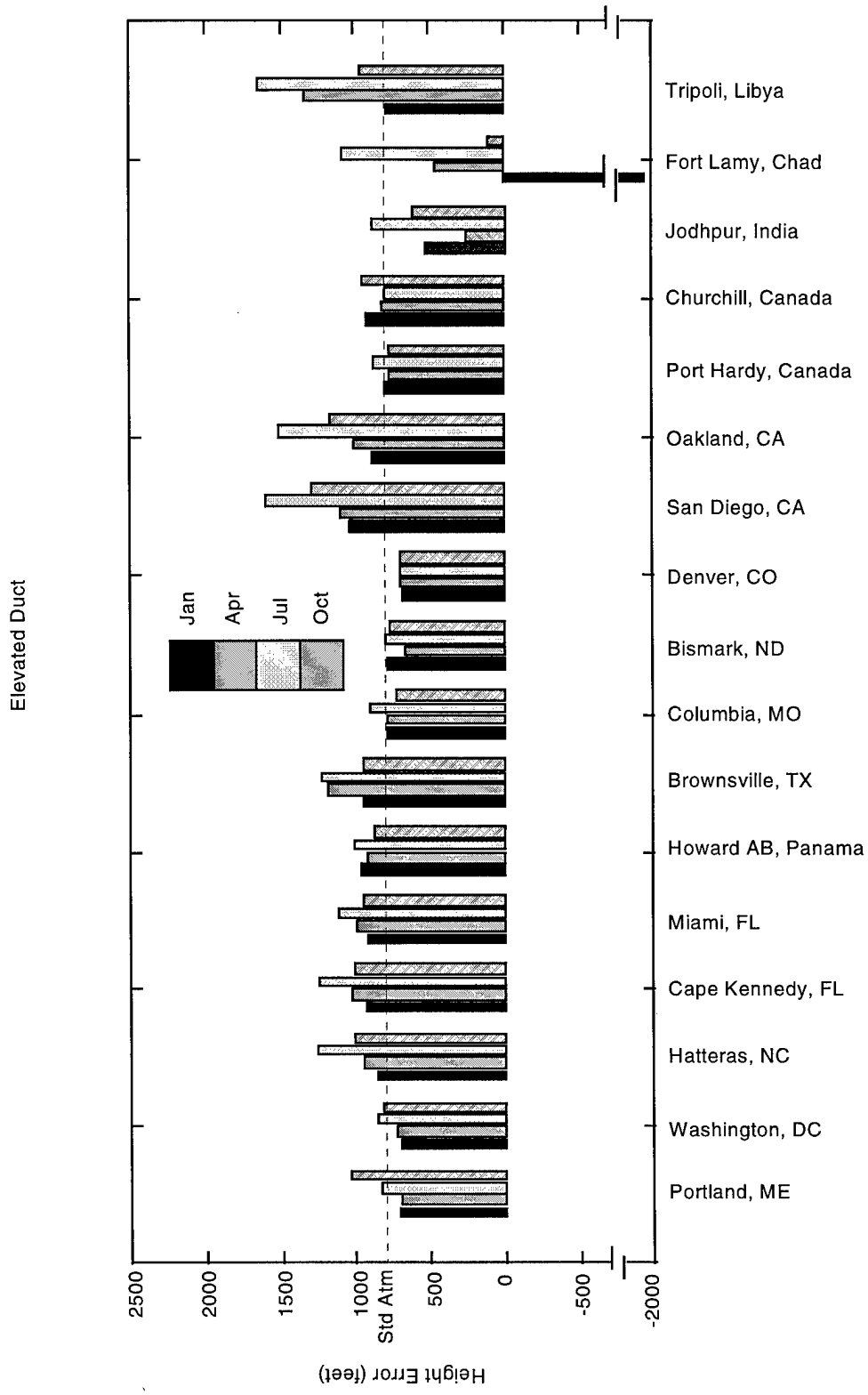

Figure 4.7 Climate variation -- Elevated Ducting, Seasonal Comparisons

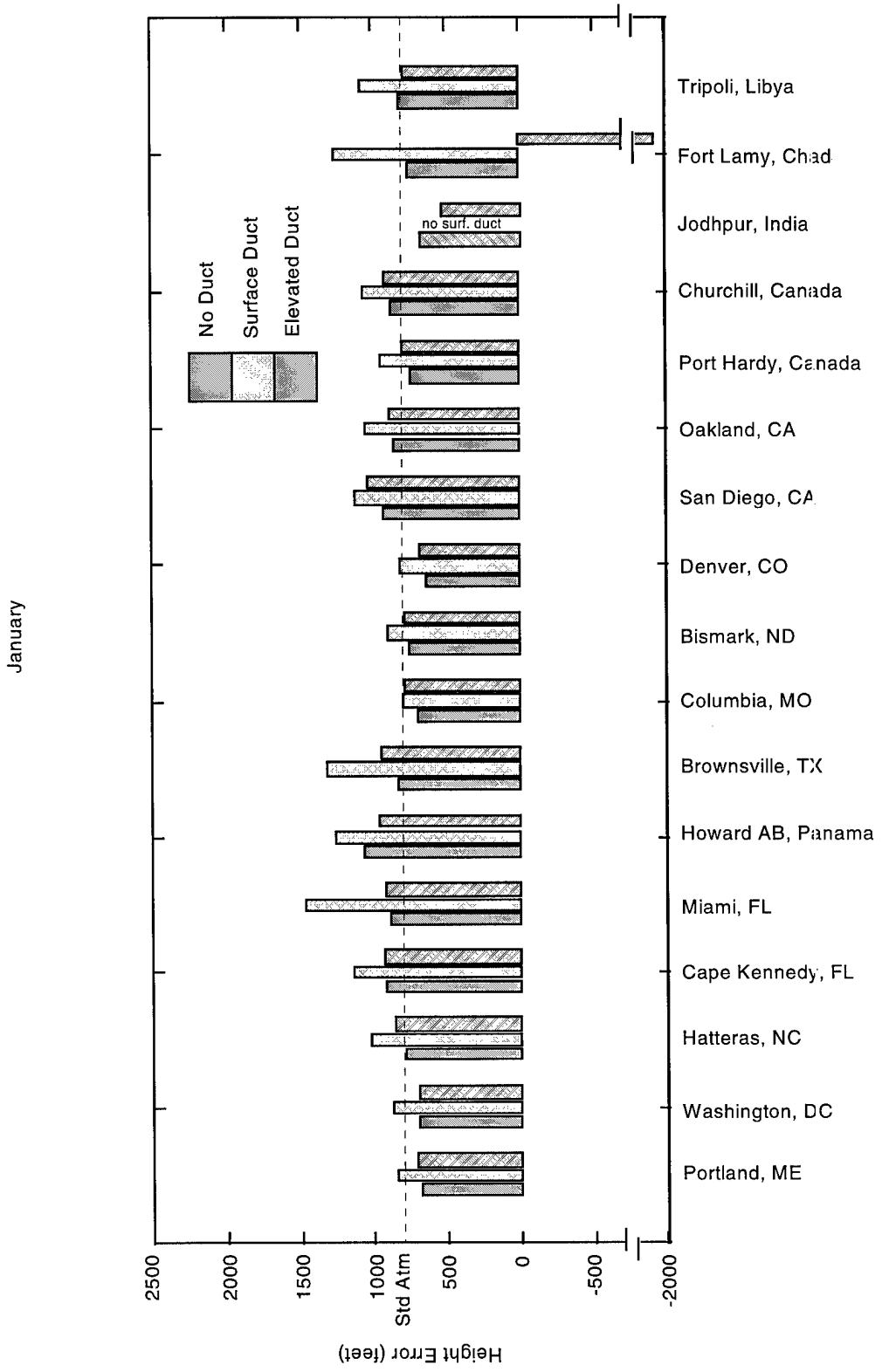

Figure 4.8 Climate variation -- January, Ducting Comparisons

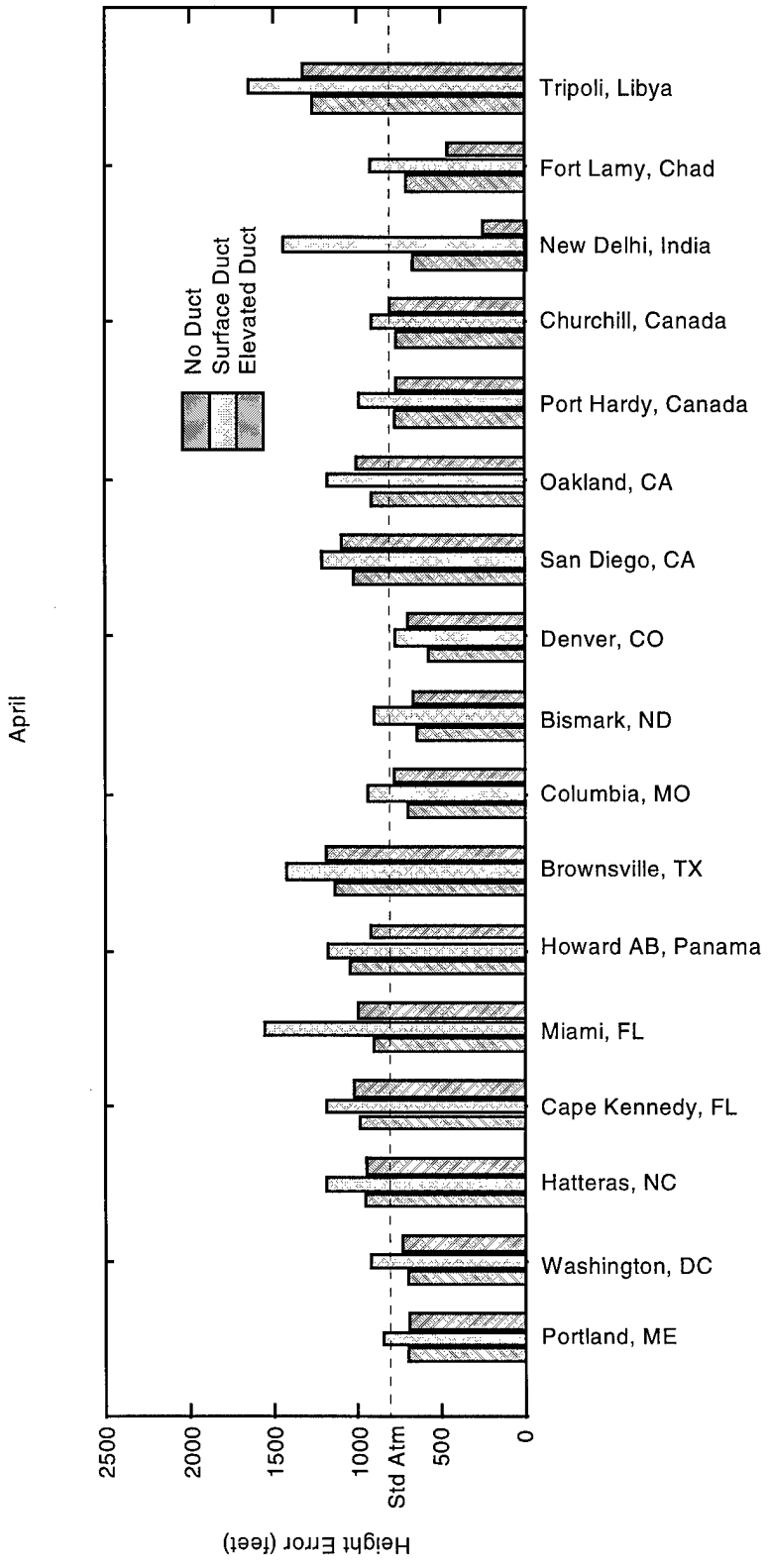

Figure 4.9 Climate variation -- April, Ducting Comparisons

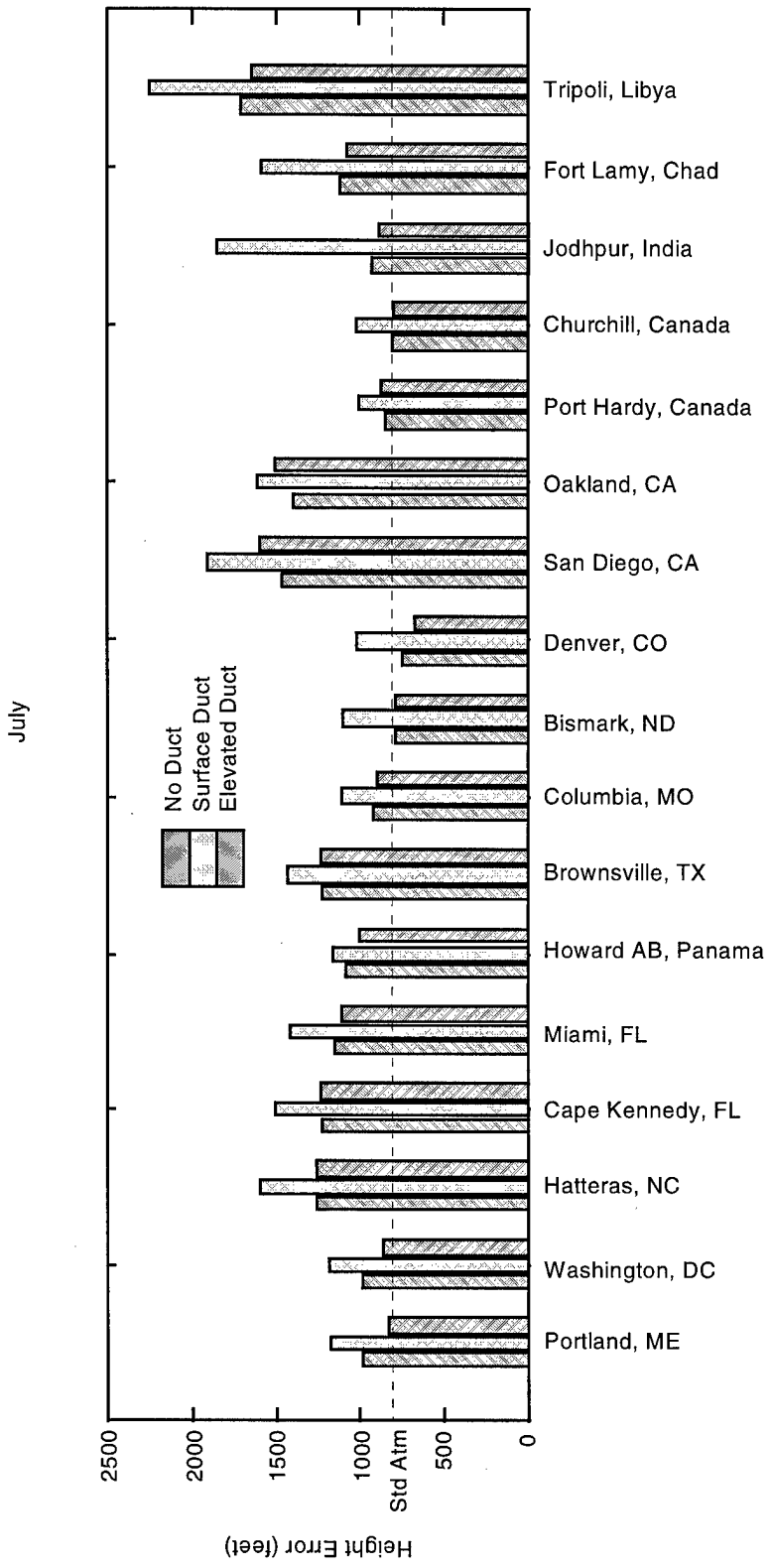

Figure 4.10 Climate variation -- July, Ducting Comparisons

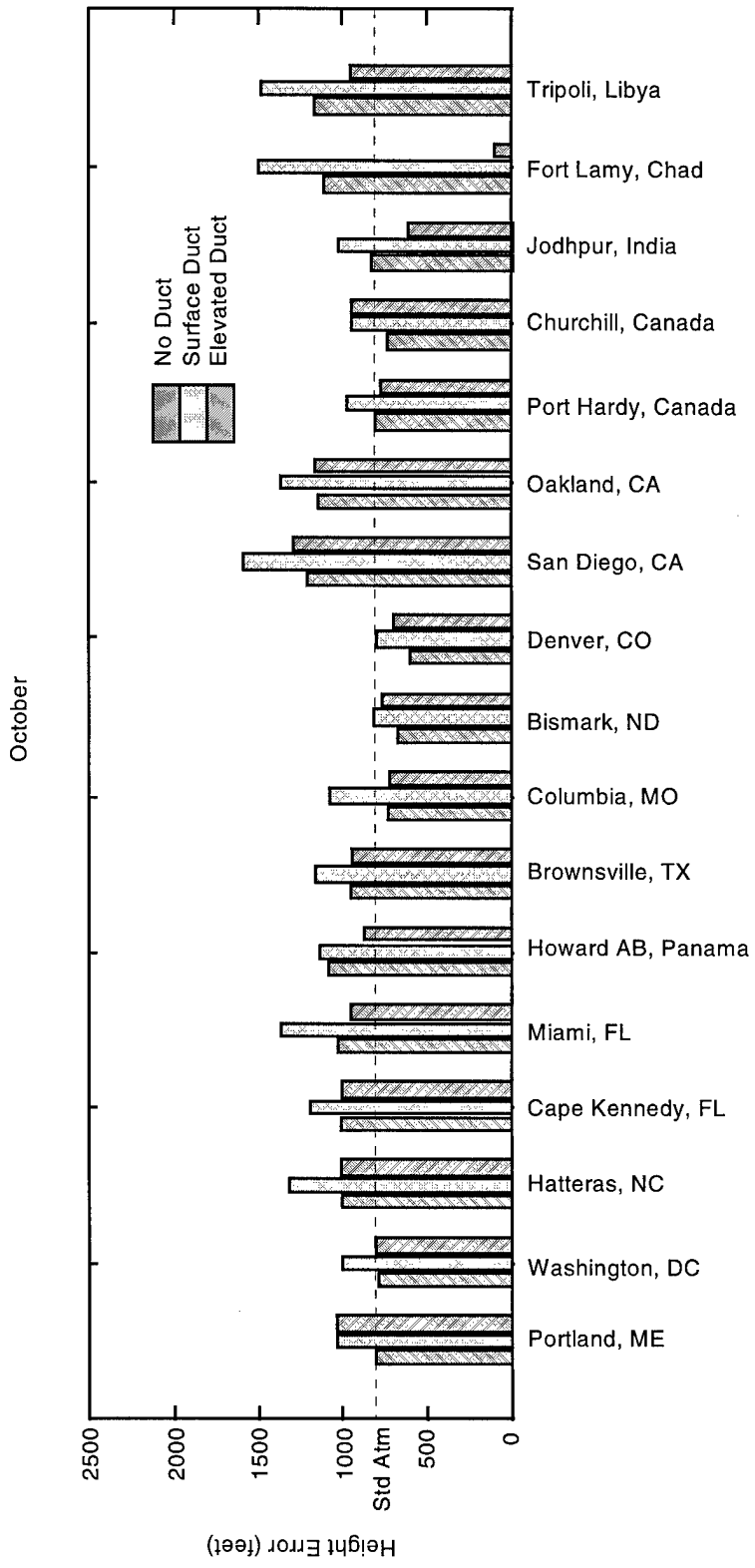

Figure 4.11 Climate variation -- October, Ducting Comparisons

Capability of Model to Handle All Types of Refractive Effects

The convenient assumption in developing a radar beam bending model would be that the radar is on the ground and the target is in the air, well above any ducting effects and within the line-of-sight range of the radar. Unfortunately, such is not the case. A general purpose model must be able to respond reliably to any conceivable situation. In this vein, the next test presents the model with radar-target-atmospherics combinations representing most, if not all, possible combinations of radar, duct and target, to determine where the weak points are, if any exist.

To perform this test, a specially modified version of the driving module, CR1main_tst, was used, and the variable *plotit* in CRraytrace9 was set to 1 allowing all estimate-traces to be plotted along with the final trace. In the plots that follow, the solid line, if any, represents the final raytrace to the target (represented by the star), and the dashed lines represent estimate-raytraces leading up to the final. These estimate-traces were numbered in order by CLIMAREF, but in many cases their proximity caused the numbers to be obscured. Dashed horizontal lines represent the boundaries of a duct. Further, all plots are of the flat-earth variety. Since the superrefracted rays have a radius of curvature greater than that of the earth's surface the standard upward paths seem to curve away from the "flat" earth.

The figures are organized by duct type and then labeled with path type and any other distinguishing characteristics. Path type is upward path, short downward path, long downward path, or ducted path. There are also variations on these and at times, because of ducting distortion, the path type definitions become blurred.

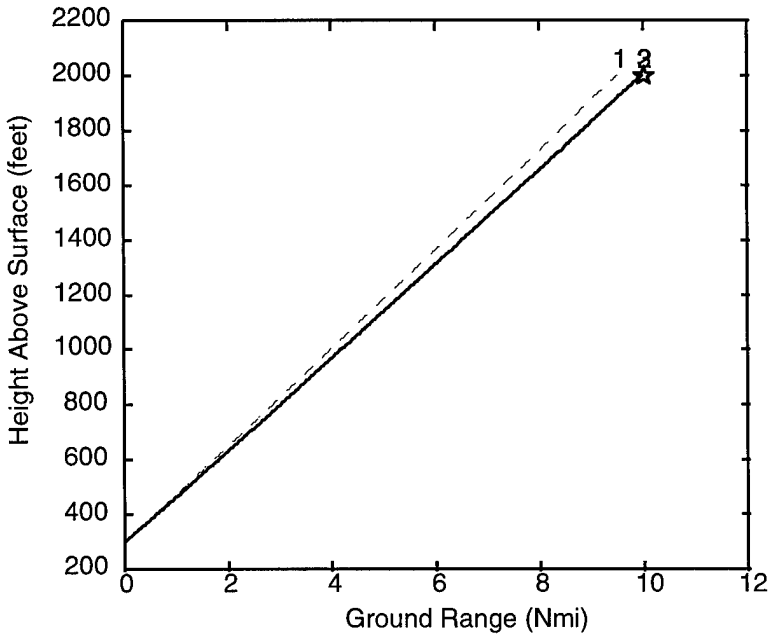

Figure 4.12 No duct -- upward path

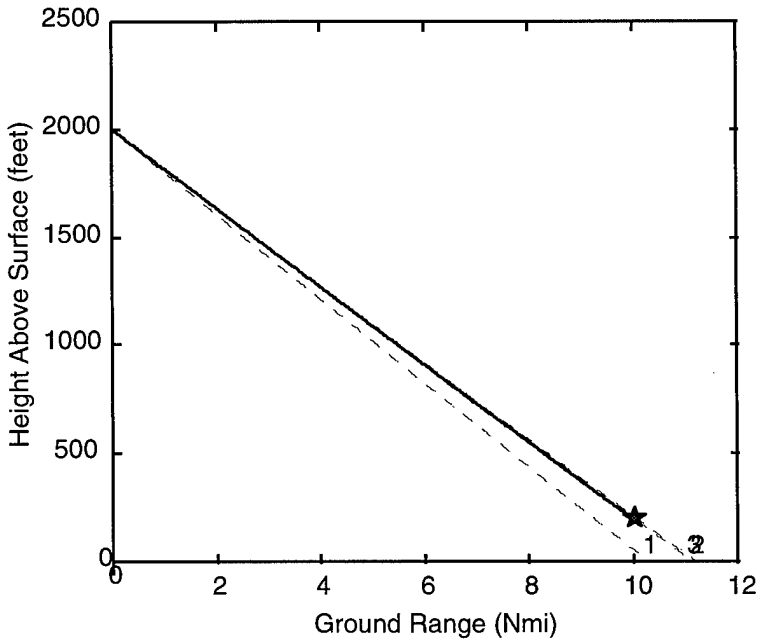

Figure 4.13 No duct -- short, downward path (target reached before ray hits surface)

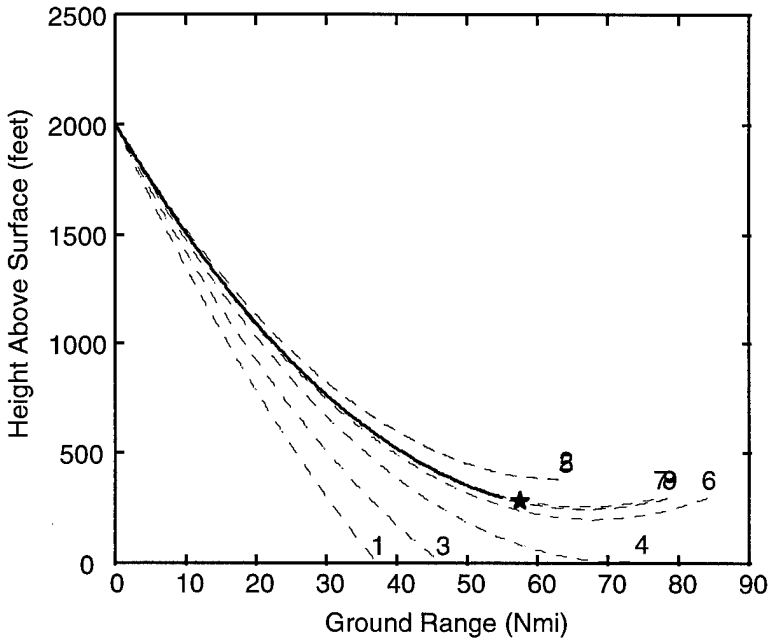

Figure 4.14 No duct -- short downward path (target reached before tangent point)

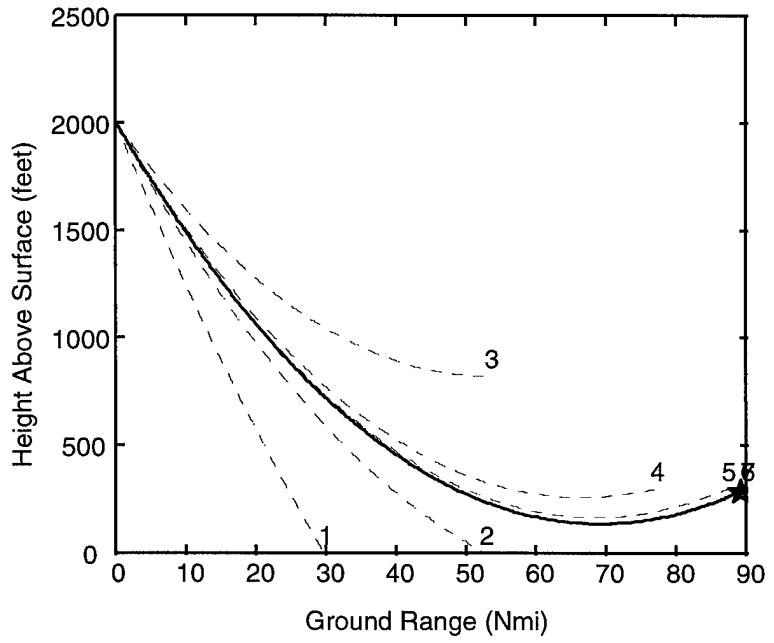

Figure 4.15 No duct -- long, downward path (target lower than radar)

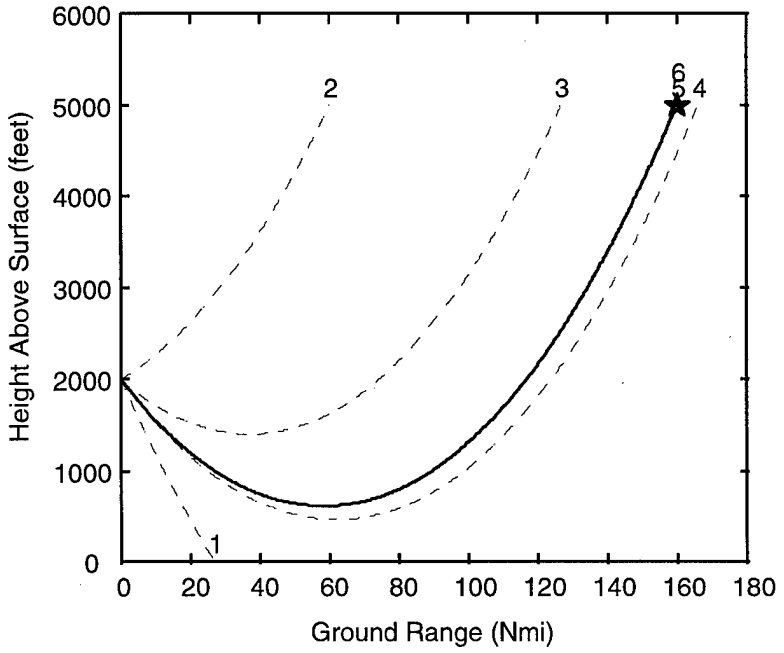

Figure 4.16 No duct -- long, downward path (target above radar)

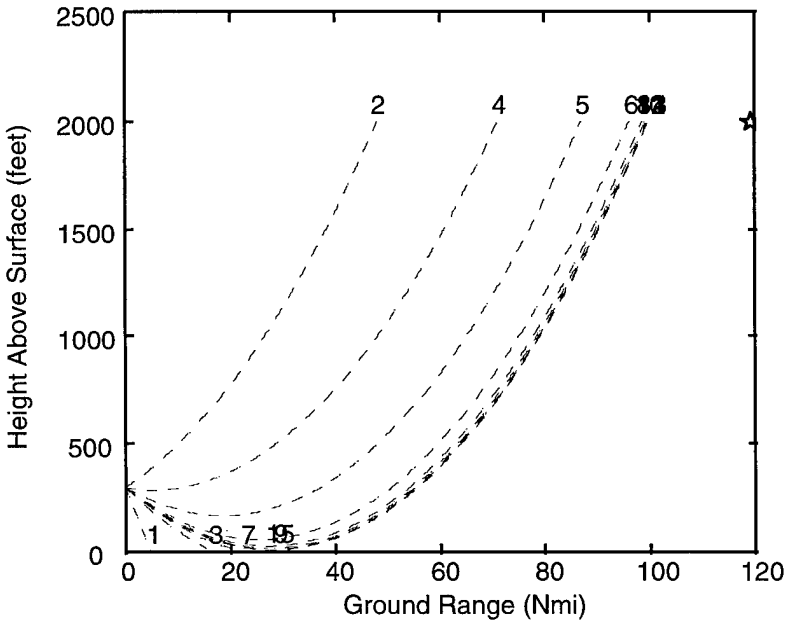

Figure 4.17 No duct -- target over radio horizon

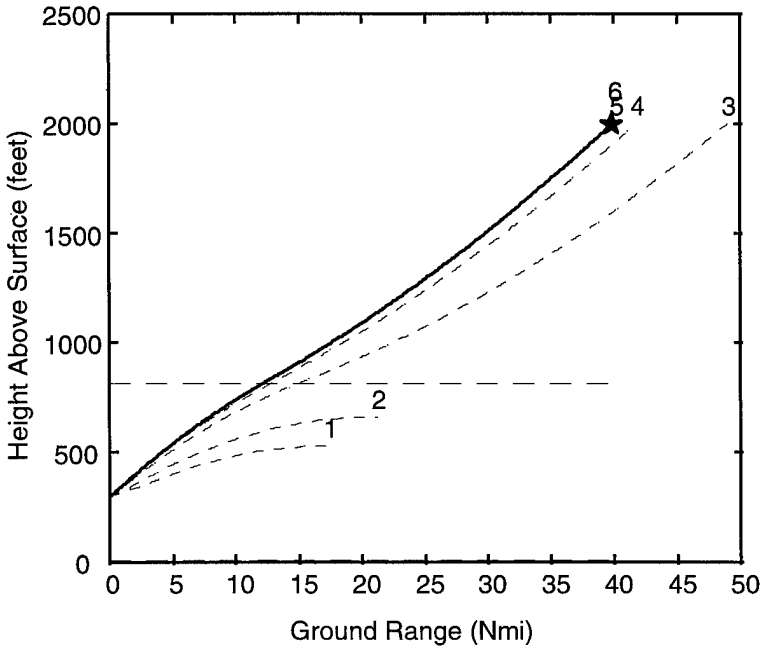

Figure 4.18 Surface duct -- upward path

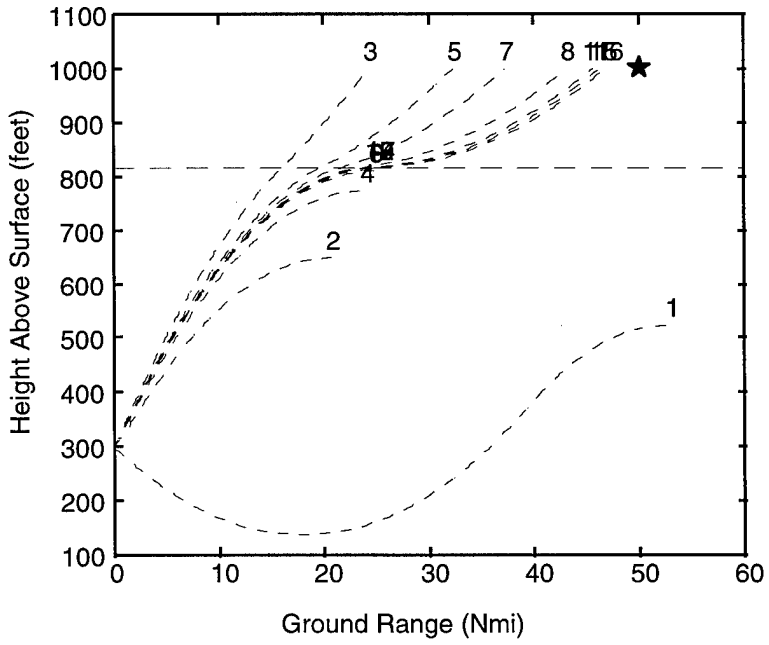

Figure 4.19 Surface duct -- upward path (target in radio hole)

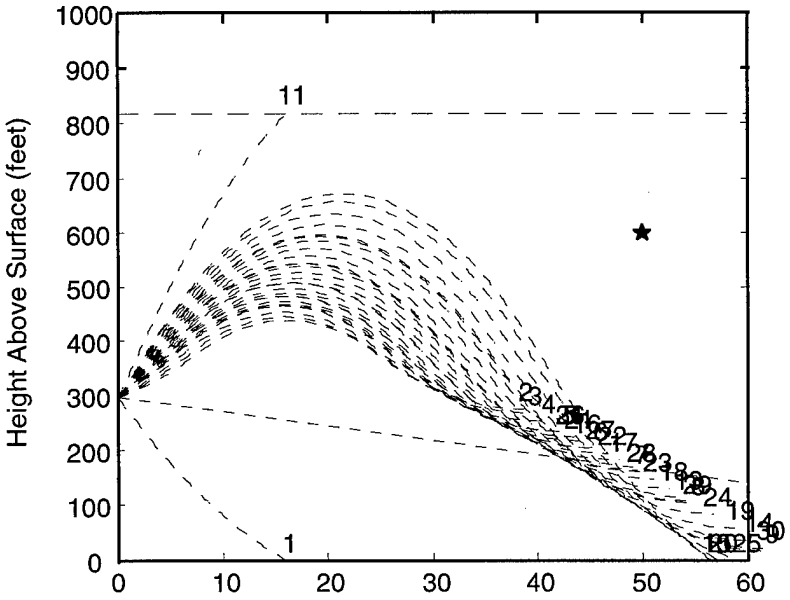

Figure 4.20 Surface duct -- ducted path

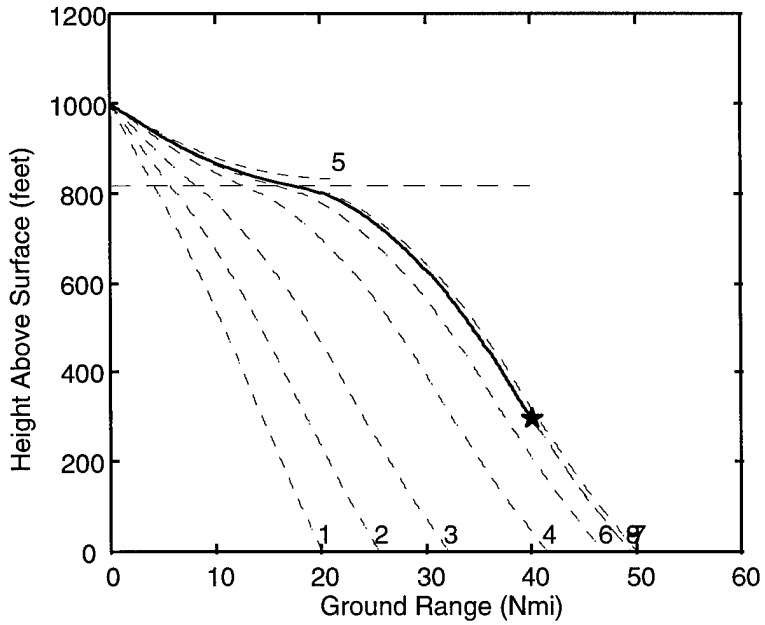

Figure 4.21 Surface duct -- short, downward path (radar above duct, target inside duct)

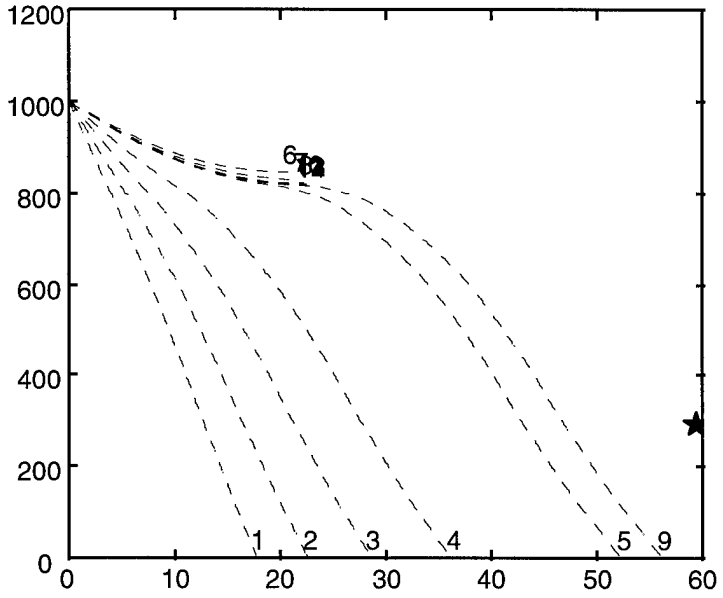

Figure 4.22 Surface duct -- downward path (radar abv duct, target in duct, in radio hole)

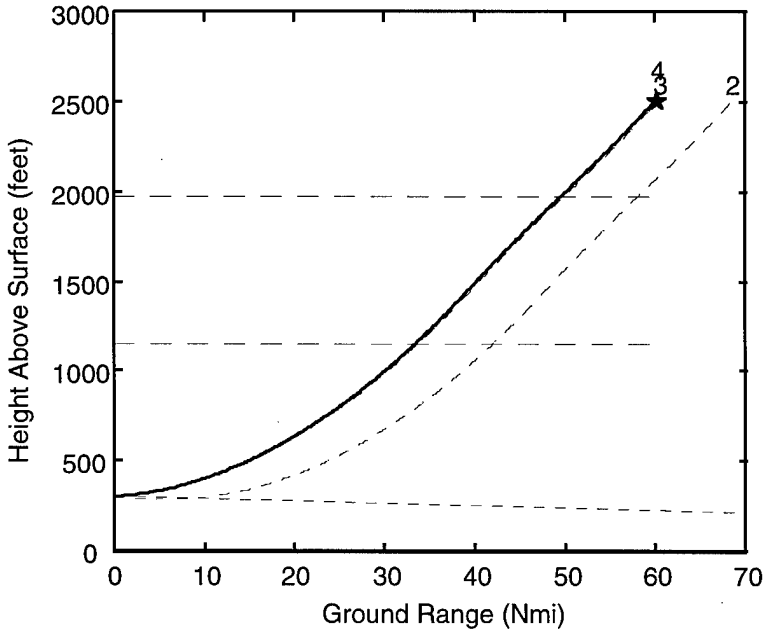

Figure 4.23 Elevated duct -- upward path (radar below duct, target above duct and far)

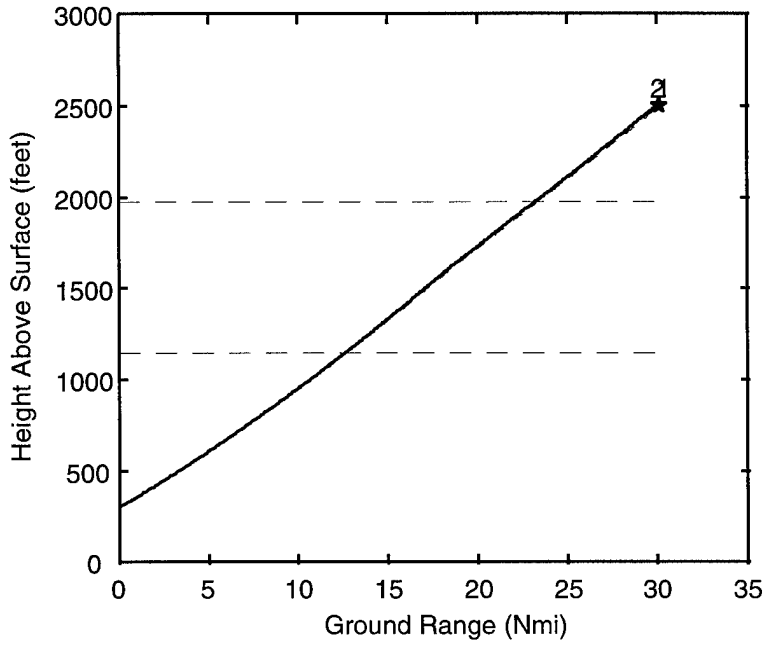

Figure 4.24 Elevated duct -- upward path (radar below duct, target above duct and near)

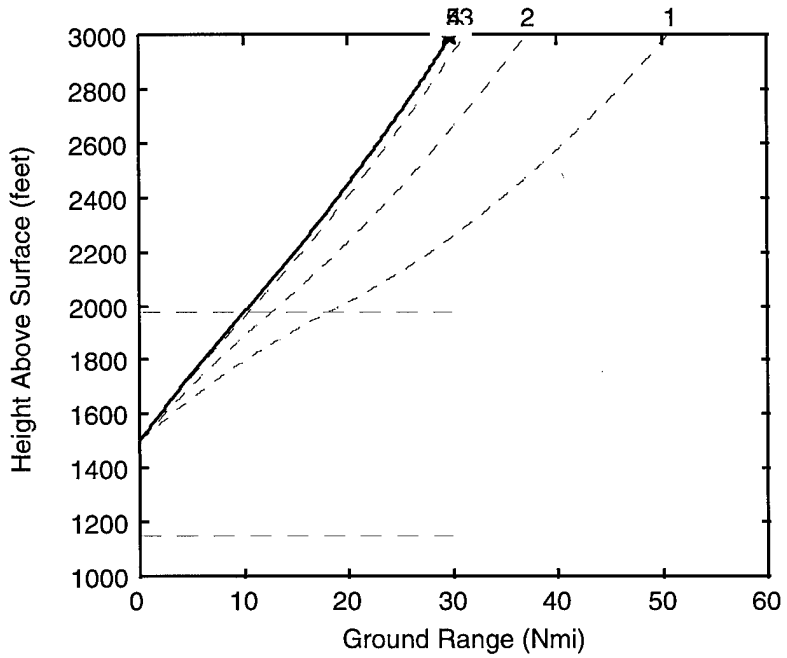

Figure 4.25 Elevated duct -- upward path (rdr in duct, tgt abv duct, before radio hole)

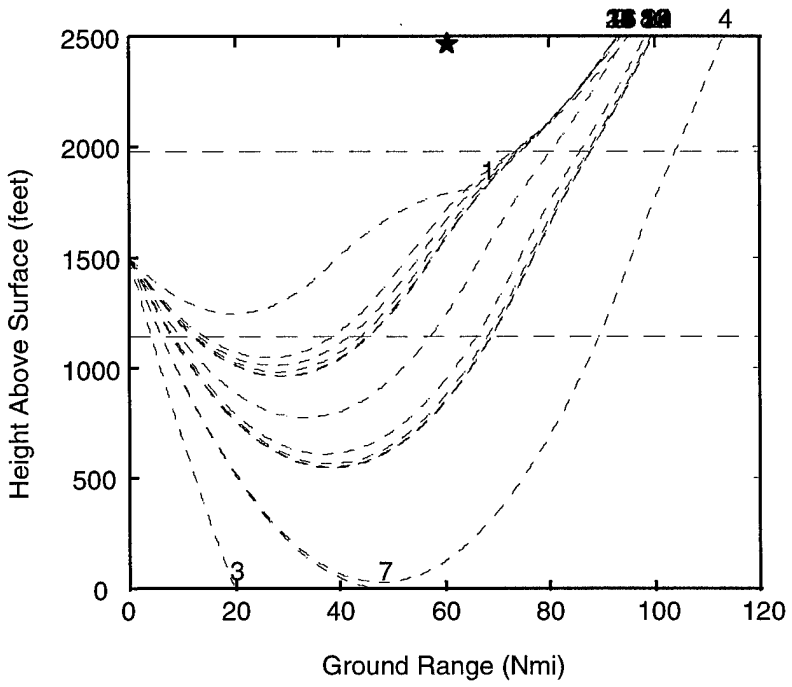

Figure 4.26 Elevated duct -- long, downward path (rdr in dct, tgt abv dct, in radio hole)

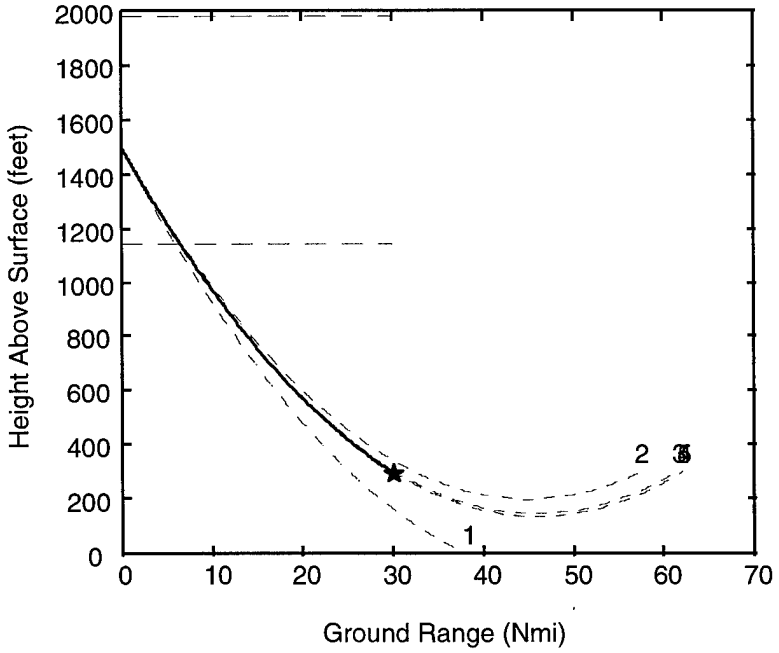

Figure 4.27 Elevated duct -- short, downward path (radar in duct, target below duct)

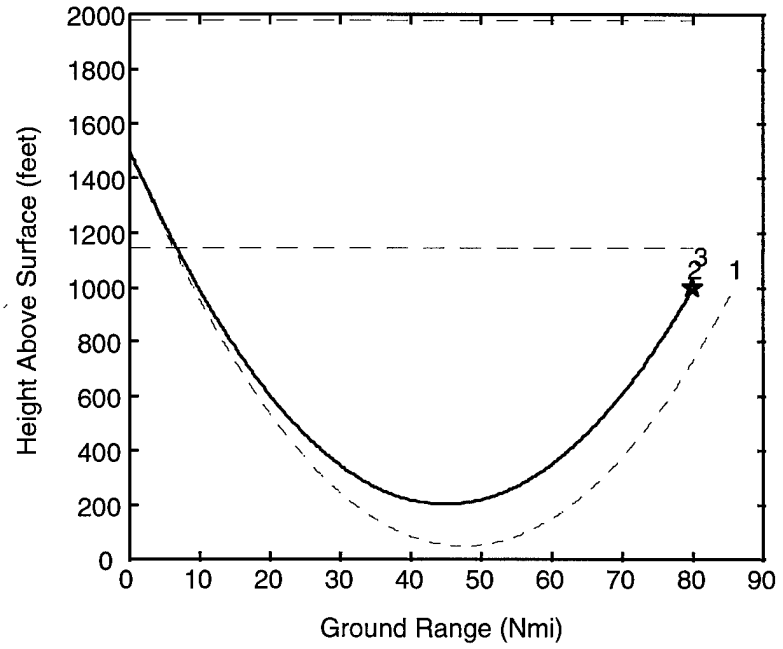

Figure 4.28 Elevated duct -- long, downward path (radar in duct, target below duct)

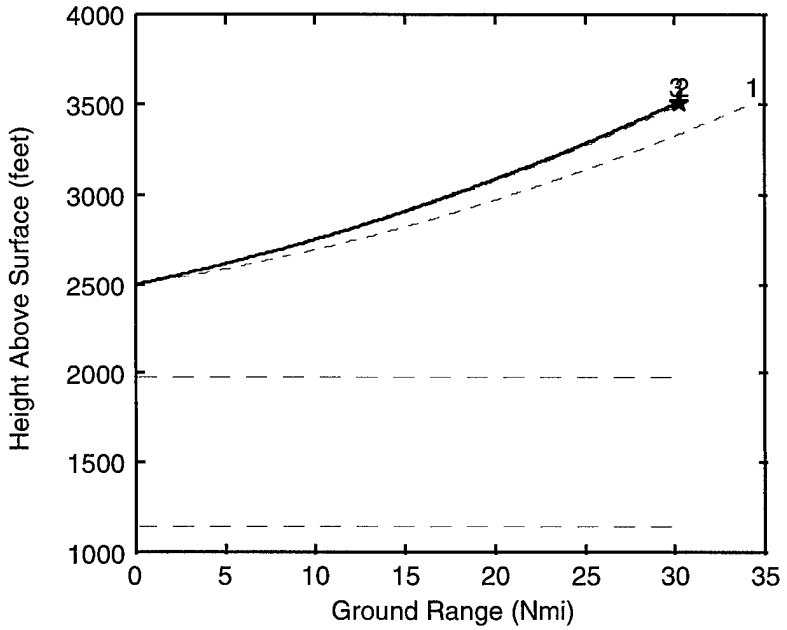

Figure 4.29 Elevated duct -- upward path (radar above duct, target above duct)

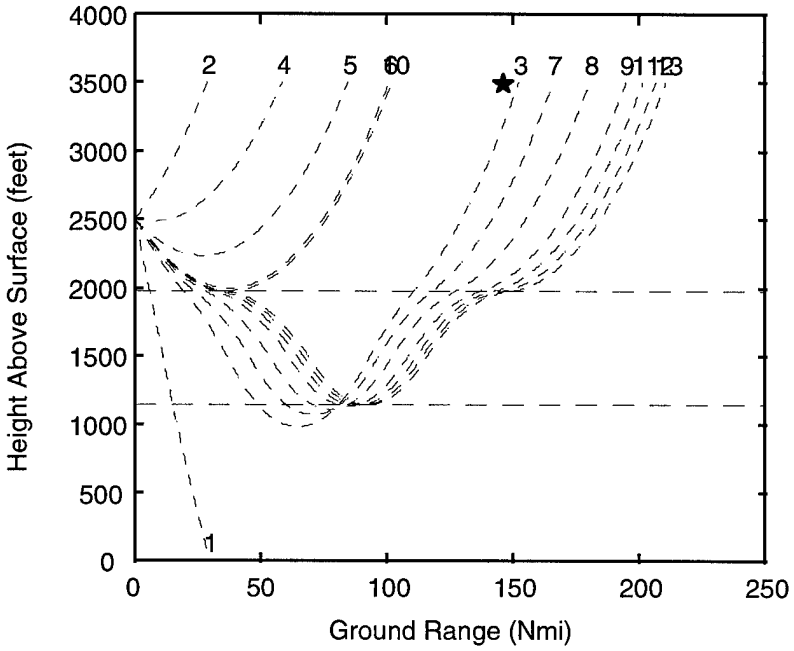

Figure 4.30 Elevated duct -- long, downward path (radar above duct, target above duct)

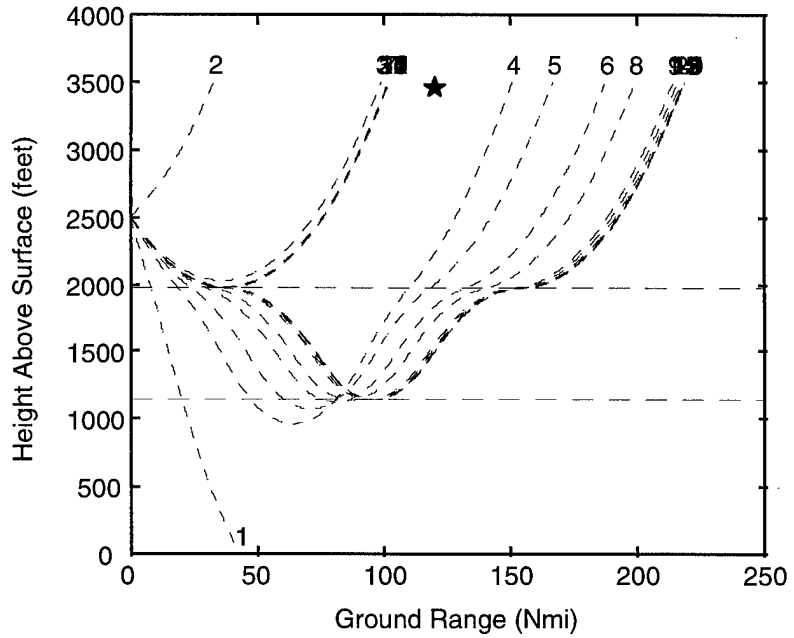

Figure 4.31 Elevated duct -- long, downward path (radar above duct, target above duct in radio hole)

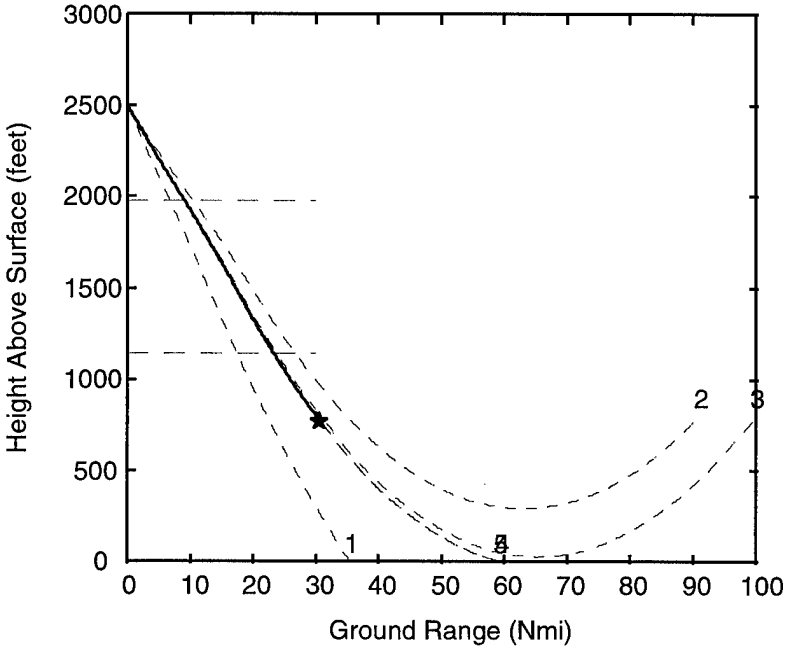

Figure 4.32 Elevated duct -- short, downward path (radar above duct, target below duct)

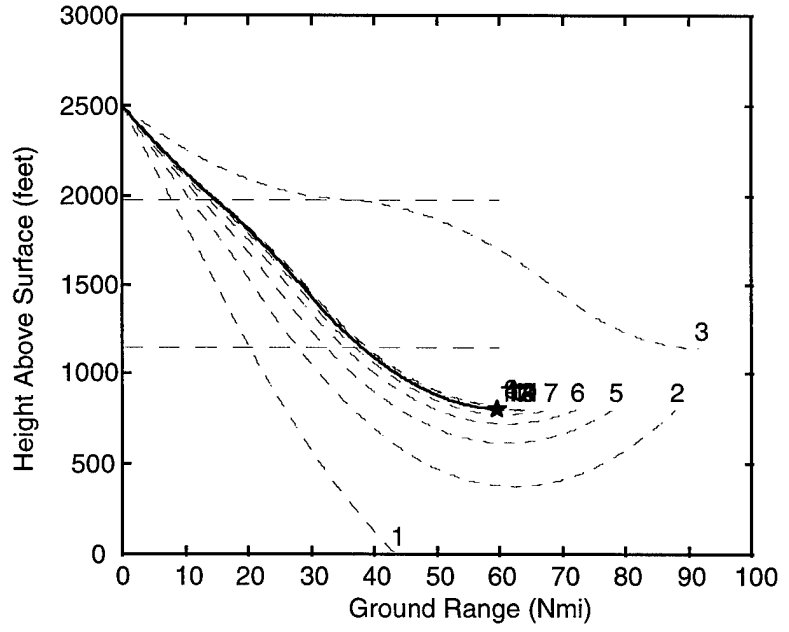

Figure 4.33 Elevated duct -- short, downward path (radar above duct, target below duct)

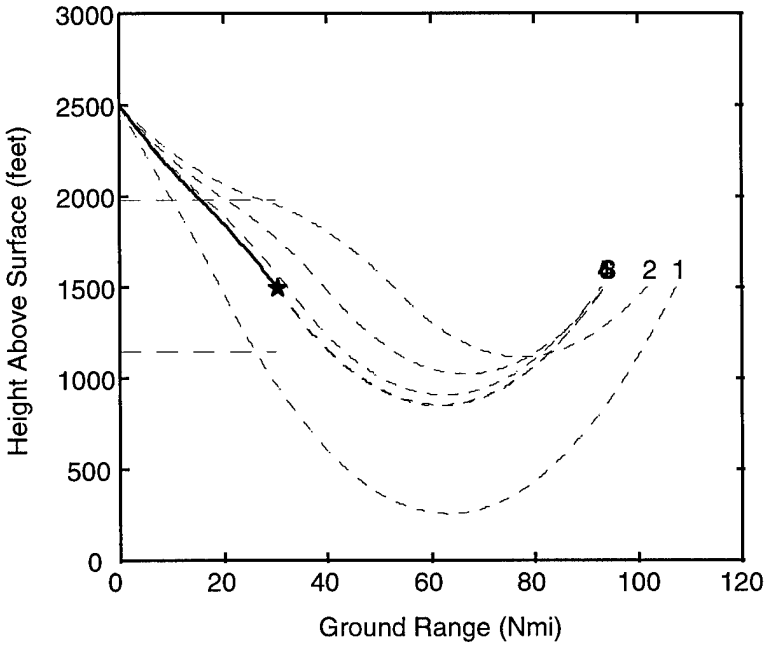

Figure 4.34 Elevated duct -- short, downward path (radar above duct, target in duct)

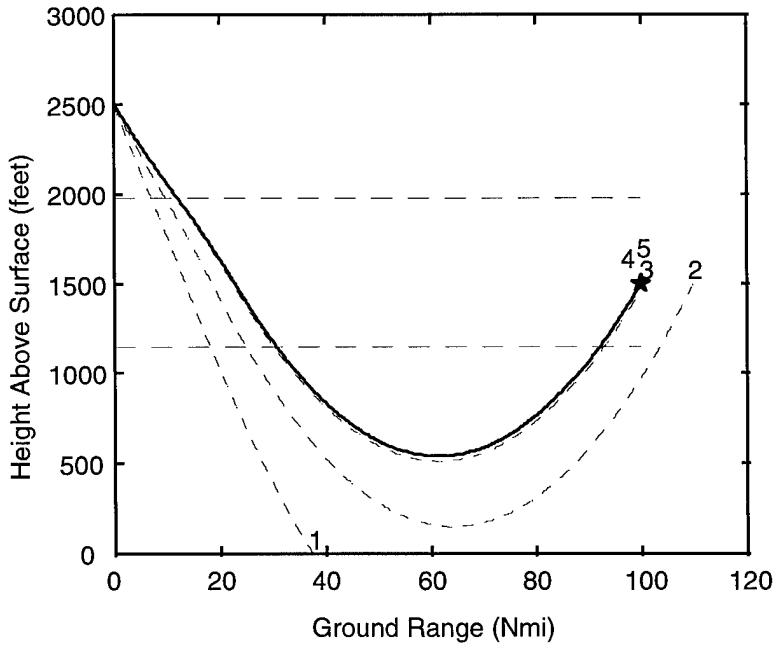

Figure 4.35 Elevated duct -- long, downward path (radar above duct, target in duct)

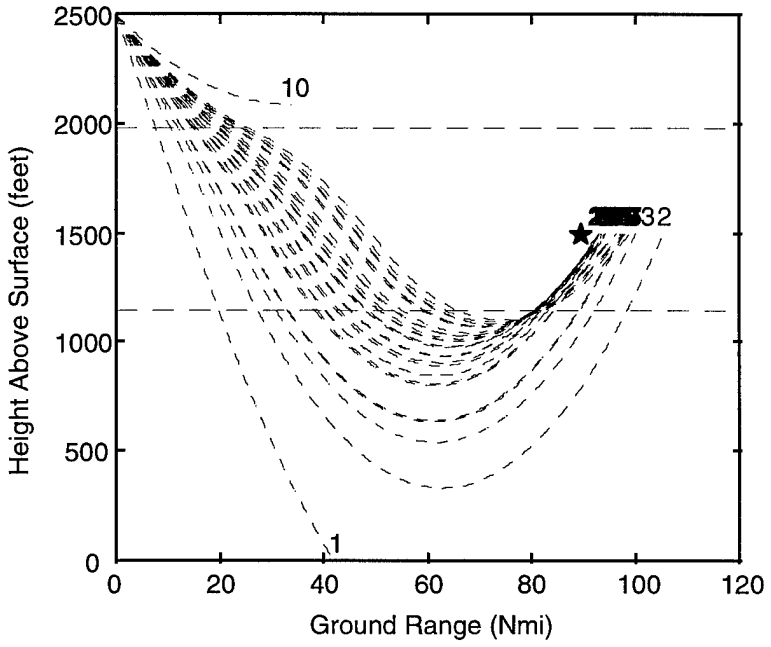

Figure 4.36 Elevated duct -- long, downward path (radar above duct, target in duct)

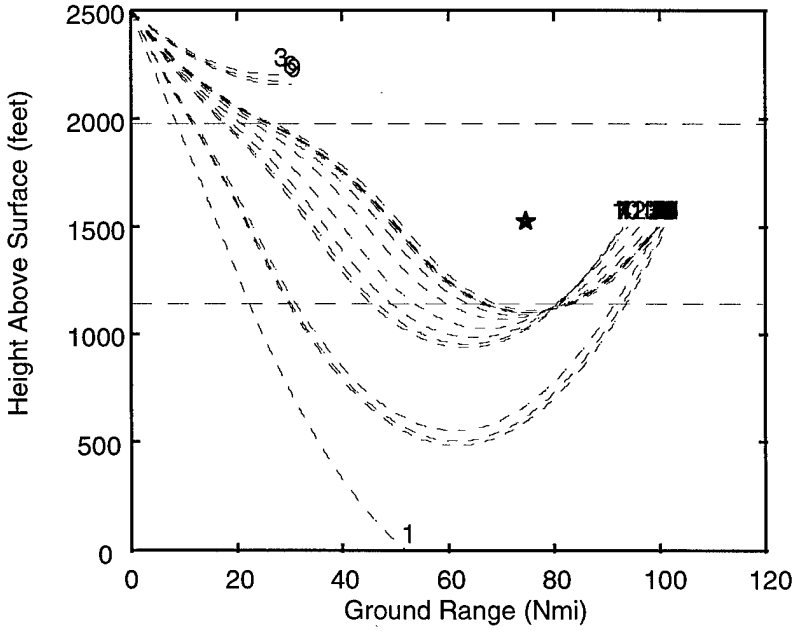

Figure 4.37 Elevated duct -- short, downward path (rdr abv dct, tgt in dct, in radio hole)

CLIMAREF correctly converged on the initial takeoff angle (to within the 10^{-6} radian tolerance) in 20 of the 26 representative scenarios presented in Figure 4.12 through Figure 4.37. There were no problems at all when no duct was present. When the target was over the horizon, the program responded with an error message to that effect. Even when ducting was present, the program responded correctly to many odd situations. Particularly, for the situations illustrated in Figure 4.19 and Figure 4.22 CLIMAREF correctly reported the target was in a radio hole. Although some situations took more iterations to find the target than others, in the simple cases three usually sufficed.

Unfortunately, six of the scenarios baffled CLIMAREF and it timed out after attempting the maximum 30 estimations. Careful examination of these cases (Figure 4.20, Figure 4.26, Figure 4.30, Figure 4.31, Figure 4.36, and Figure 4.37) reveal two distinguishing characteristics of traces that failed: 1) both the radar and the target were in the duct together and the path was a ducted path, or 2) the path was a long downward path in which the rays crossed (apparently as an effect of an elevated duct).

The immediate reasons for these two types of breakdown are readily discernible: In a duct (at least in the mathematical kind used in CLIMAREF), there are many paths (hence takeoff angles) that will lead to a given target. Because of how the rays are refracted, rays starting from a variety of takeoff angles will, at times, cross causing more ambiguity. A similar mechanism causes the rays in the downward path through the elevated duct to cross, again resulting in ambiguity.

Without further discussion, a fundamental problem is apparent. One of the limitations of geometrical optics (see chapter 2) is that adjacent rays must remain

approximately parallel to each other within a wavelength. In other words, in a valid raytrace, rays can not cross. This is an important observation that is treated further in the next chapter.

Numerical analysis provides further insight into the problem. The estimation algorithm used by CLIMAREF depends upon accurate knowledge of $\delta\beta/\delta\alpha_0$, that is, how much the subtense of the ray endpoint changes for a given change in the takeoff angle. This derivative must be such that the estimation can start from an initial guess (four-thirds earth in this case) and find the takeoff angle that will result in the correct subtense. Figure 4.38 through Figure 4.41 were created using the RAYSD test routine to plot traces for several different angles under various circumstances. In each figure, one or more horizontal lines were plotted to intersect the traces at a constant height (representing the target height, or trace endpoint height). The $\beta(\alpha_0)$ values at the intersections were plotted against the α_0 values as shown in the accompanying figures.

In Figure 4.38 and Figure 4.39 where there is no ray crossover, the β vs. α_0 plots are continuous. Note in Figure 4.39 the rightmost point is estimated since there is no trace in (a) that just touches the hypothetical target height. In Figure 4.39 there are two β values for every α_0, but the curve is still continuous. In both of these cases, $\delta\beta/\delta\alpha_0$ is defined for all β so that the estimation algorithm can eventually iterate to the correct takeoff angle. For instance, using Figure 4.39, suppose the target subtense, β_T, is 0.87 degrees. Suppose further that the initial takeoff angle estimate, α_0, is -0.325 degrees corresponding to two target height (estimated) subtenses, β_e, of 0.7 and 0.18. Using the solution that puts β_e nearer β_T, the slope of the curve tells us to decrease α_0 to get closer

to the target subtense. Continuing in this manner, specifically using equations 3-45, 3-50, and 3-51, the correct takeoff angle eventually will be found.

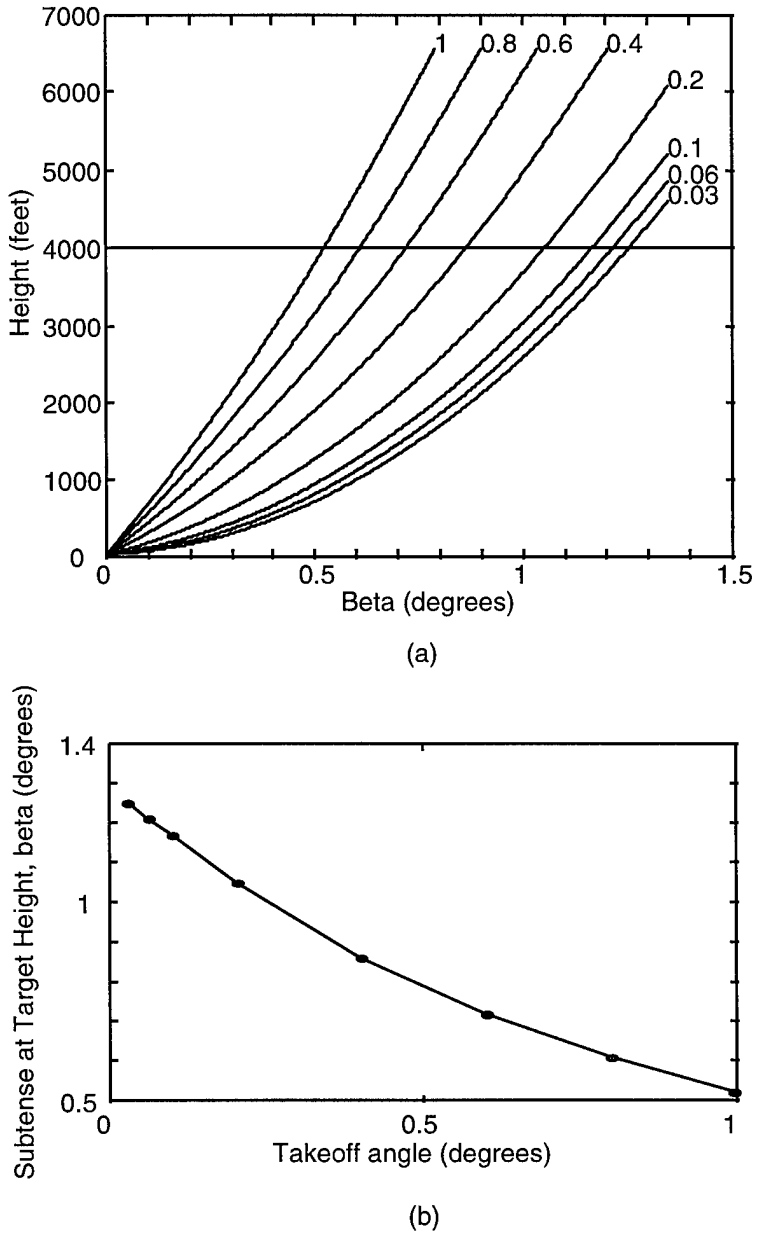

Figure 4.38 Subtense vs. Takeoff Angle Analysis (Radar Low, Target High, No Ducting), (a) traces for various takeoff angles, (b) ray subtense at 4000 feet for various takeoff angles

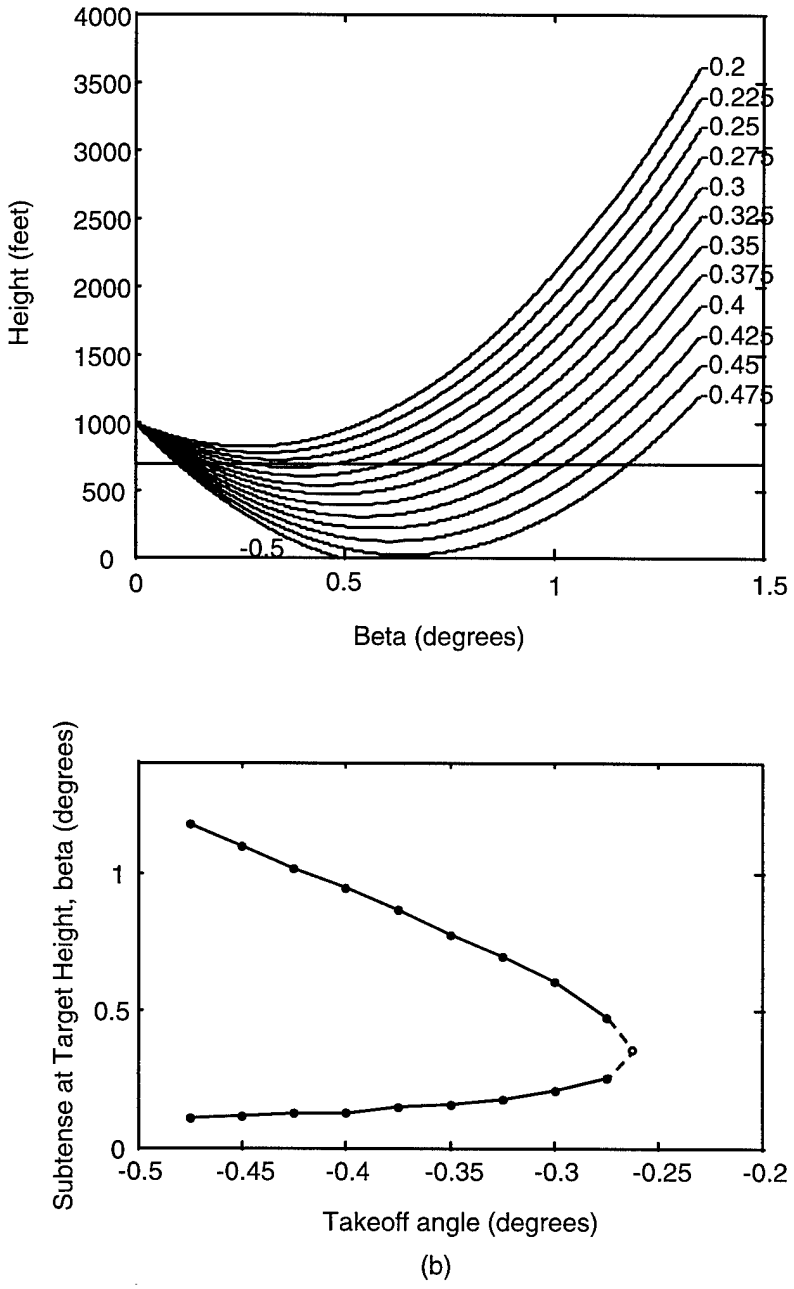

Figure 4.39 Subtense vs. Takeoff Angle Analysis (Radar High, Target Low, No Ducting), (a) traces for various takeoff angles, (b) ray subtense at 700 feet for various takeoff angles

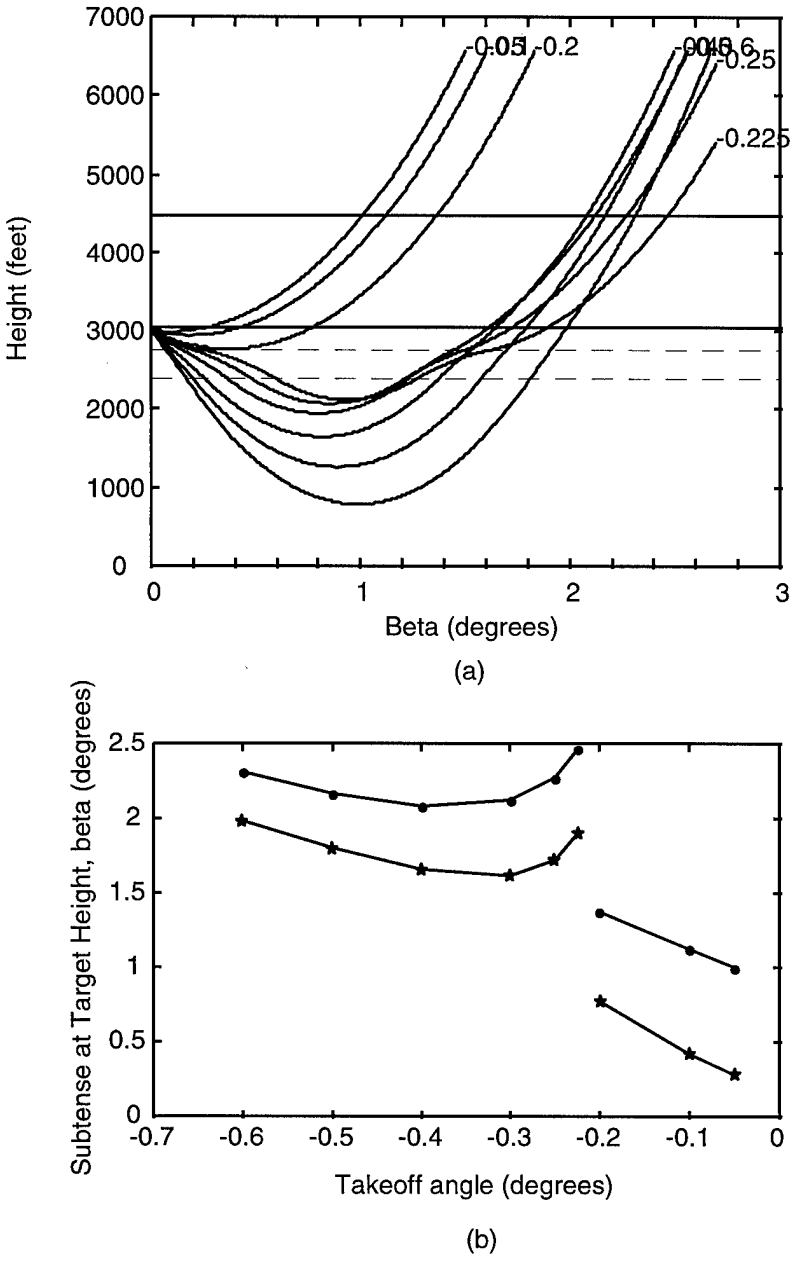

Figure 4.40 Subtense vs. Takeoff Angle Analysis (Radar High, Target Higher, Elevated Ducting), (a) traces for various takeoff angles, (b) ray subtense at 3050 feet (circle) and 4500 feet (star) for various takeoff angles

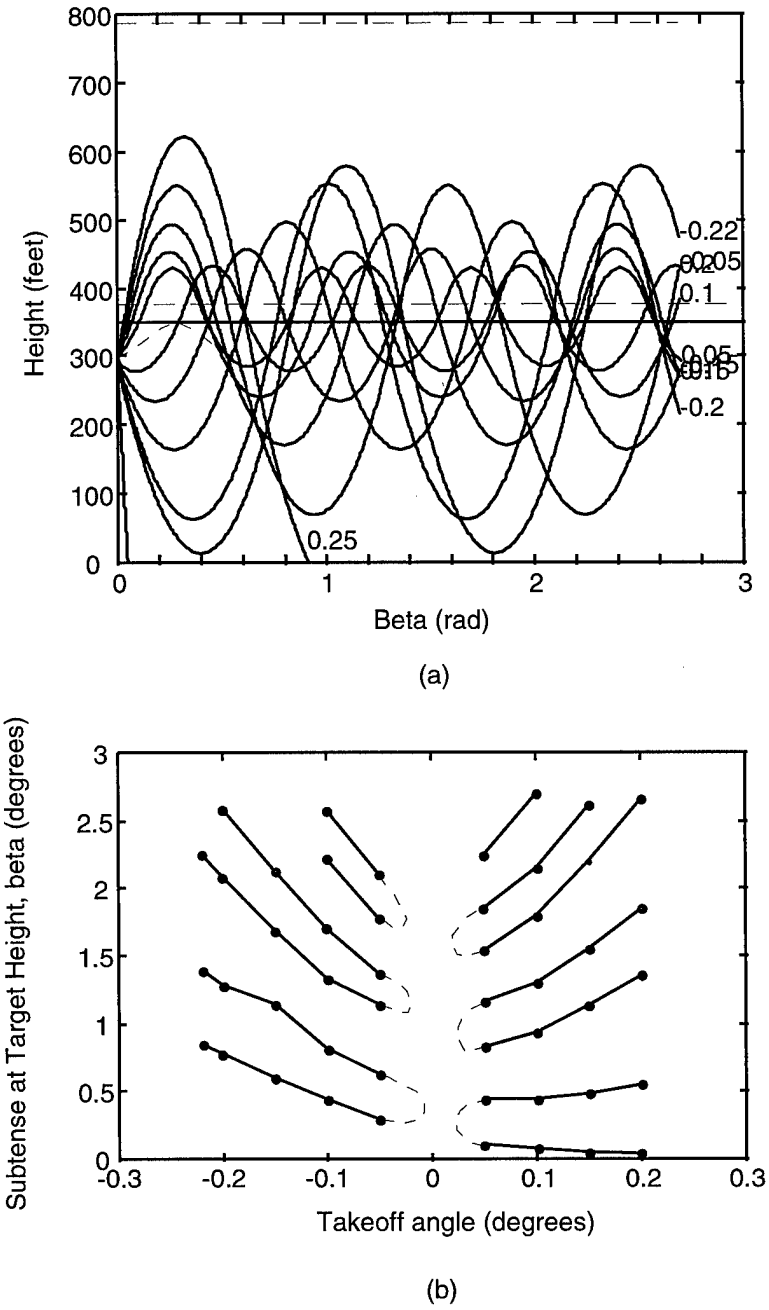

Figure 4.41 Subtense vs. Takeoff Angle Analysis (Radar High, Target Higher, Elevated Ducting), (a) traces for various takeoff angles, (b) ray subtense at 350 feet for various takeoff angles

In contrast, the situations depicted in Figure 4.40 and Figure 4.41 cause problems for the estimator. Figure 4.40(b) is an example of β vs. α_0 curves with discontinuities caused by the radio hole. By themselves, discontinuities are not a problem. They make certain subtenses impossible to reach, but that is a natural situation we want to model. However, the slope reversal at $\alpha_0 \approx -0.35$, caused by the crossover effects of the duct causes the estimator to go in the wrong direction. For example, suppose the correct takeoff angle, α_0, is -0.1 corresponding to a target subtense, β_T, of 1.13 degrees (in the 4500 feet case), and that the initial estimate is -0.4 degrees resulting in an initial estimated subtense, β_e, of 2.08 degrees. In trying to following the slope of the curve down to the target subtense, the estimator will eventually bottom out at some minimum subtense around 2.1 degrees. Of course, if the initial guess is chosen close enough to the final takeoff angle, the estimation will converge nicely. As written, however, CLIMAREF estimates based on four-thirds earth exclusively.

In the case of ducting the β vs. α_0 plot is even more contorted. Each pair of lines (one line in negative halfplane and one line in positive halfplane) represents one set of intersections of the vertically oscillating rays with the hypothetical target height. Intuitively, given a small enough takeoff angle, the curves for each pair of adjacent cycles will join as approximated by the dashed lines. The single common point of intersection occurs when the trace just barely touches the target height (instead of crossing it twice) as illustrated by the dashed hypothetical trace in Figure 4.41a.

Examination of Figure 4.41b reveals four peculiar characteristics of the ducting situation. First, traces with small enough takeoff angles will never reach the target height

at all. Second, a given subtense may be reached by traces of more than one takeoff angle. Third, a given takeoff angle can reach multiple subtenses (similar to the long, downward path illustrated in Figure 4.39). And, finally, the curves are discontinuous, not in such a way as to absolutely forbid reachability of certain subtenses, but to make the reachability of some subtenses dependent upon the initial α_0 estimate. For example, if an initial α_0 estimate of 0.1 is chosen and the target subtense is 0.75, there is no curve (no $\delta\beta/\delta\alpha_0$) the estimator can use to arrive at the necessary α_0. This is because arbitrarily large positive or negative angles will not oscillate. That is, large positive angles leave the duct and large negative angles hit the ground to be absorbed or reflected. Therefore the curves ultimately break off on either side making it impossible for some initial takeoff angles to intersect a cycle-pair that will cover a subtense range containing the target subtense. CLIMAREF is designed to accommodate the first three difficulties. This last one, however, it can not overcome using only the four-thirds earth estimation.

So CLIMAREF was tested for algorithm validity, improvement over standard atmosphere and the ability to trace in a variety of scenarios. Chapter 5 contains conclusions drawn from these results.

V. Findings and Conclusions

Attempting to simulate nature on a digital computer is a risky project comparable in its audacity to building the Tower of Babel. The test results described in the previous chapter demonstrate that CLIMAREF, the model developed for this thesis, can successfully predict radar beam paths and height error with more accuracy than four-thirds earth and standard atmosphere. Additionally, they indicate areas of the modeling problem that require more study. At this point, an attempt is made to draw some conclusions from those results in order to guide those whose task it may be to complete the Tower.

Validation: CLIMAREF vs. Blake and CLIMAREF vs. RAYS

The test against Blake is particularly significant since NAIC from the beginning designated Blake as the standard reference. Happily, the simple test passed with flying colors proving that the algorithms in CLIMAREF, at least for simple situations, are as good as the best.

Likewise, the close match between RAYSD and RAYS shows that CLIMAREF matches the industry standard as well as can be determined given the limited output capability of RAYS.

Minimum Elevation Angle

The tests described in Chapter 4 indicate CLIMAREF will not be able to complete a trace if the initial takeoff angle is so small that the N-gradient causes it to reach an extrema in the first layer in which bending is calculated. Although time did not permit extensive testing to determine the relationship between takeoff angles, layer thicknesses, and N-gradients, a few general conclusions can be made.

The takeoff angle used in the small negative angle test was $\alpha_0 = -5.6530 \times 10^{-5}$. CLIMAREF chose this angle to launch a downward trace that would pass through a tangent point and hit the target on the upswing. The target was five meters above the radar at a range of ten kilometers. When the target was raised one meter or lowered five meters, the problem went away. Although the specified target height and range do not directly correspond to the initial estimated takeoff angle (since this angle only defines the first of several iterations needed to find the correct angle), some conclusions can be drawn. For instance, it can safely be said that the small angle problem at a range of ten kilometers is only a problem when the target height is within a few meters of the radar height. Extrapolating to a range of one hundred kilometers, we might expect small angle problems within a few tens of meters of the radar height. Obviously, the significance of the problem depends on the application.

Although this limited test found no problems resulting from a small positive angle, the same effects described in Chapter 4 for small negative angles will presumably be experienced using small positive angles within a duct. This is because the steep negative M-gradients in the upper portion of a duct will cause a positive-going ray to

reach an extrema and bend downwards – behaving similarly to a downward path in a non-ducted atmosphere.

Additional measures need to be devised to allow CLIMAREF to handle these small angles. A simple, if costly, solution is to decrease the layer thickness to something less than one meter (as it is currently set). This reduction of the layer thickness will allow smaller angles to be used, but it will not eliminate the problem altogether. Furthermore, the computing time will increase by approximately the layer reduction factor since that many more layers will have to be traced through to reach a solution.

A similar, but more efficient solution might be to reduce the layer thickness on the fly only when necessary to avoid the small angle problem. It may take more iteration to find the necessary layer thinness, but extra time only would be required when a problem exists. For the vast majority of raytracing situations there will be no small angle problem.

A third solution, simpler but less effective, is to artificially eliminate the problem by disallowing small angles. Anytime a small takeoff angle coming out of the estimator causes a problem, it could be amplified just enough to eliminate the error. The negative impact is that such a solution would likely create an artificial radio hole, making some targets impossible to see.

In any case, small angles are currently a weak spot in CLIMAREF and more testing will need to be performed to determine how best to solve the problem.

Climate Variation

The climate variation test proves without a doubt that climatology-based raytracing outperforms the standard atmosphere model with respect to accuracy of prediction. With the target at 10,000 feet and 60 nautical miles out, CLIMAREF predicted height error magnitudes ranging from 101.2 to 2256.0 feet. These are, respectively, 702.8 and 1452.0 feet away from the height error calculated using standard atmosphere, 804.0 feet. Although the overall mean of 987.0 feet was close to standard atmosphere, overall average deviation from standard atmosphere was about 400 feet. A particularly unusual result was calculated for Fort Lamy, Chad with elevated ducting in January: the height error was actually negative at –1973.1 feet. Such radical departures from standard atmosphere will be useful to radar engineers using AMBER to more accurately predict radar performance.

The climate variation test provides insight not only into the utility of CLIMAREF, but also into the propagation effects that can be expected under various climatic conditions. Note that these results, as children of the HEPC database, represent mean conditions only. No variation data is available or represented.

In addition to proving the superior accuracy of CLIMAREF, the data provides many insights into the climatological aspects of this subject. For example, the extreme climates of Jodhpur (monsoon region), Chad (the Sudan), and the coast of Libya (Mediterranean climate) are reflected in the wide-ranging height errors. Particularly notable is the negative height error corresponding to January in Chad under elevated ducting conditions. This unusual effect occurred because the ray was subrefracted, that

is, it actually bent away from the earth. Obviously, the superrefractive case is more typical, but subrefraction can and does occasionally occur. On the other hand, places with more moderate climates like Port Hardy, Churchill, Denver, Bismarck, and Columbia are notable for their lack of variation and for how closely they agree with the standard atmosphere.

The conclusion is obvious. Climate does affect radar beam bending to a large extent. An appreciation for how significant the effect is may be gained by considering the Federal Aviation Administration mandates 1000 feet vertical separation between air traffic patterns as an acceptable safety margin. The variation of the error data presented, being on the same order of magnitude, makes the effects of climate worth noting. Of course, the significance ultimately depends on the application of the model, but the FAA standard is a good benchmark.

Capability of Model to Handle All Types of Refractive Effects

These tests prove that CLIMAREF can model most radar-target-atmosphere scenarios with only a few exceptions. Again, the model can recognize when the target is in a radio hole and when it is over the horizon. It can trace upwards or downwards and can properly work through the tricky business of a tangent point. Furthermore, it can differentiate between a target on the short downward path or the long downward path. Also, it can model many ducting effects, albeit with a few more iterations of the estimator. It works properly for the most common situations.

Nonetheless, CLIMAREF is not perfect. It can not satisfactorily trace when the duct causes the traces to cross or when the path to the target is a pure ducted path.

Probably the most striking observation about both situations is that the second limitation of raytracing (discussed in Chapter 2) is being violated: that is, neighboring rays must remain close to parallel within one wavelength. Further research is required to determine exactly why the model atmosphere violates this condition. Most likely, the steep gradients inherent in the inversions are the problem. Depending on the frequency in use, these gradients may also violate the first condition of geometric optics (the refractive index must not vary appreciably in one wavelength). So, it may be that completely different methods need to be used to model the more serious effects of ducting.

On the other side, EREPS RAYS, which is a component of the premiere modeling package for this sort of thing, traces in and through the ducts matching CLIMAREF trace for trace, with rays oscillating and crisscrossing all through the duct. So, either both models are wrong to raytrace in the duct, or the limitations do not apply in this case (for some reason) and problems in CLIMAREF must be overcome another way.

Apart from considerations of the applicability of raytracing, the β vs. α_0 plots at the end of the last chapter suggest that part of the problem has to do with the initial elevation angle estimate. Both scenarios in which tracing will potentially break down (Figure 4.40, and Figure 4.41) can be made to work if the initial takeoff angle estimate is close enough to the final required value. By taking the effects of the ducts into account, it is possible a more sophisticated estimation procedure can be developed that will make these disturbing anomalies irrelevant. Alternatively, logic could be employed to

recognize the traps caused by such effects in order to redirect the estimation and iteration procedure around them.

Nevertheless, the question of whether or not these techniques violate the basic assumptions of geometric optics must be answered and the answers must be dealt with. Since most analysis of ducting is performed using waveguide theory and physical optics, it may be that these disciplines are the only way to find the path of the energy through the duct, if indeed a well-defined path exists at all. While CLIMAREF as it stands is a worthy and useful tool because of the wide-variety of scenarios it can model, further study will be required to resolve these questions if it is ever to be useful and reliable under all circumstances.

Recommendations for Further Research

Due to time limitations, CLIMAREF was not developed as fully as it could be. No doubt many improvements can be made. Here are a few ideas.

First, compare CLIMAREF's predictions against actual height error statistics. The great difficulty in doing this ultimate test is getting the data. Most ground-based radars already make an attempt to compensate for beam bending. Therefore the height-measurements collected and stored are not pure. Possibly, the raw data could be tapped from the radar receiver during a dedicated test. If enough data were taken, statistics could be derived and compared to CLIMAREF predictions. Such a test would be a true measure of the model's worth.

Deciding how to trace through both the surface duct and the elevated duct at the same time could enhance the worth of the model. First, the double duct will have to be properly constructed. Patterson (1987: 15-16) describes the construction of each duct separately, but says nothing about two. Then, all the issues regarding radio holes and the unique paths produced by such a combination will have to be studied and accommodated with additional logic built into the model.

Another idea is to apply the interpolation routines to the ducting statistics as well as the surface statistics. Care must be taken to determine when these statistics can and can not be averaged.

To make the climatology database more accurate and useful, several tasks might be accomplished: Variation statistics could be researched and added to the mean data in the database. This would give the modeler a better idea of the range of height error he can expect in a given climatic situation. Also, the database could be expanded to provide a finer resolution of radiosonde stations in certain areas of interest.

Finally, to be really useful, CLIMAREF could take into account reflections and multipath and compute the power loss to the target using physical optics.

Conclusion

CLIMAREF, then, has been found to be a good tool for simulating radar beam bending. It performs well in most situations, and breaks down in some. However, the troubling issues do not seem to be irresolvable. This exploration of the issues involved with climatology-based, geometric optics-based prediction of radar beam bending is by

no means the first or the last word on the subject. However, it is the author's hope that it will play a small part in advancing the state-of-the-art of radar modeling.

Appendix A

CLIMAREF MATLAB Code

Note: Because of wraparound some of this code, as printed, is improperly formatted

```
function CR1main
global MON DYNT RLAT RLONG REL RAZ THT TRG
global ISOLATED USESTAT
global NS N1K SEL DUCTFLG MULTSTATFLG
global GMSB OHSB MTSB MDSB MFSB PSB GMEL OHEL MTEL
global MDEL MFEL PEL P2EL PSBEL PHs PMs PHe PMe PHn PMn
global R0 HEIGHTS BETAES TRGAPP ALFG ALF0
global THTAPP THTERR THTERR100 TRGERR TRGERR100 DUCTHTS ERRMSG
%CLIMAREF Main module, "cr1main.m"
%This is the main loop.  It controls all other processes
%
%VARIABLES:
%ALF0 - takeoff angle of refracted path to radar
%ALFG - geometric elevation angle of target at radar
%ang - multipurpose angle variable
%another - user input whether or not to run program again (string: y/n)
%beta - subtense counter
%BETAES - list of betas defining subtenses of every point on the trace
%betastep - rgstep in terms of subtense
%DUCTFLG - indicates type of ducting user chose
%endloop - flag to signify user termination of the program
%ERRMSG - error message (if any) output from CR9raytrace
%HEIGHTS - list of heights of every point on the raytrace
%htsft - htskm converted to feet
%htskm - heights in kilometers, used for plotting geometric path on flat
earth plot
%htstep - distance between height grid lines on curved earth plot
%intype - input data by file or manually
%ISOLATED - flag indicates radar site has no radiosonde stations around
it
%maxhtft - maximum height from surface ray reaches (in feet)
%maxrad - maximum distance from center of earth that the ray reaches
%maxrng - maximum ground range of target
%maxrngNmi - maximum ground range of target in Nmi
%MULTSTATFLG - indicates whether user chose 2 or 3 stations to
interpolate
%N1K - refractivity at 1km above surface
%NS - refractivity at surface
%p,q - generic cartesian coordinates
%PEL - probability of an elevated duct present (from duct stats)
%plottype - flat earth, 'f', or curved earth, 'c'
%PSB - probability of a surface duct present (from duct stats)
%R0 - radius from center of earth to surface (=a+SEL)
%REL - radar elevation in kilometers
%relft - radar elevation in feet
%rgstep - distance (on curved earth plot) between ground range ticks
%seeplot - y or n, whether or not user wants to see the plot
%tabeta - subtense to target based on apparent range and ray
%        initial angle of elevation
%tbeta - subtense to target based on geometric range and geometric
```

```
%        initial angle of elevation
%THTAPP - apparent (measured) target height
%ticklength - length of ground range tick marks
%TRG - actual target range
%TRGAPP - apparent (measured) target range
%trgparts - geometric range segments
%useduct - s,e, or n, whether or not user wants to use duct info for
%           the raytrace
%x,y,x1,y1,x2,y2 - multipurpose cartesian coordinates
%
%
%
%
%
endloop=0;
another=[];
intype=[];
MULTSTATFLG=0;
disp(' ')
while isempty(intype)
   intype=input('Input parameters Manually or from the preset File
(m/f): ','s');
   if isempty(intype)|(intype~='m'&intype~='M'&intype~='f'&intype~='F')
      disp('M or F, please.')
      intype=[];
   end
end
if intype=='F'|intype=='f'
   CR2in_pre   %Call pre-set user input module
else
   CR2in          %Call user input module
end

CR3findnerstats  %Find nearest stations to radar
if ISOLATED==0  %Run these if the radar DOES have stations around it
   CR4calcdist %Find distances of nearest stations
   CR5pickstat %Allow user to choose a radiosonde station
   CR6loadNdata %Retrieve refractivity, elevation values for station

else
   disp(' ')
   disp('Your radar is too far away from any radiosonde station in the')
   disp('database.  The refractivity profile will be calculated using')
   disp('the standard atmosphere (universal average).')
   NS=313;
   N1K=271;
end

if length(NS)>1 %If loadNdata returned more than one NS,
   MULTSTATFLG=1;
   CR7interp       %interpolate
end

if NS==0
   disp(' ')
   disp('No data for this station.  Run again and choose a different
station.')

else
```

```
   CR8ductstats %get duct statistics

   if ~PSB&~PEL,disp('No ducting data for this station.'),end

   if USESTAT~=999&~MULTSTATFLG&(PSB|PEL)

      disp(' ')
      disp('SURFACE-BASED DUCTS')
      disp(['Surface to Inflection Pt N-unit Gradient: ' num2str(GMSB)])
      disp(['Optimum Ht (layer base): ' num2str(OHSB) 'km'])
      disp(['Duct Thickness: ' num2str(MTSB) ' km'])
      disp(['M-Unit Deficit: ' num2str(MDSB)])
      disp(['Max. Frequency Trapped: ' num2str(MFSB) ' MHz'])
      disp(['Percent of Time Duct Occurs: ' num2str(PSB) ' %'])
      disp(' ')
      disp('ELEVATED DUCTS')
      disp(['Surface to Inflection Pt N-unit Gradient: ' num2str(GMEL)])
      disp(['Optimum Ht (layer base): ' num2str(OHEL) ' km'])
      disp(['Duct Thickness: ' num2str(MTEL) ' km'])
      disp(['N-Unit Deficit: ' num2str(MDEL)])
      disp(['Max. Frequency Trapped (MHz): ' num2str(MFEL) ' MHz'])
      disp(['Percent of Time Duct Occurs: ' num2str(PEL) '%'])
      disp(['Probability of >1 Elevated Duct: ' num2str(P2EL) ' %'])
      disp(' ')
      disp(['Probability of Surface-Based and Elevated Duct: '
num2str(PSBEL) ' %'])

      useduct=[];
      disp(' ')
      while isempty(useduct)
         disp('Take into account ducting:')
         if PSB&PEL
            useduct=input('Surface duct, Elevated duct, or No duct
(s/e/n)? ','s');
            if
isempty(useduct)|(useduct~='s'&useduct~='S'&useduct~='e'&...
                  useduct~='E'&useduct~='n'&useduct~='N')
               disp('S, E, or N, please.')
               useduct=[];
            end
         elseif ~PSB&PEL
            useduct=input('Elevated duct or No duct (e/n)? ','s');
            if isempty(useduct)|(useduct~='e'&useduct~='E'&...
                  useduct~='n'&useduct~='N')
               disp('E or N, please.')
               useduct=[];
            end
         elseif PSB&~PEL
            useduct=input('Surface duct or No duct (s/n)? ','s');
            if isempty(useduct)|(useduct~='s'&useduct~='S'&...
                  useduct~='n'&useduct~='N')
               disp('S or N, please.')
               useduct=[];
            end
         end
      end

      if useduct=='S'|useduct=='s'
         DUCTFLG=1;
```

```
      elseif useduct=='E'|useduct=='e'
         DUCTFLG=2;
      elseif useduct=='N'|useduct=='n'
         DUCTFLG=0;
      end
   else
      DUCTFLG=0;
   end

   CR9raytrace %do raytracing to construct ray path

   %Display Calculated Values to MatLab Command Window
   disp(' ')
   disp(' ')
   disp(['Actual Height: ' num2str(THT*3280.84) 'ft'])
   disp(['Apparent Height: ' num2str(THTAPP*3280.84) 'ft'])
   disp(['Height Error: ' num2str(THTERR*3280.84) 'ft'])
   disp(['Height Percent Error: ' num2str(THTERR100)])
   disp(' ')
   disp(['Actual Range: ' num2str(TRG*.53996) 'Nmi'])
   disp(['Apparent Range: ' num2str(TRGAPP*.53996) 'Nmi'])
   disp(['Range Error: ' num2str(TRGERR*.53996) 'Nmi'])
   disp(['Range Percent Error: ' num2str(TRGERR100)])

   %Plot and Display Information

   if isempty(ERRMSG)
      plottype=[];
      disp(' ')
      while isempty(plottype)
         plottype=input('Curved earth, Flat earth, No plot (c/f/n)?
','s');
         if
isempty(plottype)|(plottype~='c'&plottype~='C'&plottype~='f'&plottype~='
F'&plottype~='n'&plottype~='N')
            disp('C, F, or N, please.')
            plottype=[];
         end
      end
  else  %if there's an error message, don't plot anything
     plottype='n';
     disp(' ')
     disp('!!!!!!!!!!!!!!!!!!!!!!!!!!!!!!!!!!!!!!!!!!!!!!!!!!!!!!!!!!!!')
     disp(ERRMSG)
     disp('!!!!!!!!!!!!!!!!!!!!!!!!!!!!!!!!!!!!!!!!!!!!!!!!!!!!!!!!!!!!')
     disp(' ')
  end



  relft=REL*3280.84;

  if plottype=='C'|plottype=='c'

      %plot bent path
      ang=[(pi/2)-BETAES];
      x=[R0+HEIGHTS].*cos(ang);
      y=[R0+HEIGHTS].*sin(ang);
      plot(x,y,'r')
```

```
hold on

%plot geometric path
p=[x(1),x(1)+TRG*cos(ALFG)];
q=[y(1),y(1)+TRG*sin(ALFG)];
plot(p,q,'c')

%plot straightline path based on TRGAPP and inital ray angle,ALF0
p=[x(1),x(1)+TRGAPP*cos(ALF0)];
q=[y(1),y(1)+TRGAPP*sin(ALF0)];
plot(p,q,'m')

%plot earth surface (technically, the local geoid -- using radius
%of curvature instead of the actual local earth's radius)
ang=[pi/2-BETAES(length(BETAES)):.0001:pi/2];
x=R0*cos(ang);
y=R0*sin(ang);
plot(x,y)

%plot concentric circles around earth
ang=[pi/2-BETAES(length(BETAES)):.0001:pi/2];
if THTAPP>REL
   maxrad=R0+THTAPP;
else
   maxrad=R0+REL;
end

maxhtft=(maxrad-R0)*3280.84;
if maxhtft>=30000
   htstep=10000;
elseif maxhtft<30000&maxhtft>=10000
   htstep=5000;
elseif maxhtft<10000&maxhtft>=5000
   htstep=1000;
else
   htstep=500;
end

for r=[R0:htstep/3280.84:maxrad]
   x=r*cos(ang);
   y=r*sin(ang);
   plot(x,y,'b:')
end


%Plot ground range tick marks & labels on earth surface
maxrng=TRG*cos(ALF0);
maxrngNmi=maxrng*.53996;

if maxrngNmi>30
   rgstep=10;
elseif maxrngNmi<=30&maxrngNmi>15
   rgstep=5;
else
   rgstep=1;
end

betastep=rgstep/(R0*.53996);
ticklength=.02*(maxrad-R0);
```

```
    for beta=[0:betastep:maxrng/R0]
       x1=R0*cos(pi/2-beta);
       y1=R0*sin(pi/2-beta);
       x2=(R0+ticklength)*cos(pi/2-beta);
       y2=(R0+ticklength)*sin(pi/2-beta);
       plot([x1,x2],[y1,y2])
       if beta
          text(x2,y2,num2str(beta*R0*.53996),'VerticalAlignment',...
             'bottom','HorizontalAlignment','Center') %add Nmi labels
       end
    end

    %plot duct boundaries if applicable
    if DUCTFLG
       ang=[pi/2-BETAES(length(BETAES)):.0001:pi/2];
       for ductht=[1:2:3]
          if ductht %i.e. don't plot a zero-level duct boundary
             x=(DUCTHTS(ductht)+R0)*cos(ang);
             y=(DUCTHTS(ductht)+R0)*sin(ang);
             plot(x,y,'g--')
          end
       end
    end

    %arrange and label axes
    axis tight
    set(gca,'ytick',[R0:htstep/3280.84:maxrad])
    set(gca,'ytickLabel',[0:htstep:maxhtft])
    set(gca,'xtick',[])
    xlabel('Ground Range (Nmi)')
    ylabel('Altitude (feet)')
    set(gca,'FontSize',8)
    set(gca,'FontName','Times New Roman')

    hold off

elseif plottype=='F'|plottype=='f' %Plot type is flat earth

    %plot bent path
    gndrngs=BETAES*R0*.53996; %conversion factor changes km to Nmi
    htsft=HEIGHTS*3280.84;
    plot(gndrngs,htsft,'r')
    hold on

    %plot geometric path
    trgparts=[0:TRG/length(BETAES):TRG];
    htskm=(sqrt((R0+REL)^2+trgparts.^2-2*(R0+REL)*trgparts*...
       cos(pi/2+ALFG))-R0);
    gndrngs=R0*.53996*asin(trgparts*sin(pi/2+ALFG)./(R0+htskm));
    htsft=htskm*3280.84;
    plot(gndrngs,htsft,'-.c')

    %plot straightline path based on TRGAPP and inital ray angle,ALF0
    trgparts=[0:TRGAPP/(length(BETAES)-1):TRGAPP];
    htskm=(sqrt((R0+REL)^2+trgparts.^2-2*(R0+REL)*trgparts*...
       cos(pi/2+ALF0))-R0);
    gndrngs=R0*.53996*asin(trgparts*sin(pi/2+ALF0)./(R0+htskm));
    htsft=htskm*3280.84;
    plot(gndrngs,htsft,'-.m')
```

```
      %plot duct heights (if applicable)
      if DUCTFLG
         plot([0,gndrngs(length(gndrngs))],...
               [DUCTHTS(1)*3280.84,DUCTHTS(1)*3280.84],'--g')
         plot([0,gndrngs(length(gndrngs))],...
               [DUCTHTS(3)*3280.84,DUCTHTS(3)*3280.84],'--g')
      end

      xlabel('Ground Range (Nmi)')
      ylabel('Height above sea level (ft)')

      legend('Actual Path','Direct Path','Apparent Path','Duct
Boundaries')
   end
end

clear
```

```
%CLIMAREF User Input module "CR2in.m"
%This module allows the user to input the following data:
%month (integer 1-12)
%day or night (1=day, 0=night)
%radar latitude in degrees (between -70 and +80)
%radar longitude in degrees
%radar elevation entered in feet AGL, converted to km
%radar pointing azimuth in degrees (north=0)
%actual target height entered in feet AGL, converted to km
%actual straight line distance, radar to target in Nmi converted to km
%
%INPUT VARIABLES
%none
%
%INTERNAL VARIABLES
%dyntstr - string form of DYNT, can equal D,N, or B
%relft - radar elevation in feet
%thtft - target height in feet
%trgnm - target range in Nmi
%
%OUTPUT VARIABLES
%MON - month of interest (integer 1-12)
%RLAT - latitude of radar (-70 to +80 deg)
%RLONG - longitude of radar (deg)
%REL - elevation of radar (km)
%RAZ - azimuth radar is pointing to (deg)
%THT - actual target height (km)
%TRG - actual target range (km)

redo=1;
while redo==1

   MON=[];
   dyntstr=[];
   RLAT=[];
   RLONG=[];
   relft=[];
   RAZ=[];
   thtft=[];
   trgnm=[];
   crct=[];

   disp(' ')
   disp('Please input the following information:')
   disp(' ')

   while isempty(MON)
      MON=input('Month (1-12): ');
      if isempty(MON)|round(MON)~=MON|MON<1|MON>12
         disp('You must enter a month number (1-12)')
         MON=[];
      end
   end

   while isempty(dyntstr)
      dyntstr=input('1200Z,000Z, or avg of both (D/N/B): ','s');
      if
isempty(dyntstr)|(dyntstr~='d'&dyntstr~='D'&dyntstr~='n'&dyntstr~='N'&dy
ntstr~='b'&dyntstr~='B')
```

```
         disp('You must indicate day,night, or both')
         dyntstr=[];
      end
   end

   if dyntstr=='D'|dyntstr=='d'
      DYNT=1;
   elseif dyntstr=='N'|dyntstr=='n'
      DYNT=0;
   else  %both day and night (avg)
      DYNT=2;
   end

   while isempty(RLAT)
      RLAT=input('Radar latitude (-70 to +80 deg): ');
      if isempty(RLAT)|RLAT<-70|RLAT>+80
         disp('You must enter a latitude value between -70 and +80
degrees')
         RLAT=[];
      end
   end

   while isempty(RLONG)
      RLONG=input('Radar longitude (+/- deg): ');
      if isempty(RLONG)|RLONG<-180|RLONG>180
         disp('You must enter a longitude value between -180 and +180
degrees')
         RLONG=[];
      end
   end

   while isempty(relft)
      relft=input('Radar elevation (feet AGL): ');
      if isempty(relft)|relft<0
         disp('You must enter a positive elevation value')
         relft=[];
      end
   end
   REL=relft*.0003048;  %convert feet to kilometers

   while isempty(RAZ)
      RAZ=input('Radar azimuth (deg) - default=0 (north): ');
      if isempty(RAZ)
         RAZ=0;
         disp('The radar is pointing to 0 degrees (north)')
      end
      if RAZ<0|RAZ>360
         disp('You must enter an azimuth value between 0 and 360
degrees')
         RAZ=[];
      end
   end

   while isempty(thtft)
      thtft=input('Actual Target Height (feet AGL): ');
      if isempty(thtft)|thtft<0
         disp('You must enter a positive target height')
         thtft=[];
      end
```

```
   end
   THT=thtft*.0003048;  %convert feet to kilometers

   while isempty(trgnm)
      trgnm=input('Actual Target Range (Nmi): ');
      if isempty(trgnm)|trgnm<0
         disp('You must enter a positive target range value')
         trgnm=[];
      end
   end
   TRG=trgnm*1.852; %convert Nmi to kilometers

%Check to see if all the entries are correct
   while isempty(crct)
      disp(' ')
      crct=input('Are all the above entries correct (y/n)? ','s');
      if isempty(crct)|(crct~='y'&crct~='Y'&crct~='n'&crct~='N')
         disp('Please answer Y for yes, or N for no.')
         crct=[];
      end
   end

   if crct=='Y'|crct=='y'
      redo=0;
   end

end   %process will drop out of while-loop here as long as crct was 'y'


%Clear unneeded internal variables
clear dyntstr relft thtft trgnm

pack

%Now return to CRmain
```

```
%CLIMAREF Input module -- preset data
%This module allows the user to input the following data:
%MON - month (integer 1-12)
%DYNT - day or night (1=day, 0=night)
%RLAT - radar latitude in degrees
%RLONG - radar longitude in degrees
%REL - radar elevation in km MSL
%RAZ - radar pointing azimuth in degrees (north=0)
%THT - actual target height in km MSL
%TRG - actual straight line distance from radar to target in Nmi
%
MON=7;
DYNT=0;
RLAT=42;
RLONG=-80;
REL=.3;
RAZ=0;
%THT=3.048;
THT=input('THT (km)');
%TRG=111.1;
TRG=input('TRG (km)');
disp(' ')
disp('Radar Parameters:')
disp(' ')

disp(['Month: ' num2str(MON)])
disp(['Day/Night: ' num2str(DYNT)])
disp(['Radar Lat: ' num2str(RLAT)])
disp(['Radar Long: ' num2str(RLONG)])
disp(['Radar Elevation (km): ' num2str(REL)])
disp(['Radar Azimuth: ' num2str(RAZ)])
disp(['Target Height (km): ' num2str(THT)])
disp(['Target Range (km): ' num2str(TRG)])
```

```
function CR3findnerstats
global ISOLATED RLAT RLONG NEARMSQS NEARSTATS
%CLIMAREF Load climate data module, submodule 1 (CR3findnerstats.m)
%This submodule find the nine MSQs surrounding the radar and the record
%numbers of all the radiosonde stations within those MSQs.  If there
%aren't any it sets a flag.

%INPUT VARIABLES:
%RLAT - radar latitude (deg)
%RLONG - radar longitude (deg)

%INTERNAL VARIABLES:
%lat - lat of msq of interest (radar lat +/- 0 or 10)
%listind - used to index msqlist
%long - long of msq of interest (radar long +/- 0 or 10)
%msq - msq number of record currently being examined
%msqind - indices the nine msqs surrounding the radar
%msqlist - list of all msqs in the order they appear in the data file,
%          the index of the first record bearing the given msq number,
%           and the number or records bearing that msq number (msqlist
%           is stored as a data file until it is needed by the program
%ordflag - flag indicating near MSQs are in order
%pmmsqind - index of msq immediately west of PM from southernmost
%           to northernmost
%pmmsqs - all the msqs immediately west of PM from south to north
%sortptr - pointer used to track MSQs in bubble sort
%swapflag - flag used in sort to indicate a swap of positions has
happened
%tempmsq - temporary holder used in sort
%
%OUTPUT VARIABLES:
%NEARMSQS - numbers of the 9 marsden squares surrounding the radar
%NEARSTATS - indices of all stations in the 9 marsden squares
surrounding
%            the radar (variable length vector)
%ISOLATED - flag indicated there are no radiosonde stations in any of
%           the nine MSQs surrounding the radar (a value of 1 indicates
%           isolation)

ISOLATED=0;
%************Find 9 MSQ's nearest the radar**************************
pmmsqs=[516 480 440 408 372 336 300 1 37 73 109 145 181 217 253];
msqind=0;   %MSQ index
for lat=[RLAT-10:10:RLAT+10];       %cover all msq's surrounding the
   for long=[RLONG-10:10:RLONG+10]; %radar, 3 rows and three columns
      msqind=msqind+1;  %increment index

      if long>180 %if RLONG near 180 merid, nearby msq's need new
         long=long-360; %latitude reference calculated
      end
      if long<-180  %likewise
         long=long+360;
      end

      if lat<-70|lat>80         %if msq doesn't exist, set it to 0 and
         NEARMSQS(msqind)=0;  %go on to the next one
      else
         pmmsqind=floor(lat/10)+8;  %find the msq immediately to the
         if long<=0  %Calculate msq of interest
```

```
            NEARMSQS(msqind)=pmmsqs(pmmsqind)+floor(abs(long/10));
         else
            NEARMSQS(msqind)=pmmsqs(pmmsqind)+35-floor(long/10);
         end

      end
   end
end
%*********************************************************************

%************************Sort list of nearby MSQs*****************
ordflag=0;   %set 'ordered' flag
while ordflag==0
   swapflag=0;
   for sortptr=[9:-1:2];
      if NEARMSQS(sortptr)<NEARMSQS(sortptr-1)
         tempmsq=NEARMSQS(sortptr-1);
         NEARMSQS(sortptr-1)=NEARMSQS(sortptr);
         NEARMSQS(sortptr)=tempmsq;
         swapflag=1;
      end
   end
   if swapflag==0
      ordflag=1;
   end
end
%*********************************************************************



%*********Find all radiosonde stations within the 9 nearest MSQs*****
msqlist=load('msqlist');
listind=0;
msq=0;
NEARSTATS=[];
for msqind=[1:9];    %go through all near msqs
   if NEARMSQS(msqind)~=0     %skip the out-of-range msqs
      endlist=0;
      while msq~=NEARMSQS(msqind)&endlist==0
         listind=listind+1;       %flip through list of msqs until you
         msq=msqlist(listind,1);  %find the one you want
         if listind==length(msqlist)&msq~=NEARMSQS(msqind)  %If we've
            endlist=1;  %reached the end of the list w/out finding our
            listind=0; %msq, we have to end the while loop and reset
         end           %listind
      end
      if endlist==0      %only add to NEARSTATS if we found our msq

   NEARSTATS=cat(1,NEARSTATS,transpose([msqlist(listind,2):msqlist(listi
nd,2)+msqlist(listind,3)-1]));
      end   %   ^- add the record numbers indicated in msqlist to the
   end      %      list of nearby stations
end

if isempty(NEARSTATS)
   ISOLATED=1;
end
```

```
function CR4calcdist
global RLAT RLONG NEARSTATS
%CLIMAREF Load climate data module, submodule 2 (CR4calcdist.m)
%This submodule calculates the distances from the radar to all the
%stations listed in NEARSTATS.  It then sorts the stations from nearest
%to furthest.

%INPUT VARIABLES:
%RLAT - radar latitude
%RLONG - radar longitude
%NEARSTATS - list of indices of stations in the nine MSQs nearest
%            to the radar

%INTERNAL VARIABLES:
%a,b,c - earth radius related parameters (see code below)
%az - azimuth angle from radar to station (radians)
%complat - 90-latitude for a given station (deg)
%comprlat - 90-latitude for the radar site (deg)
%deg2rad - degrees to radians conversion factor
%dellat - diff in lat between a station and the radar (deg)
%dellong - diff in long between a station and the radar (deg)
%dists - vector of distances between radar and stations in NEARSTATS
%elevs - binary elevation values
%fid - file ID - ID# given to radio.dbf
%latraw - binary latitude value
%lats - vector of latitudes for all stations in NEARSTATS (deg)
%longraw - binary longitude value
%longs - vector of longitudes for all stations in NEARSTATS (deg)
%namesandels - matrix binary codes for letters in all the station names
%ordflag - flag indicating near stations in order (nearest to furthest)
%psi - angle between radar and a station radians)
%rc - local radius of curvature
%sortptr - pointer used to track stations in bubble sort
%stat - index used to point to stations within NEARSTATS
%status - dummy variable for I/O
%swapflag - flag used in sort to indicate a swap of positions has
happened
%tempstat - temporary holder used in sort
%top10 - The number of stations to keep (either 10, or if there aren't
%        that many, the number that there are
%xr,yr,zr - 3-D cartesian coords of the radar(neglecting radar altitude)
%xs,ys,zs - 3-D cartesian coords of station (neglecting station
altitude)



%OUTPUT VARIABLES:
%NEARSTATS - see INPUT VARIABLES above, BUT NOW it:
%            1. is sorted nearest to furthest
%            2. contains distances from radar to station in the
%               2nd column
%            3. contains the ascii values of the characters in the
%               station names in the remaining 29 columns
%            4. by the time it's output, it contains only the
%               10 nearest stations

deg2rad=2*pi/360;  %degrees to radians conversion factor

fid=fopen('radio.dbf','r');  %open file for read-only
```

```
for stat=[1:length(NEARSTATS)];
   %First read the lat/longs for each station in NEARSTATS
   status=fseek(fid,642+(NEARSTATS(stat)-1)*944+38,'bof'); %positions
                        %pointer to start of latitude in each record
   latraw=transpose(fread(fid,6));  %read raw (binary) latitude
   lats(stat)=str2num(char(latraw)); %convert to number and store

   status=fseek(fid,642+(NEARSTATS(stat)-1)*944+44,'bof'); %Do same
   longraw=transpose(fread(fid,7));              %for longitude
   longs(stat)=-str2num(char(longraw)); %NOTE: Data uses negative long.
   %values to denote East Long., but this model uses negative
   %to denote West Long. to be consistent with the National Climatic
   %Data Center (NOAA) (hence the negative sign)



   %Next, calculate the local radius of curvature, RC, in the direction
   %from the radar to the station in question
   if sign(RLAT)==sign(lats(stat))
      dellat=lats(stat)-RLAT; %Calc diff between lat/long of station and
   else
      dellat=sign(lats(stat))*(abs(lats(stat))+abs(RLAT)); %if the two
      %points straddle the equator, we just add the two abs val lats
   end
   if sign(RLONG)==sign(longs(stat)) %check for longs straddling either
                              %the prime meridian or the int'l date line
      dellong=longs(stat)-RLONG;  %radar site
   else
      if abs(RLONG)<90 %i.e. close to zero
         dellong=sign(longs(stat))*(abs(RLONG)+abs(longs(stat)));%sites
                                                  %straddling zero deg
      else
         dellong=sign(longs(stat))*(360-abs(RLONG)-abs(longs(stat)));
                                                 %sites straddling 180
      end
   end

   az=pi/2-atan2(dellat,dellong); %Calc az from radar to station
   a=6378.139; %max earth radius (km)
   b=6356.750; %min earth radius (km)
   c=a^2/b^2-1; %intermediate value

rc=a^2/(b*sqrt(1+c*cos(RLAT*deg2rad)^2)*(1+c*cos(RLAT*deg2rad)^2*cos(az)
^2));
   %^-radius of curvature (to be used in place of earth's radius)

   %Next, calculate the surface distance from the radar to the station
   complat=90-lats(stat); %compliment of lat(for spherical coord system)
   xs=rc*sin(complat*deg2rad)*cos(longs(stat)*deg2rad); %convert to
cartesian coords
   ys=rc*sin(complat*deg2rad)*sin(longs(stat)*deg2rad);
   zs=rc*cos(complat*deg2rad);
   comprlat=90-RLAT; %compliment of lat(for spherical coord system)
   xr=rc*sin(comprlat*deg2rad)*cos(RLONG*deg2rad); %convert to cartesian
coords
   yr=rc*sin(comprlat*deg2rad)*sin(RLONG*deg2rad);
   zr=rc*cos(comprlat*deg2rad);
```

```
   psi=abs(acos((xs*xr+ys*yr+zs*zr)/rc^2)); %calc angle between radar
                                            %and station
   dists(stat,1)=psi*rc;
end

%Concatenate distances to NEARSTATS
NEARSTATS=cat(2,NEARSTATS,dists);

%Clear the internal variables
clear deg2rad stat latraw lats longraw longs dellat
clear dellong az a b c rc complat xs ys zs comprlat xr yr zr psi dists

%Sort by distance (closest to furthest)
ordflag=0;   %set 'ordered' flag
while ordflag==0
   swapflag=0;
   for sortptr=[size(NEARSTATS,1):-1:2];
      if NEARSTATS(sortptr,2)<NEARSTATS(sortptr-1,2)
         tempstat=NEARSTATS(sortptr-1,:);
         NEARSTATS(sortptr-1,:)=NEARSTATS(sortptr,:);
         NEARSTATS(sortptr,:)=tempstat;
         swapflag=1;
      end
   end
   if swapflag==0
      ordflag=1;
   end
end

%Take the top 10 nearest stations
if size(NEARSTATS,1)<10
   top10=size(NEARSTATS,1);
else
   top10=10;
end
NEARSTATS=NEARSTATS(1:top10,:);

%Get the station names and elevations
for stat=[1:size(NEARSTATS,1)];
   status=fseek(fid,642+(NEARSTATS(stat)-1)*944+8,'bof'); %Get
   name=transpose(fread(fid,29));      %station names as well
   status=fseek(fid,642+(NEARSTATS(stat)-1)*944+51,'bof');
   elevraw=transpose(fread(fid,4));
   elev=double(num2str(round(str2num(char(elevraw))*3.28084)));
   if length(elev)<5
      for zros=[1:5-length(elev)]
         elev=[32 elev];
      end
   end
   namesandels(stat,:)=[name elev];
end
NEARSTATS=cat(2,NEARSTATS,namesandels);
%close file, radio.dbf
status=fclose(fid);
```

```
function CR5pickstat
global USESTAT
global NEARSTATS
%CLIMAREF Pick Station data module (CR5pickstat.m)
%This module allows the user to choose a radiosonde station from
%a list of the nearest stations.  Average N data from this station
%will be used to calculate the refractivity profile

%INPUT VARIABLES:
%NEARSTATS - Matrix consisting of:
%  Col 1 - indices (in database) of all stations in the nine Marsden
%          squares surrounding the radar
%  Col 2 - surface distances of the stations from the radar
%  Col 3 - names of the stations in binary form (i.e. each character in
%          the station name is represented by its (decimal) ascii code

%INTERNAL VARIABLES:
%statind - index for for-next listing all the stations
%s - string of near station data and tabs for formatting display

%OUTPUT VARIABLES:
%USESTAT - vector containing the index(ices) of the station(s) to use
%for the N-profile.  May contain up to three indices.

format short
disp(' ')
disp('Index     Name                      Height (ft MSL)     Distance
(km)')
s=sprintf(['999' '\t' 'Standard Atmosphere           --- ' '\t' '\t' '
---']);
disp(s)
for statind=[1:size(NEARSTATS,1)];
   s=sprintf([num2str(NEARSTATS(statind,1)) '\t'
char(NEARSTATS(statind,3:36)) '\t' '\t' num2str(NEARSTATS(statind,2))]);
   disp(s);
end

disp(' ')
disp('Average data from one,two,or three of these radiosonde stations
must')
disp('be used to construct the refractivity profile.  They are listed
in')
disp('from nearest to furthest.  You must select the station(s) you
wish')
disp('to use.  Be sure to consider topography, and not only distance
when')
disp('making your decision (e.g. may want to choose a station halfway
between')
disp('radar and target).  Note:  If you elect to use STANDARD
ATMOSPHERE,')
disp('you may not select any other stations.')

USESTAT=[];
while isempty(USESTAT)
   disp(' ')
   disp('Enter the indexes of up to THREE stations (if you enter more
than')
   USESTAT=input('one, enclose the numbers in square brackets, e.g [123
321]:  ');
```

```
      if isempty(USESTAT)|length(USESTAT)>3
         disp('Enter 1,2, or 3 station index numbers')
         USESTAT=[];
      end
      if length(USESTAT)>1
         saplus=0;
         for i=[1:length(USESTAT)] %Check to make sure the STD ATM
            if USESTAT(i)==999 %selection wasn't chosen along with
               saplus=1;   %real stations
            end
         end
         if saplus  %If STD ATM was chosen along with other stations...
            disp(' ')
            disp('You may not use STANDARD ATMOSPHERE along with other
station data')
            disp('It must be used by itself')
            USESTAT=[];
         end
         if
(length(USESTAT)==2&USESTAT(1)==USESTAT(2))|(length(USESTAT)==3&(USESTAT
(1)==USESTAT(2)|USESTAT(1)==USESTAT(3)|USESTAT(2)==USESTAT(3)))
         %Check to make sure duplicate number wasn't entered
            disp(' ')
            disp('You entered duplicate numbers')
            USESTAT=[];
         end
      end
end
```

```
function CR6loadNdata
global NS N1K SEL
global USESTAT MON
%CLIMAREF Load climate data module, submodule 3 (CR6loadNdata.m)
%This submodule loads Ns and N1k from the database for the station of
%interest

%INPUT VARIABLES:
%USESTAT - index of station of interest
%MON - month of interest

%INTERNAL VARIABLES:
%delm1k - m-gradient (numeric)
%delm1kraw - raw (binary) m-gradient
%deln1k - n-gradient (ngradient=mgradient-156)
%fid - file id
%monstart - position in record of the start of the data for the month of
interest
%n1k - scalar value of IOR at 1km AGL for one particular station
%ns - scalar value of ns for one particular station - is cat'd onto the
NS vector eventually
%nsraw - raw (binary) surface refractivity
%sel - scalar value of the station elevation for one particular station
%selraw - raw (binary) surface elevation
%stat - index to USESTAT in for/next loop
%status - dummy variable for i/o operations


%OUTPUT VARIABLES:
%NS - surface index(ices) of refraction
%N1K - index(ices) of refraction at 1km above surface
%SEL - station elevations (km)


if USESTAT~=999
   fid=fopen('radio.dbf','r');  %open file for read-only

   NS=[];
   N1K=[];
   SEL=[];
   for stat=[1:length(USESTAT)]
      status=fseek(fid,642+(USESTAT(stat)-1)*944+51,'bof'); %positions
                        %pointer to start of elevation in each record
      selraw=transpose(fread(fid,6));  %read raw (binary) elevation
      sel=.001*str2num(char(selraw)); %convert to number (km) and store
      SEL=cat(2,SEL,sel); %tack onto SEL vector

      monstart=642+(USESTAT(stat)-1)*944+55+(MON-1)*74; %pointer to
start of data
                                        %for each month in the record

      status=fseek(fid,monstart+12,'bof'); %pointer to start of Ns in
                                        %each record
      nsraw=transpose(fread(fid,3));  %read raw (binary) Ns
      ns=str2num(char(nsraw)); %convert to number and store
      NS=cat(2,NS,ns);
      status=fseek(fid,monstart+15,'bof'); %pointer to start of Ns in
                                        %each record
      delm1kraw=transpose(fread(fid,3));  %read raw (binary) Ns
```

```
      delm1k=str2num(char(delm1kraw)); %convert to number and store
      deln1k=delm1k-156; %
      n1k=ns+deln1k;  %Calculate N at 1k from surface N and gradient
      N1K=cat(2,N1K,n1k);
   end
   status=fclose(fid);
else
   SEL=0;
   NS=313;  %User chose standard refraction
   N1K=271.0612;
end

%disp(['NS=' num2str(NS) ' N1K=' num2str(N1K)]) %for testing only
```

```
function CR7interp
global USESTAT NEARSTATS RLAT RLONG NS N1K SEL
%%CLIMAREF Interpolate module (CR7interp.m)
%This submodule interpolates NS and N1K from data recorded for 2 or 3
%stations

%INPUT VARIABLES:
%USESTAT - indices of stations of interest
%NEARSTATS - 1. contains indexes of nearest ten stations in col 1
%            2. contains distances from radar to station in col 2
%            3. contains the ascii values of the characters in the
%               station names in the remaining 29 columns
%            4. is sorted nearest to furthest
%
%RLAT - radar latitude
%RLONG - radar longitude
%USESTAT - vector of station indexes to be used in interpolation
%NS - surface IOR vector (for both, or all three stations) - indexed
%     to match USESTAT
%N1K - 1K above surface IOR vector (for both, or all three stations)
%       -- indexed to match USESTAT
%SEL - surface elevations of stations


%INTERNAL VARIABLES:
%a,b,c - earth radius related parameters (see code below)
%a,b,cns,cn1k,csel - direction numbers for the line used in the line-
interp
%Ans,An1k,Bns,Bn1k,C - direction numbers for plane used in plane-interp
%az - azimuth angle from radar to station (radians)
%ce - intermediate constant for N-profile calculation (in this case for
normalization of NS and N1K
%complata - 90-latitude for first station site (deg)
%complatb - 90-latitude for second station (deg)
%d23a,d23b - two possible alternative values for the dist from station 2
to station 3 (only one is correct)
%dellat - diff in lat between a station and the radar (deg)
%dellong - diff in long between a station and the radar (deg)
%dist - index in distance-finding for/next loop to station a
%distb - index in distance-finding for/next loop to station b
%dists - vector of distances between stations (1-2) or (1-2,2-3,3-1)
%Dns,Dn1k - parameter which locates plane in space
%latraw, longraw - binary version of lat & long for station
%lats, longs - lats and longs for stations in USESTAT
%n1kmsl - N1k normalized to sea level (i.e. N at 1km MSL)
%nsi,n1ki - interpolated values of ns and n1k still normalized to MSL
%nsmsl - Ns normalized to sea level (i.e. N at 0km MSL)
%numdists - number of distances between stations to be calculated
%psi - angle between station a and station b radians)
%rc - local radius of curvature
%rdists - vector of distances from radar to each station (r-1,r-2) or
(r-1,r-2,r-3)
%stat - index to USESTAT in for/next loop
%status - dummy variable for i/o
%x1,y1,x2,y2,x3,y3 - station coordinates (for interpolation purposes)
%xa,ya,za - 3-D cartesian coords of station a (neglecting radar
altitude)
%xb,yb,zb - 3-D cartesian coords of station b(neglecting station
altitude)
```

```
%xp - x-coordinate of point on projection of line (onto 2d plane) that's
closest to the radar
%xr,yr - radar coordinates (for interpolation purposes)
%y3a,y3b - two possible alternative values for y3 (only one is correct)




%OUTPUT VARIABLES:
%NS - interpolated index of refraction at interpolated surface
%N1K - interpolated index of refraction at 1km above interpolated
%        surface (MSL)
%SEL - interpolated station elevation (km) (interpolated surface)


deg2rad=2*pi/360;  %degrees to radians conversion factor

fid=fopen('radio.dbf','r');  %open file for read-only

%%%%%%Read the lat/longs for each station in NEARSTATS%%%%%
for stat=[1:length(USESTAT)];
   status=fseek(fid,642+(USESTAT(stat)-1)*944+38,'bof'); %positions
                          %pointer to start of latitude in each record
   latraw=transpose(fread(fid,6));  %read raw (binary) latitude
   lats(stat)=str2num(char(latraw)); %convert to number and store

   status=fseek(fid,642+(USESTAT(stat)-1)*944+44,'bof'); %Do same
   longraw=transpose(fread(fid,6));              %for longitude
   longs(stat)=-str2num(char(longraw)); %NOTE: Data uses negative long.
   %values to denote East Long., but this model uses negative
   %to denote West Long. to be consistent with the National Climatic
   %Data Center (NOAA) (hence the negative sign)
end
status=fclose(fid);
%%%%%Calc distances between the stations%%%%%%
if length(USESTAT)==2
   numdists=1; %If there're two stations calc one distance
else
   numdists=3; %If there're three stations calc three distances
end
for dist=[1:numdists]
   distb=dist+1; %indexing the second station
   if distb==4
      distb=1;
   end
   %calculate the local radius of curvature, RC, in the direction
   %from the first station to the second station
   if sign(lats(dist))==sign(lats(distb))
      dellat=lats(distb)-lats(dist); %Calc diff between
      %lat/long of station a and station b
   else
      dellat=sign(lats(distb))*(abs(lats(distb))+abs(lats(dist))); %if
the two
      %points straddle the equator, we just add the two abs val lats
   end
   if sign(longs(dist))==sign(longs(distb)) %check for longs straddling
either
```

```
                                %the prime meridian or the int'l date line
      dellong=longs(distb)-longs(dist);  %radar site
   else
      if abs(longs(dist))<90 %i.e. close to zero

dellong=sign(longs(distb))*(abs(longs(dist))+abs(longs(distb)));%sites
                                                    %straddling zero deg
      else
         dellong=sign(longs(distb))*(360-abs(longs(dist))-
abs(longs(dist)));
                                                  %sites straddling 180
      end
   end

   az=pi/2-atan2(dellat,dellong); %Calc az from radar to station
   a=6378.139; %max earth radius (km)
   b=6356.750; %min earth radius (km)
   c=a^2/b^2-1; %intermediate value

rc=a^2/(b*sqrt(1+c*cos(lats(dist)*deg2rad)^2)*(1+c*cos(lats(dist)*deg2ra
d)^2*cos(az)^2));
   %^-radius of curvature (to be used in place of earth's radius)

   %Next, calculate the surface distance from the first station (a) to
   %the second station (b)
   complatb=90-lats(distb); %compliment of lat(for spherical coord
system)
   xb=rc*sin(complatb*deg2rad)*cos(longs(distb)*deg2rad); %convert to
cartesian coords
   yb=rc*sin(complatb*deg2rad)*sin(longs(distb)*deg2rad);
   zb=rc*cos(complatb*deg2rad);
   complata=90-lats(dist); %compliment of lat(for spherical coord
system)
   xa=rc*sin(complata*deg2rad)*cos(longs(dist)*deg2rad); %convert to
cartesian coords
   ya=rc*sin(complata*deg2rad)*sin(longs(dist)*deg2rad);
   za=rc*cos(complata*deg2rad);
   psi=abs(acos((xb*xa+yb*ya+zb*za)/rc^2)); %calc angle between radar
                                             %and station
   dists(dist)=psi*rc;
end

%also extract distances from radar to stations from NEARSTATS
for stat=[1:length(USESTAT)] %go through list of 2 or 3 stations
   for nstat=[1:size(NEARSTATS,1)] %go through list of 10 NEARSTATS
      if USESTAT(stat)==NEARSTATS(nstat,1)
         rdists(stat)=NEARSTATS(nstat,2);
      end
   end
end

%%%%%%%%Construct triangle using three distances: (r-1,r-2,1-2)%%%%%%%
%%%%%%%%This routine is used whether you have two stations or three%%%
%%%%%%%%This routine essentialy flattens out the surface of the%%%%%%%
%%%%%%%%earth in order to do a simple planar or linear interpolation%%
xr=0; %establish radar as center of coord system
yr=0;
x1=rdists(1); %position station 2 on the x axis to the right of radar
y1=0; %Note: absolute orientation of this system doesn't matter for
```

```
%      interp, only relative orientation
x2=(rdists(2)^2-dists(1)^2+rdists(1)^2)/(2*rdists(1));  %Calc x2,y2
y2=sqrt(rdists(2)^2-x2^2); %Based on the other two points--in addition
%to its arbitrary orientation, this triangle may also be flipped
%(mirror image).  This doesn't matter either for the interpolation

%%%%%%%Locate third station (another triangle) if there is one%%%%%%%
%%%%%%%This is used only for the planar (3-station) interpolation%%%%
if length(USESTAT)==3 %locate third station if there is one
   x3=(rdists(3)^2-dists(3)^2+rdists(1)^2)/(2*rdists(1));
   y3a=sqrt(rdists(3)^2-x3^2);  %station three is either above or
   y3b=-y3a;%                    below the x-axis
   d23a=sqrt((x2-x3)^2+(y2-y3a)^2);
   d23b=sqrt((x2-x3)^2+(y2-y3b)^2);
   if abs(d23a-dists(2))<abs(d23b-dists(2)) %To figure out which, we
      y3=y3a;% simply calculate both, figure out the two distances to
   else %station 2, and see which one matches the actual distance
      y3=y3b; %the closest
   end
end


%%%%%%Normalize NS & N1K (all stations) to 0ft MSL%%%%%%%%%
ce=log(NS./N1K);
nsmsl=NS.*exp(-ce.*(-SEL)); %calc N at sea level
n1kmsl=NS.*exp(-ce.*(-SEL+1)); %calc N, 1km above sea level

%%%%%%Linear Interpolation (for 2 stations)%%%%%%%%%%%%%%%%
%construct 3 sets of lines in 3d space - one using nsmsl for z,
%another using n1kmsl for z, and the third using SEL for z
if length(USESTAT)==2
   a=x2-x1; %parametric coefficients for lines
   b=y2-y1;
   cns=nsmsl(2)-nsmsl(1);
   cn1k=n1kmsl(2)-n1kmsl(1);
   csel=SEL(2)-SEL(1);
%Find point on projection (of line onto 2d plane) closest to radar
   xp=(a*xr/b+b*x1/a-y1+yr)/(b/a+a/b); %We only need x-coord--it's a
line!
%Find z-value (ns or n1k)
   nsi=cns*(xp-x1)/a+nsmsl(1); %Note: We're redefining NS,N1K,& SEL as
   n1ki=cn1k*(xp-x1)/a+n1kmsl(1); %scalar interpolated values
   SEL=csel*(xp-x1)/a+SEL(1);
else %i.e. there are 3 stations
   Ans=(y2-y1)*(nsmsl(3)-nsmsl(1))-(nsmsl(2)-nsmsl(1))*(y3-y1);
   An1k=(y2-y1)*(n1kmsl(3)-n1kmsl(1))-(n1kmsl(2)-n1kmsl(1))*(y3-y1);
   Asel=(y2-y1)*(SEL(3)-SEL(1))-(SEL(2)-SEL(1))*(y3-y1);
   Bns=(nsmsl(2)-nsmsl(1))*(x3-x1)-(x2-x1)*(nsmsl(3)-nsmsl(1));
   Bn1k=(n1kmsl(2)-n1kmsl(1))*(x3-x1)-(x2-x1)*(n1kmsl(3)-n1kmsl(1));
   Bsel=(SEL(2)-SEL(1))*(x3-x1)-(x2-x1)*(SEL(3)-SEL(1));
   C=(x2-x1)*(y3-y1)-(y2-y1)*(x3-x1);
   Dns=-Ans*x1-Bns*y1-C*nsmsl(1);
   Dn1k=-An1k*x1-Bn1k*y1-C*n1kmsl(1);
   Dsel=-Asel*x1-Bsel*y1-C*SEL(1);


   nsi=(-Ans*xr-Bns*yr-Dns)/C;  %Redefine NS,N1K,& SEL as scalars with
   n1ki=(-An1k*xr-Bn1k*yr-Dn1k)/C;%the interpolated values
   SEL=(-Asel*xr-Bsel*yr-Dsel)/C;
```

```
end


%De-normalize NS and N1k back to the interpolated SEL
ce=log(nsi/n1ki);
NS=nsi*exp(-ce*SEL); %calc N at surface
N1K=nsi*exp(-ce*(SEL+1)); %calc N, 1km above surface
```

```
function CR8ductstats
global USESTAT MON DYNT SEL MULTSTATFLG
global GMSB OHSB MTSB MDSB MFSB PSB GMEL OHEL MTEL
global MDEL MFEL PEL P2EL PSBEL NS N1K
global PHs PMs PHe PMe PHn PMn
%CLIMAREF Load climate data module, submodule 4 (CR8ductstats.m)
%This submodule loads ducting statistics from the database for
%the station of interest

%INPUT VARIABLES:
%USESTAT - index of station of interest
%MON - month of interest
%DYNT - day, night, or both readings (1=day, 0=night, 2=both)

%INTERNAL VARIABLES:
%fid - file id
%monstart - position in record of the start of the data for the month of
interest
%p2elx100 - prob >1 elev duct occurs (%x100)
%pel00 - % of 0000Z radiosonde readings in which elev. ducts occurred
%pel12 - % of 1200Z radiosonde readings in which elev. ducts occurred
%psb00 - % of 0000Z radiosonde readings in which surf. ducts occurred
%psb12 - % of 1200Z radiosonde readings in which surf. ducts occurred
%psbelx100 - prob surf-based and elev duct both occur simultaneously
(%x100)
%status - dummy variable for i/o operations

%OUTPUT VARIABLES:
%(heights in kilometers unless otherwise specified)
%GNEL - elevated duct N-unit gradient
%GNSB - surface based duct N-unit gradient
%NDEL - elevated duct N-unit deficit
%NDSB - surface based duct N-unit deficit
%NFEL - elevated duct trapping frequency
%NFSB - surface based duct trapping frequency
%NTEL - elevated duct thickness
%NTSB - surface based duct thickness
%OHEL - elevated duct optimum height
%OHSB - surface based duct optimum height
%P2EL - probability of >1 elevated duct
%PEL - elevated duct percent chance of occuring (day, night, or avg)
%PHe - vector of key heights (km) in elevated duct profile
%PHn - vector of key heights (km) in no-duct profile
%PHs - vector of key heights (km) in surface duct profile
%PMe - vector of M values corresponding to heights in PHs
%PMn - vector of M values corresponding to heights in PHs
%PMs - vector of M values corresponding to heights in PHs
%PSB - surface based duct percent chance of occuring (day, night or avg)
%PSBEL - probability of surface-based AND elevated duct occuring

%Initialize variables
PHs=[];
PMs=[];
PHe=[];
PMe=[];
PHn=[];
PMn=[];

%Get Ducting Data
```

```
if USESTAT~=999&~MULTSTATFLG
   fid=fopen('radio.dbf','r');  %open file for read-only

   monstart=642+(USESTAT-1)*944+55+(MON-1)*74; %pointer to start of
                                %data for each month in the record

   status=fseek(fid,monstart+18,'bof'); %pointer to start of duct data

   ductdatraw=transpose(fread(fid,56));  %read entire list of raw
                                %(binary) duct statistics

   %Now, break it out and convert the binary data to actual numbers
   GMSB=str2num(char(ductdatraw(1:4))); %convert gmsb from binary, to
   %                                    a string, then to a number
   OHSB=str2num(char(ductdatraw(5:7)))/1000; % x/1k to convert to km
   MTSB=str2num(char(ductdatraw(8:10)))/1000;
   MDSB=str2num(char(ductdatraw(11:13)));
   MFSB=str2num(char(ductdatraw(14:17)));
   psb12=str2num(char(ductdatraw(18:20)));
   psb00=str2num(char(ductdatraw(21:23)));
   if DYNT==0  %determine which parameter to use depending on user
      PSB=psb00;  %input of day, night, or both
   elseif DYNT==1
      PSB=psb12;
   else
      PSB=(psb00+psb12)/2;
   end
   GMEL=str2num(char(ductdatraw(24:27)));
   OHEL=str2num(char(ductdatraw(28:31)))/1000;
   MTEL=str2num(char(ductdatraw(32:34)))/1000;
   MDEL=str2num(char(ductdatraw(35:37)));
   MFEL=str2num(char(ductdatraw(38:41)));
   pel12=str2num(char(ductdatraw(42:44)));
   pel00=str2num(char(ductdatraw(45:47)));
   if DYNT==0  %determine which parameter to use depending on user
      PEL=pel00; %input of day, night or both
   elseif DYNT==1
      PEL=pel12;
   else
      PEL=(pel00+pel12)/2;
   end
   p2elx100=str2num(char(ductdatraw(48:51)));
   psbelx100=str2num(char(ductdatraw(52:56)));
   P2EL=p2elx100/100;
   PSBEL=psbelx100/100;

   status=fclose(fid);

   %Calculate duct heights and associated M values
   M1K=N1K+1*(1e6/6378);
   %  Surface Duct Calculations
   PHs(1)=0;  %all heights in km
   PMs(1)=NS;
   PHs(2)=OHSB;
   PMs(2)=NS+GMSB*OHSB;
   PHs(3)=MTSB;
   PMs(3)=PMs(2)-MDSB;
   PHs(4)=PHs(3)+1;
   PMs(4)=PMs(3)+(M1K-NS);
```

```
    %  Elevated Duct Calculations
    PHe(1)=0;  %all heights in km
    PMe(1)=NS;
    PHe(2)=OHEL;
    PMe(2)=NS+GMEL*OHEL;
    PHe(3)=OHEL-(MDEL/GMEL)+MTEL;
    PMe(3)=PMe(2)-MDEL;
    PHe(4)=PHe(3)+1;
    PMe(4)=PMe(3)+(M1K-NS);
    %  No-Ducting Calculations
    PHn(1)=0;
    PMn(1)=NS;
    PHn(2)=1;
    PMn(2)=M1K;
    if ~PHs(2) %Happens if the prob of surf duct is zilch, so we
       PHs(2)=PHs(4); %just calculate the two levels needed for
       PMs(2)=PMs(4); %the exponential model
       PHs(3:4)=[];
       PMs(3:4)=[];
    end
    if ~PHe(2) %Happens if the prob of elev duct is zilch, so we
       PHe(2)=PHe(4); %just calculate the two levels needed for
       PMe(2)=PMe(4); %the exponential model
       PHe(3:4)=[];
       PMe(3:4)=[];
    end
else %Standard atmosphere or interpolation - no ducting
    GMSB=0;
    OHSB=0;
    MTSB=0;
    MDSB=0;
    MFSB=0;
    PSB=0;
    GMEL=0;
    OHEL=0;
    MTEL=0;
    MDEL=0;
    MFEL=0;
    PEL=0;
    P2EL=0;
    PSBEL=0;
    %  No Ducting Profile Calculations
    M1K=N1K+1*(1e6/6378);
    PHn(1)=0;
    PMn(1)=NS;
    PHn(2)=1;
    PMn(2)=M1K;
end
```

```
function CR9raytrace
global DUCTFLG PHs PHe PHn PMs PMe PMn RAZ REL RLAT SEL THT TRG
global ALF0 ALFG BETAES R0 HEIGHTS THTAPP THTERR THTERR100 TRGAPP
global TRGERR TRGERR100 DUCTHTS ERRMSG

%CLIMAREF Raytrace with ducting module (CR9raytrace_d.m)
%This module uses the refractivity data from the selected radiosonde
%station to trace the bending of a ray from the radar to the given
%target whether or not a duct exists

%INPUT VARIABLES:
%DUCTFLG - flag indicating what type, if any, ducting will be taken into
account
%PHs,PHe,PHn - M-profile heights
%PMs,PMe,PMn - M-profile M-values into account (0=none,1=sfc,2=elev)
%RAZ - radar azimuth (direction it's pointing)
%REL - radar elevation (AGL)
%RLAT - radar latitude
%SEL - radiosonde station height (MSL)
%THT - target height (AGL) (actual) (km)
%TRG - target range (actual) (km)

%INTERNAL VARIABLES:

%a,b,c - intermediate variables for radius of curvature calc
%A,B,C,delz - intermediate values in calculating height of extrema
%alfga,alfgb - intermediate variables for calculating ALFG
%a0 - estimate of initial take-off angle required to hit target
%a0hiB - highest a0 of a trace that reached target ht but missed tgt
%a0lastgood - last a0 estimate that was "in the clear" -- used for
%             splitting the difference
%a0loB - lowest a0 of a trace that reached target ht but missed tgt
%a0magtoolo - lower limit of takeoff angle when radar and target are in
%             the duct together.  Takeoff angle <= this will result in
%             trace never reaching the target height
%a0magtoohi - upper limit of takeoff angle when radar and target are in
the
%          duct together
%a0toohi - an a0 estimate above a0toohi will either put the trace in a
%          duct unnecessarily or cause the ray to overshoot the target
%          on a downward slope
%a0toolo - an a0 estimate below a0toolo will either put the trace into
%          a duct unnecessarily or cause the ray to "hit dirt"
%          unnecessarily
%angtol - tolerance for subtense matching (constant=1e-6)
%bend - index into profile heights, ph
%beta1 - subtense over current layer
%beta43,rc43,trg43 - subtense,radius of curvature,and target range
%                    modified for 4/3 earth
%betae - total subtense up to this point in the estimated trace
%betat - actual subtense between radar and target
%botductht - height of bottom of duct
%bothinduct - flag indicating both radar and target are in the duct
%botrng,toprng - defines levels at top and bottom of a profile layer
%cantfind - flag indicating the estimation is not working to find the
%          target, probably because of ducting effects
%ce - intermediate constant in calculation of N
%clostsub - when trace has reached target height multiple times,
%          clostsub is the index into hitBETAES,and hitdBda0,
```

```
%           indicating which is the closest to the target
%cosia1,cosia0,cosia2 - cosine of a1,a0,a2
%db1da0 - incremental subtense change with initial el angle
%dbda0 - total subtense change with initial el angle
%deg2rad - degres to radians conversion
%dh - height increment
%gam - intermediate var -- n-gradient in layer
%h - height vector, contains heights of all defined levels
%hitbetae - subtenses of points at which target height was reached
%hitdBda0 - total change in subtense with change in a0, stored for
%           every point at which target height was reached
%hitdirtflg - flag indicating ray has hit the ground
%hithole - flag indicating target appears to be in a radio hole (val=1)
%           -- duct steers all radio energy away from it -- OR over
%           the radio horizon (val=2)
%hittarg - flag indicating target hit (value indicates which hit,
%           if more than one, was the target)
%maxalt - maximum altitude for defining refractivity profile
%maxminflg - indicates an extrema (ray is tangent to a shell
%              concentric with the earth) has been reached
%Mgrad - M gradient, used for deteriming bottom of elevated duct
%missby - subtense angle (pos or neg) by which the trace missed target
%N - refractivity at every level from surface to maxalt
%n0 - index of refraction at surface
%N1,h1 - N and h values for lower level defining current layer
%N2,h2 - N and h values for upper level defining current layer
%Nm,hm - N and h values at extrema
%nummms - extrema counter
%outoduct - flag indicating trace has left the duct
%ph,pM - M-profile heights and M values
%pN - N-profile N-values
%psi1 - amount of bending ray underwent in current layer
%R0 - (rc+SEL) radius from earth center to surface (station) elevation
%rta,rtb - intermediate variables for calculating ALFG
%stepstohit - number of steps it took to get to each point at which
%              target height was reached
%stoptrace - flag indicating trace must be stopped - value indicates
%              reason for stop (see notes)
%trgapp1 - range from point 1 to point 2 for a single layer --
%              accumulated to calculate TRGAPP, the total apparent range

%OUTPUT VARIABLES:
%ALF0 - initial angle of elevation for iteration
%ALFG - geometric elevation angle (el angle of straight line between
%        radar and target
%BETAES - stored betaes for plotting later
%HEIGHTS - stored step heights for plotting later
%R0 - local earth radius of curvature + surface elevation
%THTAPP - apparent target height
%THTERR - height error
%THTERR100 - height percent error
%TRGAPP - total apparent range
%TRGERR - range error
%TRGERR100 - height percent error
```

```
%************Set up initial variables and values**********************

maxnumtraces=30;
deg2rad=2*pi/360; %degrees to radians conversion factor
angtol=1e-6; %tolerance used to compare angles in iteration (radians)
dh=.001; %height resolution in km (recommend dh=0.00001 for best results
maxalt=5+max([THT REL]); %we won't worry about levels any
%  higher than 5km above highest point -- that'll cover ducting
maxalt=dh*round(maxalt/dh);      %round maxalt to nearest level
REL=dh*round(REL/dh);          %round radar elevation to nearest level
THT=dh*round(THT/dh);          %round target height to nearest level
%Calculate local earth radius of curvature
a=6378.139; %km
b=6356.750; %km
c=a^2/b^2-1;
rc=a^2/(b*sqrt(1+c*cos(RLAT*deg2rad)^2)*(1+c*cos(RLAT*deg2rad)^2*...
   cos(RAZ*deg2rad)^2));
%define radius to surface
R0=rc+SEL;
%Calculate N-Profile
switch DUCTFLG %determine which ducting profile, if any, to use
   case 0
      ph=PHn;
      pM=PMn;
   case 1
      ph=PHs;
      pM=PMs;
   case 2
      ph=PHe;
      pM=PMe;
end  %end of determine ducting profile
ph=dh*round(ph/dh);    %round profile heights to nearest
%                                 multiple of dh
pN=pM-ph*(1e6/6378);
pgd=(pN(2:length(pN))-pN(1:length(pN)-1))./...
   (ph(2:length(ph))-ph(1:length(ph)-1));
h=[0:dh:maxalt];  %height vector all heights (hence levels) are
%                            defined w.r.t. surface elevation
for bend=[1:length(ph)-2]
   botrng=round(ph(bend)/dh+1); %calculates bottom and top levels of
   toprng=round(ph(bend+1)/dh+1); %layer -- 'round' ensures integer
   N(botrng:toprng)=pN(bend)+(h(botrng:toprng)-h(botrng))*pgd(bend);
end %end of loop through all "bends"
ce=log(pN(length(pN)-1)/pN(length(pN)));  %intermediate constant
botrng=round(ph(length(ph)-1)/dh+1); %'round' simply ensures answer
toprng=round(maxalt/dh+1); %is integer type--no rounding really takes
place
N(botrng:toprng)=pN(length(pN)-1)*...
   exp(-ce*(h(botrng:toprng)-h(botrng)));

n0=1+N(1)*1e-6;  %index of refraction at surface
%Calculate target subtense
betat=acos(((R0+THT)^2+(R0+REL)^2-TRG^2)/(2*(R0+THT)*(R0+REL)));
%Estimate initial angle of elevation using 4/3 earth
beta43=.75*betat; %i.e. beta(effearth)=(re/re(eff))*betat
rc43=1.25*rc; %rc modified for eff earth
r043=rc43+SEL; %R0 modified for eff earthd
trg43=sqrt((r043+REL)^2+(r043+THT)^2-2*(r043+REL)*...
   (r043+THT)*cos(beta43));
```

```
if trg43==0 %if trg43 happens to be zero it will cause a ?/0 error
   %unless we modify it slightly
   trg43=1e-12;
end %end of check for trg43=0
a0=acos((r043+THT)*sin(beta43)/trg43); %Note: a0 is always positive
if (r043+THT)<((r043+REL)/cos(beta43)),a0=-a0;,end %determine whether
%  takeoff angle is + or - using pythagorean theorem (see notes,step 5)

if ~isreal(a0),a0=1e-12;end %if a0 is close to zero, it may be
calculated
%as imaginary or complex, hence this fix

%Determine whether target and radar are in a duct together
if DUCTFLG>0
   if DUCTFLG==2
      Mgrad=(pM(2)-pM(1))/(ph(2)-ph(1));
      botductht=ph(2)+(pM(3)-pM(2))/Mgrad;
   else
      botductht=0;
   end %end of DUCTFLG==2
   if REL<ph(3)&REL>botductht&THT<ph(3)&THT>botductht
      bothinduct=1;
   else
      bothinduct=0;
   end %end of height comparison
else
   bothinduct=0;
end %end of target-radar in duct together check

%************************Perform Raytracing*************************
%Initialize counters,flags,etc.
hittarg=0;
hithole=0;
a0toolo=-99;
a0toohi=99;
a0magtoolo=0;
a0lastgood=99;
ERRMSG=[];
hitbetae=[];
stoptrace=0;
a0loB=99;
a0hiB=99;
tracecount=0;
cantfind=0;
while ~hittarg&~hithole&~cantfind  %BEGINNING of estimate/iterate loop
   tracecount=tracecount+1;
   %disp(['trace # ' num2str(tracecount) ' a0=' num2str(a0,16)])

   a1=a0;  %initialize el angle #1
   dir=sign(a0);
   lvl=REL/dh+1-dir; %initialize level to one before REL (taking into
   %              account the increment at the start)--Note: level 1 is
   %              at the surface (there is no level 0)
   betae=0;
   BETAES=[0];     %Initialize beta accumulator
   TRGAPP=0;
   dBda0=0;
   cosia2=0;
   heights=[REL];  %Initialize height accumulator
```

```
   maxminflg=0;
   hitdirtflg=0;
   stoptrace=0;   %Initialize flag for stopping trace
   nummms=0;      %Initialize max/min counter
   numhits=0;     %Initialize target-height-reached counter
   hitbetae=[];   %Initialize target-height-reached subtense storage
   hitdBda0=[];  %Initialize target-height-reached dBda0 storage
   stepstohit=[]; %Initialize target-height-reached #-steps-it-took-
   %                 to-get-there storage
   outoduct=0;
   while ~stoptrace  %BEGINNING of trace loop
      lvl=lvl+dir;
      if lvl==2 & dir==-1  %if level is currently 1 above ground...
         hitdirtflg=1;
      end
      cosia1=cosia2;  %for use if there's an extrema
      if maxminflg==1  %if the previous point was an extrema...
         %!!!Note: Determine direction by sign of M-gradient--FIX--p4B-
5!!!
         dir=-dir; %swap directions
         N1=Nm; %current N and ht are at the extrema
         h1=hm;
         N2=N(lvl+dir); %since dir's been swapped around, this'll
         h2=h(lvl+dir); %  bring us back to the last level we were at

         cosia2=cosia0; %el angle of ray is opposite that of the
         %  level hit before the extrema
         maxminflg=-1; %set flag indicating current level is max/min
      else
         N1=N(lvl);
         h1=h(lvl);
         N2=N(lvl+dir);
         h2=h(lvl+dir);
         %disp(['h1=' num2str(h1) ' h2=' num2str(h2) ' cos(a1)='
num2str(cos(a1),16)])
         cosia2=(1+(N1-N2)*(1e-6)-(dir*dh/(R0+h1)))*cos(a1);
         %disp(['cosia2=' num2str(cosia2,16)])
      end %end of assign-N-and-h-values routine
      if cosia2>1 %max or min -- find ht of extrema, see Abel,pp.23,24
         A=(1/(R0+h1))*(N2-N1)*1e-6/(h2-h1);
         %  A=(1/ra)*(dn/dz)
         B=.5*(1/(R0+h1)+(N2-N1)*1e-6/(h2-h1));
         %  B=(1/2)(1/a+dn/dz)
         C=1-cosia1; %C=1-cos(alfa)
         delz=dir*abs((abs(B)-sqrt(B^2-A*C))/A);   %ht difference
         hm=h1+delz;
         Nm=N1-(h1-hm)*(N1-N2)/(h1-h2);
         N2=Nm;
         h2=hm;
         cosia2=1; %since el ang at extrema is 0, cos(ang) is 1
         cosia0=cosia1;
         maxminflg=1;  %set flag indicating next level is max/min
         nummms=nummms+1; %count number of max/mins
      end  %end of what-if-there's-an-extrema? routine
      if h1==floor(h1),disp([num2str(h1) 'km reached']),end
      n1=1+N1*1e-6;
      n2=1+N2*1e-6;
      a2=dir*acos(cosia2); %is SIGN necessary
      psi1=2*(n1-n2)/(tan(a1)+tan(a2)); %calc bending in layer
```

```
      beta1=abs(psi1+a2-a1); %calc subtense across this layer
      betae=betae+beta1;      %accumulate total subtense to this point
      %disp(['a1=' num2str(a1,16) ' a2=' num2str(a2) ' psi1='
num2str(psi1,16) ' betae=' num2str(betae,16)])
      BETAES=cat(2,BETAES,betae);  %store all subtenses for later
      heights=cat(2,heights,h2); %store all heights for later

      %Calc geometric range over layer and accumulate
      trgapp1=sqrt((R0+h1)^2+(R0+h2)^2-2*(R0+h1)*(R0+h2)*cos(beta1));
      TRGAPP=TRGAPP+trgapp1;

      %Calculate how beta changed with a0 this layer (see Abel,p.29)
      if maxminflg==1  %next level is max/min
         gam=(n2-n1)/(h2-h1); %intermediate var -- n-gradient in layer
         dB1da0=-tan(a0)/tan(a1)+(2*n0*R0*sin(a0))/...
            (tan(a1)*(n2/gam+R0+h2))-(psi1*tan(a0))/(sin(a1))^2;
      elseif maxminflg==-1 %current level is max/min
         gam=(n2-n1)/(h2-h1); %intermediate var -- n-gradient in layer
         maxminflg=0; %reset maxminflg
         %Note: dB1da0 is the same -- symmetric about the extrema
      else  %neither level is max/min
         dB1da0=-tan(a0)/tan(a1)+tan(a0)/tan(a2)-...
            (psi1*tan(a0)/(tan(a1)+tan(a2)))*...
            (1/(cos(a1)*sin(a1))+1/(cos(a2)*sin(a2))); %Calc beta
         %                                          gradient for this layer
      end  %end of calculate-dB1da0 routine
      dBda0=dBda0+dB1da0; %accumulate total beta change with a0

      %record data every time target height is reached
      if abs(h2-THT)<1e-10
         hitbetae=cat(2,hitbetae,betae);  %subtenses of "hit" points
         hitdBda0=cat(2,hitdBda0,dBda0);  %differential of "hit" points
         stepstohit=cat(2,stepstohit,length(BETAES)); %number of steps
         %it took to get to each "hit" point
      end

      if DUCTFLG
         if
REL<ph(3)&REL>botductht&(h2>ph(3)|h2<botductht),outoduct=1;,end  %Check
to see if trace started in duct           else
         %Check to see if the trace has left the duct
      end
      %***********Determine whether raytrace needs to be stopped******
      if ~bothinduct %radar and target not in duct together
         if a0>=0    %initial el angle positive (or zero)
            if nummms==1|hitdirtflg  %unwanted ducting
               stoptrace=1;
               if a0>a0toolo,a0toolo=a0;,end
            elseif h2==THT  %target height reached
               stoptrace=2;
               a0lastgood=a0;
            end  %end of el-ang-pos options
         else        %initial el angle negative
            if nummms>1   %unwanted ducting
               stoptrace=3;
               if a0<a0toohi&DUCTFLG==2,a0toohi=a0;,end %if we're
dealing with an
               %elevated duct, establish a new upper limit for the trace
angle
```

```
            elseif THT>=REL&length(hitbetae)==1 %target higher than
radar
               %                                & target height reached
               stoptrace=4;
               a0lastgood=a0;
            elseif THT<REL %target lower than radar
               if (length(hitbetae)==2)|(length(hitbetae)==1&...
                     hitdirtflg&abs(hitbetae-betat)<.5*hitbetae)
                  %target height reached twice OR height reached once
                  %near the target and trace hits the ground
                  stoptrace=5;
                  a0lastgood=a0;
               elseif ~length(hitbetae)&nummms==1 %max/min reached,but
                  %target height never reached
                  stoptrace=8;
                  if a0<a0toohi,a0toohi=a0;end
               end
            end  %end of el-ang-neg options
         end  %end of el-ang-pos-or-neg routine
      else  %radar and target ARE in duct together

         if hitbetae  %If target height has been reached
            if ~outoduct&hitbetae(length(hitbetae))>betat
            %radar and target in duct together, ray goes past target
               stoptrace=6;
               a0lastgood=a0;
            elseif outoduct
               if a0>=0 %tgt ht reached,trace left duct,a0 positive
                  stoptrace=2;
               else %a0<0
                  if THT<REL&(length(hitbetae)==2|...
                        (length(hitbetae)==1&hitdirtflg&...
                        abs(hitbetae-betat)<.5*hitbetae))
                  %target height reached twice OR height reached once
                  %near the target and trace hits the ground
                     stoptrace=5;
                     a0lastgood=a0;
                  elseif THT>REL
                     stoptrace=4;
                     a0lastgood=a0;
                  end
               end
            elseif a0>0&hitdirtflg %trace reaches target height on
upward swing,then
               %reaches max, swings down and hits the ground
               stoptrace=6;
               a0lastgood=a0;
            end
         elseif nummms>1|(nummms==1&hitdirtflg)
            %If target height has not been reached but two extremas
            %have been hit, or one & trace hit dirt
            stoptrace=9;
         end
      end  %end of radar&targ-both-in-duct-or-not check
      if hitdirtflg&a0<0&~stoptrace %initial el ang neg,ray hits
         %surface, and no other stop situation exists
         stoptrace=7;
         if a0>a0toolo,a0toolo=a0;,end
      end
```

```
      a1=a2; %Prepare to jump to next level
   end   %END of trace loop


   %!!!!!!!!!!!!!!!TEMP!!!!!!!!!!!!!!!!!!
      %plot bent path
   %plotit=input('Plot trace? (y=1/n=0)');
   plotit=0; %set plotit=1 to plot every trace
   if plotit
      gndrngs=BETAES*R0*.53996; %conversion factor changes km to Nmi
      htsft=heights*3280.83; %conv factor changes km to feet
      plot(gndrngs,htsft,'y')
      text(gndrngs(length(gndrngs)),htsft(length(htsft)),...
         num2str(tracecount),'HorizontalAlignment','center',...
         'VerticalAlignment','bottom')
      hold on
      plot(betat*R0*.53996,THT*3280.83,'*b')
      disp(['hitbetae=' num2str(hitbetae)])
      disp(['betat=' num2str(betat)])
      disp(['stoptrace=' num2str(stoptrace)])
      %disp(['hitdBda0=' num2str(hitdBda0)])
      disp('Hit any key...')
      pause
   end

   %!!!!!!!!!!!!!!!END TEMP TEST!!!!!!!!!!!!!!!!!!!!!!!!!!!!!!!



   %**************Check for target reached/inaccessible***************
   %Check for target-reached or target-inaccessible based on reason
   %for stopping trace (stoptrace)
   %stoptrace=1,3,7,8,9:  no check;reestimate directly
   if stoptrace==2|stoptrace==4|stoptrace==5|stoptrace==6
      [dummy,clostsub]=min(abs(hitbetae-betat)); %determine which
      %  "hit" subtense is nearest the target
      missby=hitbetae(clostsub)-betat; %determine proximity of "hit"
    if sign(missby)==-1  %store takeoff angles of nearest hits
      a0loB=a0;
      else
         a0hiB=a0;
      end
      if abs(missby)<=angtol,hittarg=clostsub;,end %determine if trace
      %came near enough to target to stop tracing
   end

   %Flag to stop if estimation/iteration isn't getting anywhere
   if ~hittarg&tracecount>maxnumtraces  %If more than 20 traces have
occurred
      %and still the target is not reached...
      cantfind=1;  %set flag indicating estimator can't find target
   end

   %**************Estimate new initial takeoff angle****************
   %Estimate new initial elevation angle based on reason for
   %stopping the trace (stoptrace)
   if ~hittarg&stoptrace
```

```
      a0last=a0; %Keep track of the last a0 (for various reasons)
      switch stoptrace
         case 1   %pos el ang, unwanted ducting
            if a0lastgood==99  %If every trace has been in duct...
               a0=1.5*a0;  %double initial el angle to break out of duct
            else  %If a previous trace was out of the duct...
               a0=a0toolo+(a0lastgood-a0toolo)/2; %split
               %difference between intl angs to brk out w/out jumping
               %over last good trace
               if abs(a0-a0last)<=angtol, hithole=1,end
            end
         case 2   %pos el ang, target height reached
            a0=a0+(betat-betae)/dBda0;  %use standard estimator
         case 3   %neg el ang, unwanted ducting
            if a0lastgood==99  %If every trace has been in duct...
               if DUCTFLG==1   %i.e. surface duct
                  a0=-1.5*a0;  %increase initial angle and make it
positive
                  %to break out of the duct
               else %i.e. DUCTFLG=2, elevated duct
                  a0=1.5*a0;  %increase initial el angle to break out of
duct
               end
            else  %If a previous trace was out of the duct...
               a0=a0toohi+(a0lastgood-a0toohi)/2;
               %split difference between intl angs to brk out w/out
               %jumping over last good trace
               if abs(a0-a0last)<=angtol, hithole=1,end
            end
         case 4   %neg el ang,targ ht (higher than radar) reached
            a0=a0+(betat-betae)/dBda0;  %use standard estimator
            %if betae>betat&a0<a0last,a0=.75*a0last,end %if ducting
            %causes estimator to fail and go the wrong direction,
            %fudge it down.  Eventually, betae will drop below betat
            %and a0loB and a0hiB will kick in and guide it in
         case 5   %neg el ang,targ ht (lower than radar) reached twice
            a0=a0+(betat-hitbetae(clostsub))/hitdBda0(clostsub);
         case 6   %ducting,trace reached targ ht at point beyond targ or
trace
            %reached target height and hit the dirt
            a0=a0+(betat-hitbetae(clostsub))/hitdBda0(clostsub);
            if abs(a0)<=a0magtoolo,a0=1.2*a0magtoolo;,end
            %  use standard estimator with values at hit closest to
            %  the target
         case 7  %neg el ang, hit ground (in duct or not)
            if a0lastgood==99  %If every trace has hit the dirt...
               if THT>=REL
                  a0=-.25*a0; %force pos el angle to converge on soln
               else   %i.e. Target is lower than radar
                  a0=.75*a0; %raise angle a bit in order to eventually
                  %reach the target height while remaining negative
               end
            else  %If a previous trace stayed away from dirt...
               a0=a0toolo+(a0lastgood-a0toolo)/2;
               %split difference between lowest airborne ray and
               %highest "underground" ray
               if abs(a0-a0last)<=angtol, hithole=2,end
            end
         case 8 %neg el ang, tgt below rdr, but didn't reach low enough
```

```
            if a0lastgood==99
               a0=1.2*a0; %increase angle to get down to tgt height,
then
            %              regular estimation will do the trick
            else
               a0=a0toohi+(a0lastgood-a0toohi)/2;
               %split difference between intl angs to brk out w/out
               %jumping over last good trace
               if abs(a0-a0last)<=angtol, hithole=1,end
            end
         case 9 %rdr&tgt in duct together, tgt height not reached
            a0magtoolo=abs(a0);
            a0=1.2*a0; %arbitary increment amount -- no sign change
      end

      if stoptrace

         %Ensure estimate doesn't go beyond hi/lo bounds established to
         %avoid hitting the ground and getting trapped in a duct
         if a0<=a0toolo
            a0=a0toolo+(a0last-a0toolo)/2; %split diff w/last a0
estimate
         end
         if a0>=a0toohi
            a0=a0toohi+(a0last-a0toohi)/2; %split diff w/last a0
estimate
         end

         %Ensure estimate doesn't go beyond hi/lo bounds established to
         %prevent waffling around the target without hitting it
         if a0loB~=99&a0hiB~=99&(abs(a0-a0loB)>abs(a0hiB-a0loB)|...
             abs(a0-a0hiB)>abs(a0hiB-a0loB))
         %If the limits are established & the new estimate is outside
them
            a0=(a0loB+a0hiB)/2; %redefine a0 halfway in-between limits
         end

         %Ensure estimate does not go positive if target is below radar
and
         %they are not in the duct together
         if a0>0&THT<REL&~bothinduct,a0=.25*a0last;,end

         if hitbetae>100*betat %If initial takeoff angle is too
         %small, a huge betae will result.  This knocks the estimate
         %out of that range (eventually)
            a0=10*a0last;
         end

      end

   end

end  %END of estimate and iterate loop

%****************Calculate final information**************
if hithole  %If target is in a radio hole or over the radio horizon...
   switch hithole
      case 1   %radio hole
         ERRMSG=['Target appears to be in a radio hole'];
```

```
      case 2   %over radio horizon
         ERRMSG=['Target appears to be over radio horizon'];
   end
elseif cantfind&~bothinduct
   ERRMSG=['Unable to trace to target, probably due to ambiguities
caused by ducting.'];
elseif cantfind&bothinduct
   ERRMSG=['Unable to trace to target.  Radar and Target are in the duct
together resulting in ambiguous estimation'];
else  %Target reached
   ALF0=a0;
   HEIGHTS=heights(1:stepstohit(hittarg));%Only keep those steps
   BETAES=BETAES(1:stepstohit(hittarg));%necessary to get to target
   %Calculate geometric elevation angle (i.e. Inital angle for straight
   %line path from radar to target.
   if TRG==0 %prevents potential ?/0 error
      TRG=1e-12;
   end
   alfga=asin((R0+THT)*sin(betat)/TRG)-pi/2; %calc geo el angle for long
and
   alfgb=-alfga;                          %short R0's (see notes)
   rta=sqrt((R0+REL)^2+TRG^2-2*(R0+REL)*TRG*cos(alfga+pi/2)); %calc two
rt's to
   rtb=sqrt((R0+REL)^2+TRG^2-2*(R0+REL)*TRG*cos(alfgb+pi/2)); %compare
   if abs(rta-(R0+THT))<abs(rtb-(R0+THT)) %whichever rta/b equals rt
indicates
      ALFG=alfga;             %which alfga/b is the correct geometric
   else                       %elevation angle
      ALFG=alfgb;
   end

   %Calculate measured (apparent) target height
   THTAPP=sqrt((R0+REL)^2+TRGAPP^2-2*(R0+REL)*TRGAPP*cos(ALF0+pi/2))-R0;

   %Calculate height error, range error, % error
   THTERR=THTAPP-THT; %height error
   THTERR100=THTERR*100/THT; %height percent error
   TRGERR=TRGAPP-TRG; %range error
   TRGERR100=TRGERR*100/TRG; %range percent error

   %Save duct parameters for plotting later
   if DUCTFLG>0,DUCTHTS=[botductht,ph(2),ph(3)];,end

end
```

Appendix B

Marsden Square Numbering System for the World

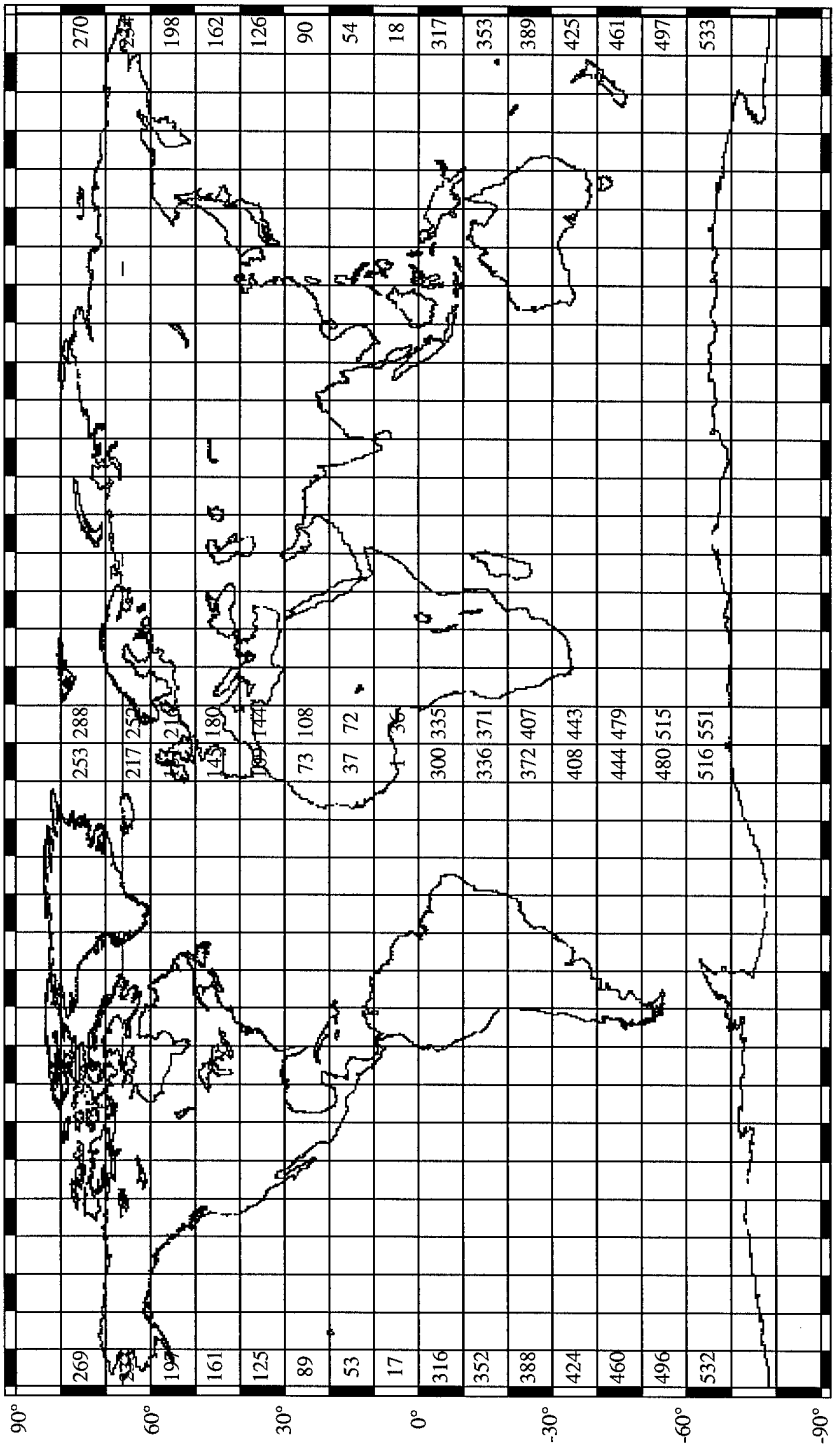

Bibliography

84th Radar Evaluation Squadron. Class Handout, Radar Evaluation Technical Training, Radar Theory Vol 1. 84 RADES, Hill AFB UT July 1998.

Abel, Michael D. *et. al.* "The Theory and Use of a Raytracing Model Developed at USAFETAC." USAFETAC/TN-82/005. USAF Environmental Technical Applications Center, Scott AFB IL, September 1982.

Bean, B.R. And E.J. Dutton. *Radio Meteorology.* National Bureau of Standards Monograph 92. Washington: GPO, 1 March 1966.

Bean, B.R. and G.D. Thayer. "Central Radio Propagation Laboratory Exponential Reference Atmosphere, " *Jour. Res. NBS*, Vol. 63D, No. 3: 315-317 (June 1959).

Blake, Lamont C. *Radar Range Performance Analysis.* Norwood MA: Artech House, Inc., 1986.

California Department of Water Resources, Division of Local Assistance. "CIMIS ETo Calculations." Equations excerpted from an article by Pruitt and Doorenbos in the *Proceedings of International Round Table Conference on "Evapotranspiration,"* Budapest, Hungary, 1977, n. pag. http://wwwdla.water.ca.gov/cimis/cimis/hq/etocal.htm. 3 Aug 1998.

Hitney, H.V. and J.H. Richter. Integrated Refractive Effects Prediction System (IREPS), Nav. Eng. Jour., 88, 2: 257-262 (April 1976)

Kalnay, E., *et. al.* "The NCEP/NCAR 40-Year Reanalysis Project," Bulletin of the *American Meteorological Society, Vol. 77, No. 3*: 437-471, (March 1996).

Kerr, Donald E. *Propagation of Short Radio Waves.* New York: McGraw-Hill Book Co., Inc., 1951.

Ko, H.W. *et. al.* "Anomalous Propagation and Radar Coverage Through Inhomogeneous Atmospheres," AGARD, CP346:25-1 - 25-11 (1994).

Ko, H. W., Sari, J. W., and Skura, J. P., "Anomalous Microwave Propagation Through Atmospheric Ducts," *Johns Hopkins APL Tech. Dig.* 4, 12–26 (1983).

Livingston, Donald C. *The Physics of Microwave Propagation.* Englewood Cliffs NJ: Prentice-Hall, Inc., 1970.

Patterson, W.L. *Advanced Refractive Effects Predictive System (EREPS) Version 1.0 User's Manual.* Technical Document 3028. San Diego: Space and Naval Warfare Systems Center, April 1998.

Patterson, W.L. Ducting Climatology Summary (DCS) software (Version 2.0, 21 January 1992) read file. San Diego: Space and Naval Warfare Systems Center, 1993.

Patterson, W.L., *et. al. Engineer's Refractive Effects Predictive System (EREPS) Version 3.0.* Technical Document 2648. San Diego: Naval Command, Control and Ocean Surveillance Center, RDT&E Division, May 1994.

Patterson, W. L. *Historical Electromagnetic Propagation Condition Database Description.* Technical Document 1149. San Diego: Naval Ocean Systems Center, September 1987.

Ryan, Frank J. *Analysis of Electromagnetic Propagation Over Variable Terrain Using the Parabolic Wave Equation.* TR1453. San Diego: Naval Ocean Systems Center, 1991.

Schelleng, J.C., C.R. Burrows, and E.B. Ferrell. "Ultra-Short-Wave Propagation." *Proc. IRE* 21, no.3: 427-63 (March 1933).

Science Applications International Corporation. *Investigation of Refraction Issues.* TR DO 30-01-04. SAIC, 30 March 1996.

Smith, E.K. and S. Weintraub. "The Constants in the Equation for Atmospheric Refractive Index at Radio Frequencies," *Proc. IRE* 41: 1035-1037 (Aug 1953).

Squires, Michael F. "Height-Error Analysis for the FAA-Air Force Replacement Radar Program (FARR)." USAFETAC/PR--91/014. USAF Environmental Technical Applications Center, Scott AFB IL, August 1991.

Weisbrod, S. and L.J. Anderson. "Simple Methods for Computing Tropospheric and Ionospheric Refractive Effects on Radio Waves," *Proc. IRE* ##: ??-?? (Sep 1958).
(Note: this entry has DTIC # ADA 056800)

Vita

Capt Todd Pittman was born 18 September 1967 at Scott Air Force Base, Illinois. In 1985 he graduated from Chittenango High School in Chittenango, New York and entered Grove City College, Grove City, Pennsylvania with a four-year ROTC scholarship to study Electrical Engineering. Upon graduating with a Bachelor of Science in Engineering (Electrical Engineering) Degree, Capt Pittman was commissioned into the United States Air Force.

Captain Pittman's first assignment was at the Air Force Communications Command Headquarters at Scott AFB where he worked as an air traffic control radar evaluation engineer and a communications test engineer until March 1994. He then traveled to Wright-Patterson AFB and Keesler AFB where he was assigned to the Air Force's Communications Systems Evaluation School as the Advanced Narrowband Radio Course Director. While at Keesler AFB, he was selected for a regular commission. In July 1997, he entered the Graduate Electrical Engineering Program, School of Engineering, Air Force Institute of Technology. Upon graduation, he will be assigned to the 84th Radar Evaluation Squadron at Hill AFB, Utah.

Permanent Address: 5888 Fieldstone Drive
Cazenovia, NY 13035